INVESTIGATION OF BEARING AND TEAROUT OF STEEL BOLTED CONNECTIONS

Final Report
submitted to the
American Institute of Steel Construction

by

Mark D. Denavit, Nicolo Franceschetti, and Andrew Shahan
Department of Civil and Environmental Engineering
University of Tennessee, Knoxville

July 2021

Abstract

The limit state of tearout can complicate the design of steel bolted connections since, in contrast to the limit states of bearing and bolt shear rupture, tearout strength can vary from bolt to bolt within a connection. Under the current AISC *Specification*, tearout strength is proportional to the clear distance, in the direction of force, between the edge of the hole and the edge of the adjacent hole or edge of the material. However, recent studies on concentrically loaded bolt groups have suggested that the use of clear distance may not accurately represent tearout strength and have proposed alternative lengths for use in strength equations. A reevaluation of the limit state of tearout is presented in this work, including a thorough evaluation of the proposed alternative tearout lengths using a large database of previously published experimental work and new experiments with various edge distances and hole types. Equations with the alternative tearout lengths were found to be more accurate than those with clear distance, especially for small edge distances. Design recommendations including the alternative tearout lengths were developed. A reliability study on the existing provisions and recommended provisions was also completed to ensure the safety of these recommendations. An alternative design approach in which the limit state of tearout is captured implicitly through reduction factors applied to the bearing and shear rupture strength was also developed. Additionally, the impact of tearout on the behavior and design of single-plate shear connections, one of the most common applications of eccentrically-loaded bolted groups, was investigated with the goal of determining if the simplified approach for considering tearout recommended in the AISC *Manual* for conventional connections is appropriate and how best to consider tearout for extended connections. Experimental testing of beam and column subassemblies with single-plate shear connections showed that small horizontal edge distances do not necessarily decrease the strength of the connection. The results of this work increase understanding of the limit state of tearout and offer improved methods of evaluating this limit state in design.

Chapter 1: Introduction

The current AISC *Specification* (AISC 2016) includes a user note that was added in the 2010 edition (AISC 2010) stating that the strength of a bearing-type bolt group in shear should be taken as the sum of the effective strengths of the individual bolts. The effective strength of a bolt is equal to the minimum strength computed for the limit states of bolt shear rupture, bearing, and tearout. By this method, it is possible, for example, to have the strength of a bolt group controlled by a combination of tearout for the bolts near an edge and bolt shear rupture for the remaining bolts. The possibility of this interaction of limit states is in contrast to a common practice where bolt shear rupture is treated as independent from bearing and tearout (e.g., Salmon et al. 2009). Evaluating the potential interaction of bolt shear rupture, bearing, and tearout complicates the design of bolt groups, primarily because the strength of an individual bolt for the limit state of tearout can vary from bolt to bolt within a group. Given the increased complexity and recently proposed alternative strength equations (Clements and Teh 2013; Kamtekar 2012), a reevaluation of the limit state of tearout is warranted to determine if changes can be made that lead to more accurate and efficient connection designs.

Theory of Bearing and Tearout

For bolts sufficiently far from edges of material and adjacent bolts, the strength of the connected material near the bolt is controlled by bearing. The limit state of bearing is characterized by plastic deformations of the connected material near the bolt hole and a long yield plateau in the load-deformation relationship. However, the connected material eventually ruptures with continued loading. In experimental testing, the peak load has been noted to occur upon reaching yield, prior to rupture or somewhere in between. However, once the yield plateau is reached, the variation in load is small.

Bearing strength has been observed to depend on the diameter of the bolt, thickness of the connected material, and the tensile strength of the connected material. The edge distance, when large, does not impact bearing strength. Bearing strength can be quantified as the product of the projected area of the bolt on the connected material and the ultimate bearing stress of the connected material, as shown in Eq. 1.

$$P = dt\sigma_b \tag{1}$$

where, P is the failure load, d is the diameter of the bolt, t is the thickness of the connected material, and σ_b is the ultimate bearing stress of the connected material, or the bearing stress at a specified level of deformation. In research and practice, σ_b is expressed in terms of F_u, the ultimate tensile strength of the material, multiplied by an empirically derived coefficient.

The primary limit state for connected material with smaller edge distance is tearout. Tearout is characterized by the rupture of the connected material on either side of the bolt, depicted in Figure 1. A tearout failure would occur when the two shear planes extending from the bolt hole to the nearest edge reach their ultimate shear strength, as described in Eq. 2.

$$P = 2l_s t\sigma_s \tag{2}$$

where P is the failure load, l_s is the shearing length to the nearest edge (plate edge or bolt hole), t is the thickness of the connected material, and σ_s is the rupture shear stress of the connected material. The rupture shear stress is commonly taken as $0.6F_u$ as was determined for block shear (Birkemoe and Gilmor 1978). However, other coefficients have been proposed through testing. The shear length is most often based on edge distance from either the edge or center of the bolt hole. Other shear lengths have been proposed and will be evaluated in this work.
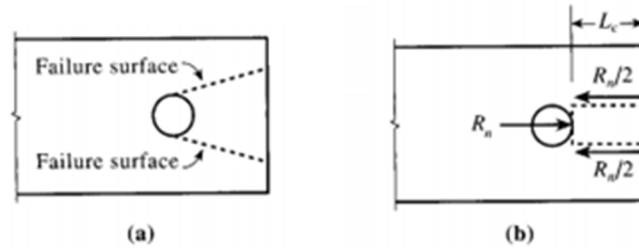
Figure 1: Comparison of Bearing and Tearout Mechanisms (Segui 2013)

Figure 2 demonstrates the load-deformation curves of specimens of varying edge distance tested by Wang et al. (2017). The second number in the specimen label indicates the edge distance. SD-10-30 had a nominal edge distance of 1.0 in., whereas SD-25-30 had a nominal edge distance of 2.5 in. Specimen SD-25-30 was the only specimen for which the strength per the AISC *Specification* (AISC 2016) was controlled by bearing. The failed specimens all show a tearout shear rupture of the connected material. However, the bearing-controlled specimen had much larger deformations. The figure depicts the decrease in strength as the edge distance is reduced.
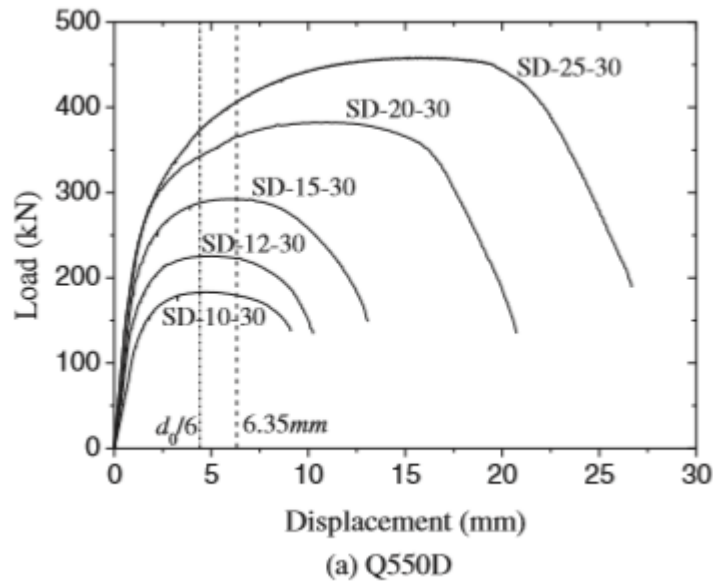
Figure 2: Load-Deformation Plots of Varying Edge Distances (Wang et al. 2017)

Splitting is another failure mode for bolted connections with small edge distances. It involves a tensile fracture initiating at the end of the connected material. The limit state of splitting is distinct from the limit state of tearout. Equations have been proposed to predict splitting strength (Duerr 2006) and some standards treat tearout and splitting separately (e.g., ASME 2017). However, splitting is not recognized within the AISC *Specification* (AISC 2016). Therefore, equations for

3

the limit state of tearout are implicitly covering splitting as well. This approach is justified since experimental results have shown the two limit states to have similar strengths.

Some experiments have also shown modes of failure for bolted connections that include out-of-plane curling of unconfined plates. A summary of failure modes in concentrically loaded bolted connections is provided in Figure 3.
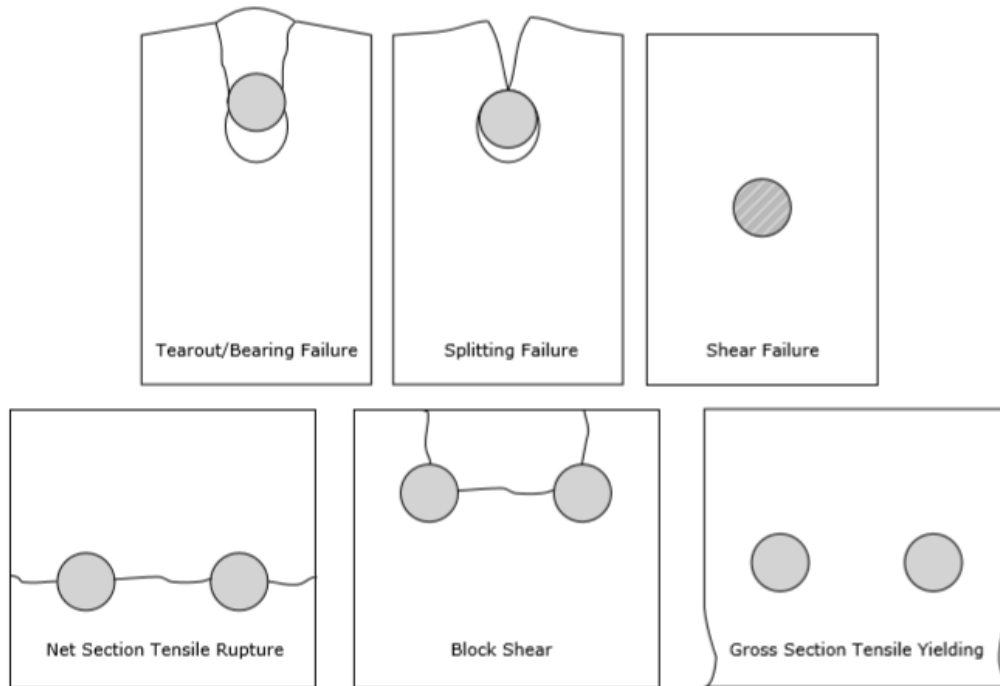
Figure 3: Common Failure Modes of Concentrically Loaded Bolted Connections

History of Provisions

Bearing of fasteners has been a consideration in the AISC *Specification* since the first edition published in 1923 (AISC 1923). However, tearout was not considered beyond the minimum edge distance requirements for construction tolerance. The appendix of the 1936 *Specification* (AISC 1936) describes a series of tension tests of riveted connections that revealed a tearout failure in the thinnest plate. The *Specification* reflected this finding by including a provision that the edge distance and/or spacing of a rivet be greater than the shearing area of the rivet divided by the plate thickness. This is significantly different from the modern tearout limit state because it is a function of geometry rather than strength. The 1936 *Specification* made an exception for the case of more than three rivets in the line of stress. The appendix justifies this as the following: "Had the specimens contained several rivets in line, this [tearout] should not have occurred, as the yielding of the end of the bar would no doubt have thrown more load back onto the interior rivets." The idea that tearout of the edge bolt can be precluded in the case of multiple bolts is revisited in later *Specifications*.

The creation of the Research Council on Riveted and Bolted Connections in 1947 led to several research projects regarding bolted connections. One outcome was an increase in the allowable

bearing stress in the 1961 AISC *Specification* (AISC 1961). The research completed by the Research Council was compiled in the *Guide to Design Criteria for Bolted and Riveted Joints* (Fisher and Struik 1974). Along with introducing LRFD design to bolted connections, tearout was reassessed using data gathered from many tests that had been completed. Two equations were suggested in the *Guide*, which were plotted as shown in Figure 4. The solid line is equivalent to Eq. 3, which is derived from the theory presented in Eq. 2.

$$P = (2t)\left(L_e - \frac{d}{2}\right)(0.7F_u) \tag{3}$$

where P is the failure load, t is the thickness of the connected material, L_e is the edge distance from the center of the bolt, F_u is the ultimate tensile strength of the connected material, and d is the diameter of the bolt.

The dashed line in Figure 4 is a simpler equation that was found to fit the data well. The dashed line can be expressed as shown in Eq. 4. and was included in the AISC *Specification* (1978).

$$P = L_e t F_u \tag{4}$$

This was the first provision that considered the reduction of allowable stress at smaller edge distances. The exception of the edge distance check for multiple bolts in a line that existed since 1936 was removed with the justification that "critical bearing stress is significantly affected by reduction of the edge distance, even with three fasteners in line" (AISC 1978).
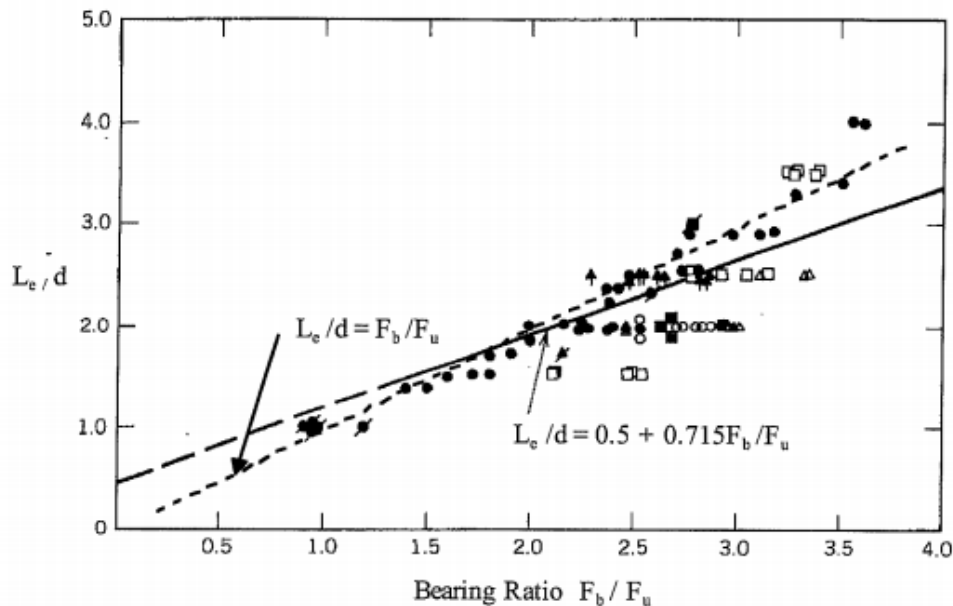
Figure 4: Experimental Data and Lines of Fit for Normalized Edge Distance vs. Bearing Ratio (Fisher and Struik 1974)

Frank and Yura (1981) identified that a connection with a bolt hole deformation of 1/4 in. has likely achieved much of the maximum strength, and further loading may limit the effectiveness of

the connection due to increasing deformation. Through experimental data, they determined a stress that would limit the deformation to 1/4 in., shown in Eq. 5.

$$\sigma_b = 2.4F_u \tag{5}$$

Frank and Yura's findings were incorporated in the 1986 Specification (AISC 1986). An additional condition was added to the provisions for the case where 1/4 in. deformation is tolerable, or as the *Specification* notes, "deformation around the bolt hole is not a design consideration." This condition allowed an additional 25% strength using a multiplier of 3.0 rather than 2.4. New criteria were added in which the tearout provision, Eq. 4, was not required to be checked if there were two or more bolts in a line, a minimum edge distance of $1.5d$ was provided, a minimum spacing of $3d$ was provided, and deformation at the bolt hole was a design consideration. These criteria were a return to previous *Specifications* that allowed an exception if several bolts were in the line of force. The exceptions were justified on the premise of load redistribution to the interior fasteners or that sufficient interior bolts in a connection would diminish the effects of reduced edge bolt hole strength if certain minimum edge distance and bolt spacing were provided.

There were no changes to the bearing and tearout provisions until the 1999 Specification (AISC 1999). According to Carter et al. (1997) there was a desire in the early 1990s to use clear distances to accommodate long-slotted and oversize holes without modification factors. Additionally, the existing provisions (AISC 1993) resulted in a discontinuity at an edge distance of 1.5d, when the bearing strength begins controlling over tearout. This is shown in Figure 5. To achieve the desired changes, a reformulation of Eq. 3 from the Guide (1974), which uses clear distance, was recommended in the 1994 RCSC Specification (Research Council on Structural Connections 1994). The experimental tests performed by Kim and Yura (1999) and Lewis and Zwerneman (1996) verified the accuracy of the new equation and concluded that the discontinuity in the 1993 *Specification* resulted in overestimations of the strength. Afterwards, the 1999 *Specification* (AISC 1999) adopted the RCSC provisions, as shown in Eq. 6 for the case where deformation is a design consideration.

$$R_n = 1.2l_c tF_u \le 2.4dtF_u \tag{6}$$

The equation was modified to imply a shear strength of $0.6F_u$ rather than $0.7F_u$ used in Eq. 3 for consistency with the block shear rupture equations (Carter et al. 1997; Kim and Yura 1999). The provisions also removed the discontinuity at $1.5d$ and made the check in terms of clear distance.

Current Provisions

The current provisions are based on the 1999 provisions. Section J3.10 of the AISC *Specification* (2016) governs bearing and tearout strength at bolt holes. The bearing strength of a bolt in a standard, oversize, or short-slotted hole is given by Eqs. 7 and 8 (J3-6a and J3-6b in the 2016 AISC *Specification*).

$$R_n = 2.4dtF_u \tag{7}$$

$$R_n = 3.0dtF_u \tag{8}$$

6

where, R_n is the nominal strength, d is the bolt diameter, t is the thickness of the connected material, and F_u is the ultimate tensile stress of the connected material.
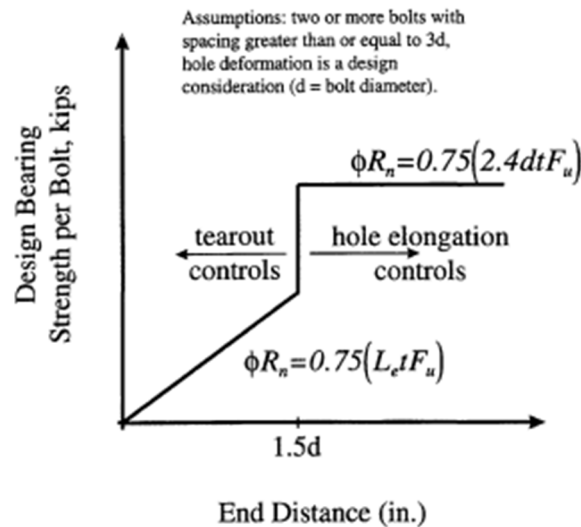
Figure 5: Bearing Strength per 1993 Specification Showing Discontinuity (Carter et al. 1997)

Eq. 7 is used when deformation at the bolt hole at service load is a design consideration, whereas Eq. 8 is used when deformation at the bolt hole at service load is not a design consideration. Significant bolt hole ovalization is expected to occur prior to reaching the full bearing strength of the connected material, which may limit the effectiveness of the connection. Frank and Yura (1981) identified 1/4 in. deformation as a practical limit to define a bearing strength which also prevents excessive ovalization.

The tearout strength of a bolt in a standard, oversize, or short-slotted hole is given by Eqs. 9 and 10 (J3-6c and J3-6d in the 2016 AISC *Specification*), where the distinction between Eqs. 9 and 10 is the same as that between Eqs. 7 and 8.

$$R_n = 1.2 l_c t F_u \tag{9}$$

$$R_n = 1.5 l_c t F_u \tag{10}$$

where, l_c is the clear distance, in the direction of force, between the edge of the hole and the edge of the adjacent hole or edge of the material.

With the revisions over time, there has come increasing recognition of potential for interaction between bolt shear rupture, bearing, and tearout in bolt groups. A user note and commentary have been included since the 2010 AISC *Specification* (AISC 2010) to indicate that the effective strength of a bearing-type fastener is equal to the minimum strength computed for the limit states of bolt shear rupture, bearing, and tearout, and that the strength of a bolt group is computed from the strength of the individual fasteners. Except for special cases, neither bolt shear rupture strength nor bearing strength will vary among the individual bolts in a group. Tearout will typically vary between the edge bolt and the interior bolts. The calculation is further complicated in eccentrically

loaded connections where the direction of loading for individual bolts, and consequently clear distance, is difficult to determine.

Objective and Scope of Research

This report describes a study undertaken to further investigate the behavior of and design provisions for steel bolted connections subject to the limit states of bearing and tearout. The study was divided into two phases. The first phase focused on concentrically loaded connections. The second phase focused on single-plate shear connections.

Specific objectives for the first phase were:

- Create a database of previous experimental tests with an emphasis on bearing and tearout limit states.

- Evaluate the accuracy of the current and alternative equations that include different tearout shear lengths and/or coefficients through analysis of the experimental database.

- Perform experimental testing to fill gaps in the existing research, particularly the use of different hole types.

- Evaluate the reliability of current and alternative equations.

- Consider simplifications to the design procedure, including alternative design methods.

- Develop recommendations for design based on the results.

Specific objectives for the second phase were:

- Create a database of previous experimental tests on eccentrically loaded connections, with an emphasis on single-plate shear connections.

- Perform experimental testing on single-plate shear connections, particularly with smaller edge distances.

- Evaluate the design procedures for single-plate shear connections

- Develop recommendations for design based on the results.

This report is arranged as follows. Chapter 2 discusses the experimental database that was created in order to evaluate general trends in experimental testing and as a source of data for analysis. Chapter 3 evaluates the existing experimental data. The accuracy of current and alternative equations was assessed using statistical analysis of the test-to-predicted ratios, among other considerations. Chapter 4 details the experimental testing of single-bolt concentrically loaded connections that investigate differing hole types and verify the results found in the previous analyses. Chapter 5 includes a reliability study using Monte Carlo simulations to evaluate the safety level of the current and alternative design equations. Chapter 6 introduces an alternative design approach that simplifies the design procedure through reduction factors on bearing and bolt shear rupture such that the tearout check can be precluded. Chapter 7 details the experimental testing of single-plate shear connections that investigate the effect of edge distance. Chapter 8 summarizes the work and presents recommendations for design.

Chapter 2: Literature Review

This literature review consists of three parts. The first part describes the creation of a database of previously published experimental tests on bolted connections. The second part includes a more qualitative review of some tests of interest, particularly those with eccentrically loaded bolt groups. The third part reviews the alternative tearout shear lengths that have been recently proposed.

Creation of Experimental Database

A database of experiments on steel bolted connections was developed as part of the literature review. Published papers and reports with relevant physical testing were collected, read, and categorized. Due to differing fields between test types, four datasets were created:

- concentrically loaded lap splice connections in tension
- concentrically loaded butt splice connections in tension
- eccentrically loaded bolt groups
- single-plate shear connections

Since the objectives of the research focus on the bearing and tearout limit states, papers and reports that describe tests that exhibited these failure modes were prioritized. However, other failures were present in the reviewed studies, mainly in the eccentrically loaded bolt groups and single-plate bolted shear connections. The number of specimens in each dataset is shown in Table 1.

Table 1: Specimen Count in the Database

Database Category	Number of Specimens	Number of Studies
Concentrically Loaded Lap Splice Connections	197	6
Concentrically Loaded Butt Splice Connections	702	14
Basic Eccentrically Loaded Bolt Groups	43	4
Single-Plate Bolted Shear Connections	42	7
Total	984	31

Criteria for Database

To be included in the database, each specimen must 1) have obtained bearing, tearout, bolt shear rupture, or other failure strength in a physical experiment; 2) be described in a published work (preferably a peer-reviewed journal publication); and 3) be capable of being accurately described by the fields in the database. Other types of tests that were outside the scope of this work included:

- Other connection types (e.g., welded connections and moment connections)
- Connections with stainless steel, thin gage cold-formed steel, or composite materials
- Connections tested at elevated temperatures

Some specimens which had conflicting data reporting of important values were also not included. Since the analyses of the concentrically loaded connection datasets was more rigorous and included calculating predicted strengths, these connections were subject to additional criteria, which are described in the next section.

Data entered for each specimen included general information, such as author of the reference and specimen name; qualitative data, such as the bolt tightness and observed failure mode; and quantitative data, such as plate thickness and material strengths. Data was entered in original units to facilitate validation. A MATLAB script was used to read the data and convert all values to consistent units and to prepare the data for the analysis performed in this work.

Concentrically Loaded Connections

The purpose of the concentrically loaded connection database was to provide a source of data to complete the analyses and to reveal any gaps in existing testing. Due to their relative simplicity, numerous concentrically loaded connections have been tested as compared to eccentrically loaded connections. Concentrically loaded specimens made up 92% of the reviewed tests. 20 of the 31 of the reviewed works contained concentrically loaded connections (899 specimens). The tests completed as part of this work were considered as well. The concentrically loaded connections were subdivided into lap splices and butt splices. A lap splice refers to a connection in which two plates are fastened with one or more bolts that are subject to a single shear plane. A butt splice refers to a connection containing two exterior plates and one interior plate fastened with one or more bolts that are subject to two shear planes. These differences justified the use of separate datasets to organize the information. Table 2 provides a summary of the experimental data sources.

Table 2: Summary of Experimental Data Sources

Reference	Connection Type	Number of Specimens Included in Database	Number of Specimens with Bearing, Tearout, or Splitting Failures
Gillett (1978)	Lap Splice	54	33
Frank and Yura (1981)	Butt Splice	16	6
Sarkar (1992)	Lap Splice	19	2
Karsu (1995)	Lap Splice	64	38
Kim and Yura (1999)	Lap Splice	41	41
Lewis and Zwerneman (1996)	Butt Splice	92	87
Udagawa and Yamada (1998)	Butt Splice	219	47
Puthli and Fleischer (2001)	Butt Splice	25	9
Rex and Easterling (2003)	Butt Splice	31	20
Udagawa and Yamada (2004)	Butt Splice	42	5
Freitas (2005)	Butt Splice	29	26
Brown et al. (2007)	Butt Splice	94	63
Cai and Driver (2008)	Butt Splice	44	23
Moze and Beg (2010)	Butt Splice	38	16
Moze and Beg (2011)	Butt Splice	24	14
Draganić et al. (2014)	Lap Splice	9	0
Moze and Beg (2014)	Butt Splice	19	8
Teh and Uz (2016)	Lap Splice	10	10
Wang et al. (2017)	Butt Splice	24	18
This Work	Butt Splice	5	5
		899	471

Additional Criteria

To be included in the concentrically loaded database, either the ultimate load, $R_{exp,u}$, or load at 1/4 in. deformation, $R_{exp,d}$, must have been recorded. For specimens where $R_{exp,d}$ was not specifically reported, but a plot of the load-deformation response of the connection was provided, the load at 1/4 in. deformation was interpolated from the plot. If the specimen reached its peak load prior to attaining 1/4 in. deformation, $R_{exp,d}$ was set equal to the ultimate load. Accordingly, $R_{exp,d}$ should be interpreted as a failure load at which peak strength is attained or the connection experiences 1/4 in. deformation, whichever occurs first. Additionally, material testing must have been conducted to determine the tensile strength, F_u, of the connected material in which failure occurred. Only specimens with standard holes were included in the database to provide consistency. A few specimens with slotted holes were identified and were evaluated separately.

Database Characteristics

In order to characterize the general trends in the tests, the variables of the datasets were plotted in histograms shown in Figure 6. The most commonly tested materials were A36 and SS400 steel, explaining the distribution of yield and ultimate strengths in Figure 6c and Figure 6d. However, various types of higher strength steels were prominent, including A572 Gr. 50, HQ590, and HQ780. Figure 6e shows that plate thickness was concentrated around 0.4 in. to 0.5 in. This concentration of plate thickness is mostly due to 219 specimens with 12 mm (0.472 in.) plates tested by Udagawa and Yamada (1998). The large majority of the specimens contained one or two bolts. Tested bolt diameters ranged from 5/8 in. to 1 in.

The bolts were untightened or there was a gap between the plates (termed loose plates) for about half of the specimens (485). Neither of these conditions satisfies the requirement in the AISC *Specification* (2016) that bolts be snug-tightened or pretensioned. Kim and Yura (1999) justified the use of loose plates in order to achieve a lower-bound strength of the connection that does not include frictional forces. While performing tests on loose connections isolates the contribution of bearing and provides a lower bound for strength, it is potentially overly conservative to base provisions on these results. The possible effects of bolt tightening on the strength of the connection will be described further in Chapter 3 and Chapter 4.

The figures demonstrate that a wide variety of conditions were tested in existing research. However, only 471 of the 899 concentrically loaded specimens failed in bearing, tearout, or the related splitting type failure. This limited the database size for analysis of these limit states.
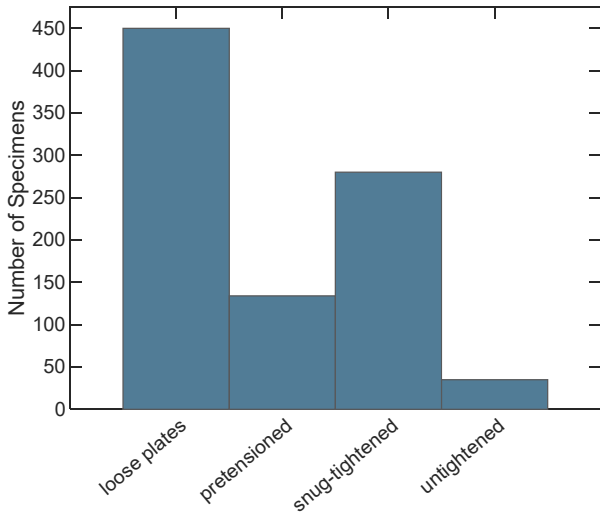
(a) Bolt tightness
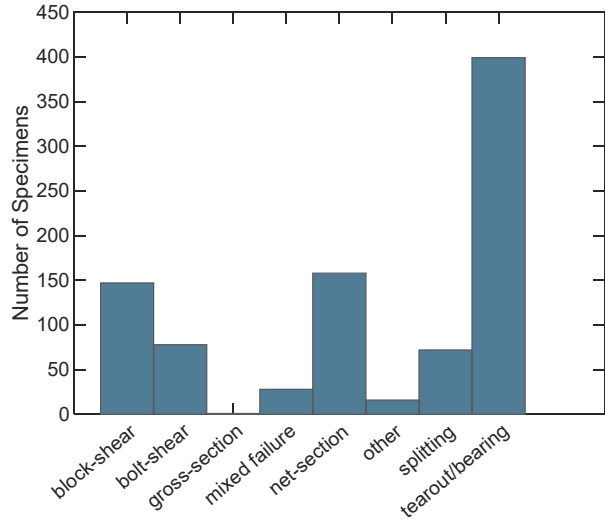
(b) Failure modes
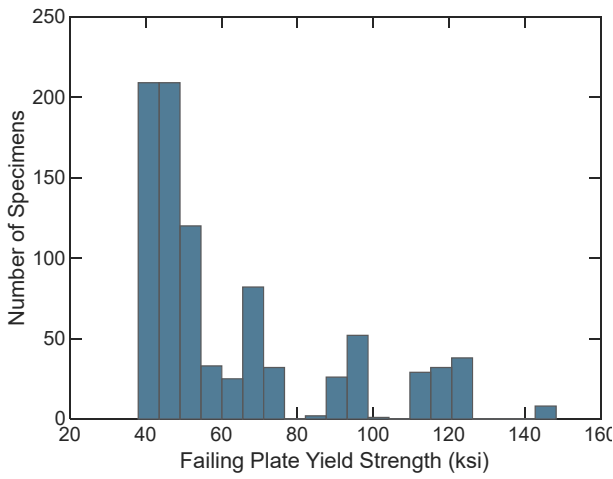
(c) Plate yield strength
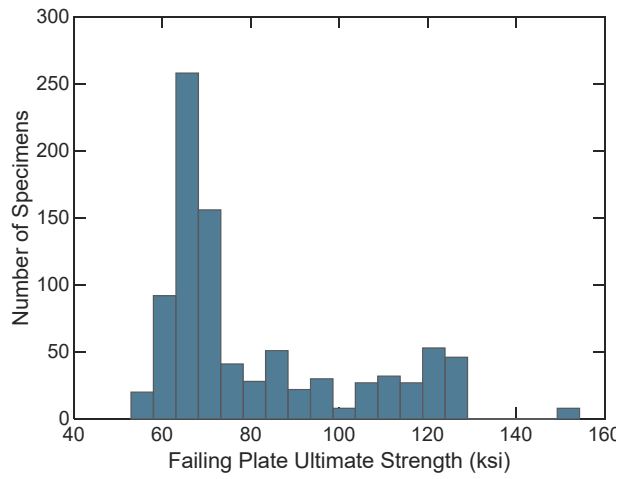
(d) Plate ultimate strength
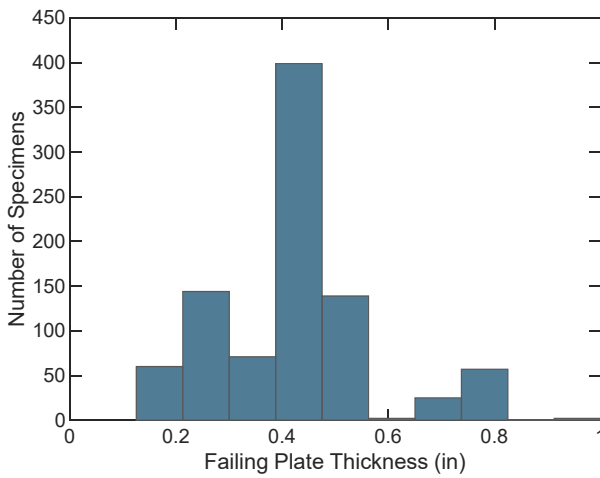
(e) Plate thickness
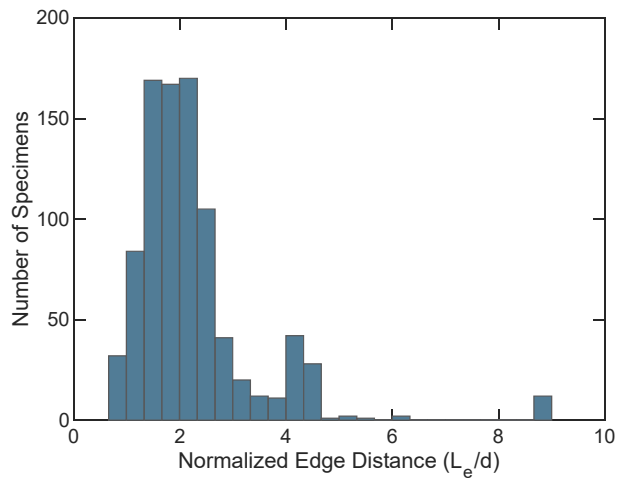
(f) Normalized edge distance

Figure 6: Number of specimens in database by property
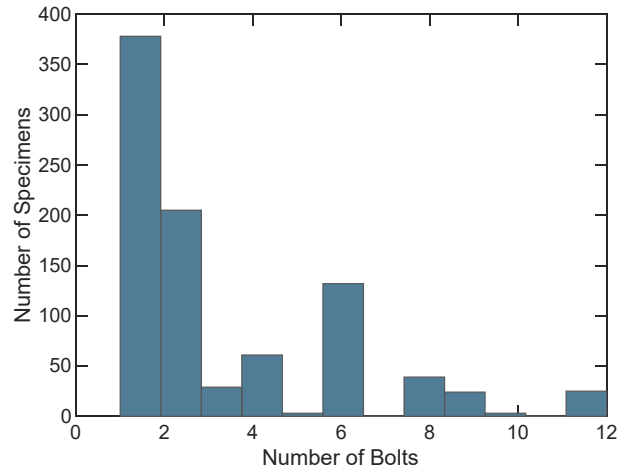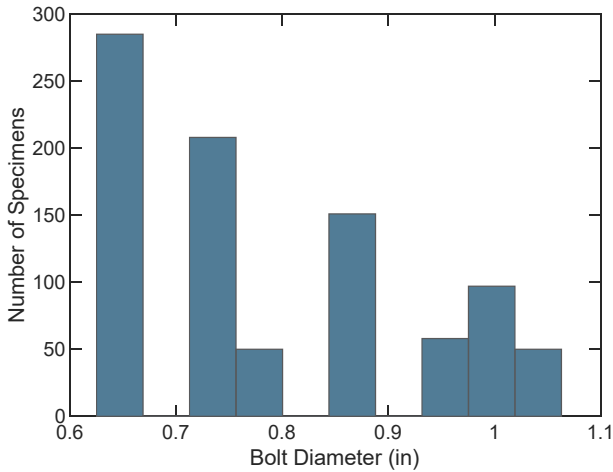
(g) Bolt diameter   (h) Number of bolts

Figure 6: Number of specimens in database by property (continued)

Eccentrically Loaded Connections

Experimental research on eccentrically loaded connections was also reviewed and included in the database. Several experimental testing methods exist for eccentrically loaded connections. The most direct method involves loading a bolted cantilevered plate at a certain distance from the support. The plate is directly subject to an eccentricity and rotation that must be accommodated by deformation of the bolt holes, bolts and plate. A more common procedure is to apply a load to a beam fastened to two columns with a plate or angle. A pinned column base and short beam is used such as to induce a rotation at the column base. The reaction force on the column is at a certain distance, or eccentricity, from the centroid of the bolt group. An example of this type of test is shown in Figure 7. Finally, the effects of eccentricity can also be tested in shear connections often used in structures. In which case, a longer span beam is loaded to induce a deflection of the beam and rotation at the connection. Although these tests are larger, they can simulate a common structural element. All these test methods can be completed with various connecting elements. The most commonly used are single plates bolted to the beam and welded to the supporting member, and all-bolted single or double angles.

Review of Database Specimens

Two datasets were created to organize the information. The first dataset is comprised of single-plate bolted shear connections. The other dataset consists of the basic eccentrically loaded bolted groups which do not include single-plate shear connections (i.e., using the first two methods described in the previous section). Specimens were required to meet the criteria for the database as described earlier. Additionally, in order to maintain comparison between reviewed specimens, the following were not included in the database:

- Single-plate shear connections that included stiffeners, slabs, or tabs

- Specimens subject to other loading such as compression

Other shear connections, such as single and double angle, were reviewed as well but not compiled in a database. Due to the variation of tests for eccentrically loaded connections, the literature was

13

reviewed for testing procedures, connection design, proposed analysis methods, and failure information that was relevant to the scope of this work.
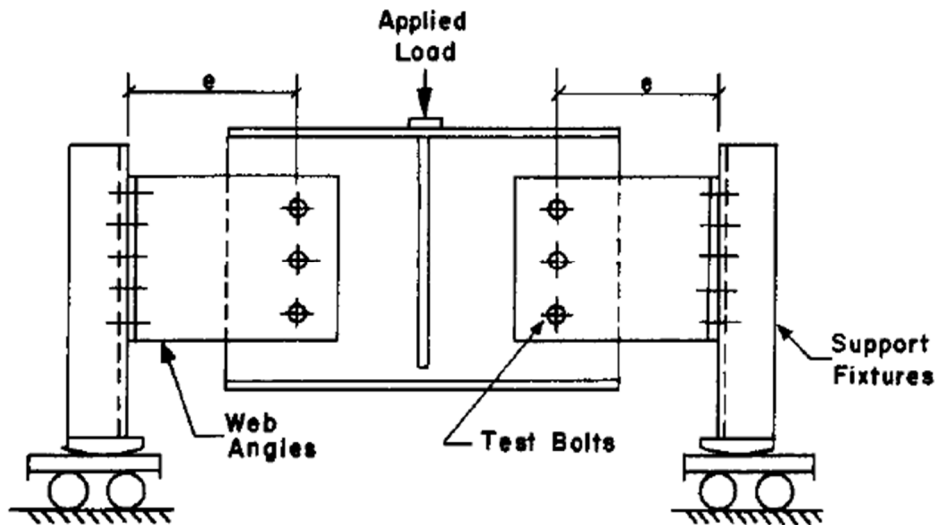
Figure 7: Eccentrically Loaded Shear Connection Set-Up (Crawford and Kulak 1971)

The studies included in the database of basic eccentrically loaded bolt groups are summarized in Table 3. The work by Crawford and Kulak (1971) included the development of the instantaneous center of rotation method. Wing and Harris (1983) and Badawi (1983) investigated bearing failures in eccentrically loaded connections. Both studies considered failure as a 0.3 in. deformation of the furthest bolt from the centroid. Although the edge distance value was not given, it is likely that the edge distance was sufficient to preclude tearout failure. Research by Nissen (2014) used several bolt lines and rows, resulting in block shearing and large deformations.

Table 3: Summary of Basic Eccentrically Loaded Bolt Groups

Author	Year	# of Tests	Testing Details	Thinnest Material	Eccentric.	Smallest Edge Dist.	Failure Modes
Crawford and Kulak	(1971)	8	Double Angles	0.50" A36	8" - 15"	Not Given	Bolt Shear
Badawi	(1983)	12	Double Angles	0.305" Gr.50	3.5" - 11.8"	Not Given	Bearing
Wing and Harris	(1983)	12	Double Angles	0.287" Gr.50	2.5" - 6.5"	Not Given	Bearing
Nissen	(2014)	11	Cantilevered Single Plate	0.394" S325	8" - 15.75"	2.66d (horiz.)	Block Shear

Note:
1. Bolts in Nissen 2014 are M12 Gr. 10.9. All other tests used 3/4" diameter A325

The studies included in the database of single-plate shear connections are summarized in Table 4. The table shows that the frequency of bearing and tearout in existing single-plate shear connection research is limited. Although bearing deformations were noticed in several of the tests, only one test by Sherman and Ghorbanpoor (2002) was described as a bearing failure. Tearout was not a failure in any of the single-plate shear connection tests investigated. The data suggests that tearout was precluded with use of center-to-edge distances of $2d$ and/or stronger plate material. The

specimens with smaller edge distances had a plate thickness of at least 3/8 in. No testing in these datasets used a plate thinner than 3/8 in. in combination with shorter edge distances, which would be more predisposed to a bearing or tearout failure. The only tests that tested the minimum edge distance were in Baldwin Metzger's research. However, the horizontal distance was set at $2d$.

Table 4: Summary of Single-Plate Shear Connections

Author	Year	# of Tests	Testing Details	Thinnest Material	Eccentric.	Smallest Edge Dist.	Failure Modes
Astaneh-Asl et al.	(1988)	5	Cantilever Beam	0.375" A36	2.75"	1.5d	Bolt Shear
Porter and Astaneh-Asl	(1990)	4	Cantilever Beam	0.375" A36	3.125"	1.5d	Bolt Shear
Sherman and Ghorbanpoor	(2002)	8	Simply Supported	0.371" A36	6.3" - 10"	2d	Other[3], Bearing
Creech	(2005)	8	Simply Supported	0.375" A36	3"	2d	Bolt Shear Beam Failure
Baldwin Metzger	(2006)	8	Simply Supported	0.39" Gr.50	3" - 10.5"	1.33d (vert.) 2d (horiz.)	Beam Failure, Bolt Shear
Marosi	(2011)	6	Cantilever Beam	0.247" Gr.50	2" - 4"	2d	Other[3]
Hertz	(2014)	3	Cantilever Beam	0.37" Gr.50	6" - 8"	2d	Other[3]

Notes:
1. Bolt holes are short-slotted in Porter and Astaneh-Asl (1990) and Sherman and Ghorbanpoor (2002)
2. Bolts in Marosi (2011) and Hertz (2014) range from 3/4" to 1" and 3/4" to 7/8" diameter A325, respectively. All other tests used 3/4" diameter A325
3. Other failures may include plate twisting, column failure, plate buckling, plate shear rupture, plate flexure, and weld fracture

Other failure modes, particularly plate failures, were more common with extended configurations in which the eccentricity to the center of the bolt group was greater than 3 in. This includes the extended configurations tested by Sherman and Ghorbanpoor (2002), Hertz (2014), and several of Marosi's (2011) specimens. Beam failures were also observed in some tests, due to insufficient lateral bracing and attempting to achieve target rotation of 0.03 radians.

Review of Single and Double Angle Bolted Connections

Birkemoe and Gilmor (1978) completed tests on a coped and uncoped double angle connection which demonstrated horizontal splitting type failures of the beam edge and large deformations. The beam was a W18x45 of grade 44W (44 ksi nominal yield stress) with a measured web thickness of 0.305 in. The edge distance from the center of bolt to edge of the beam web was 1-3/4 in. or 2.33d. Comparing to the single-plate shear connections in Table 4, the failing material was thinner but the edge distance was higher than most specimens. The test is most comparable to the ones completed by Badawi (1983) and Wing and Harris (1983), which failed with bearing deformation. The use of double angles may help preclude other failure modes of the plate and beam web, and isolate the failure to bearing, tearout, and bolt shear rupture.

Franchuk et al. (2002) investigated five single angle bolted connections with slotted holes and minimum edge distances for 1 in. and ¾ in. diameter bolts. The failing angles had a thickness of 1/4 in. with 350W steel material. Two of the tests failed in tearout of the bottom bolt combined with tilting of the middle bolt and out-of-plane movement of the angle, shown in Figure 8. The use of a thinner single angle caused the bending behavior of the angle; however, the use of minimum edge distances most likely resulted in the tearout failure.

(a) Test IV – Angle   (b) Test V – Angle
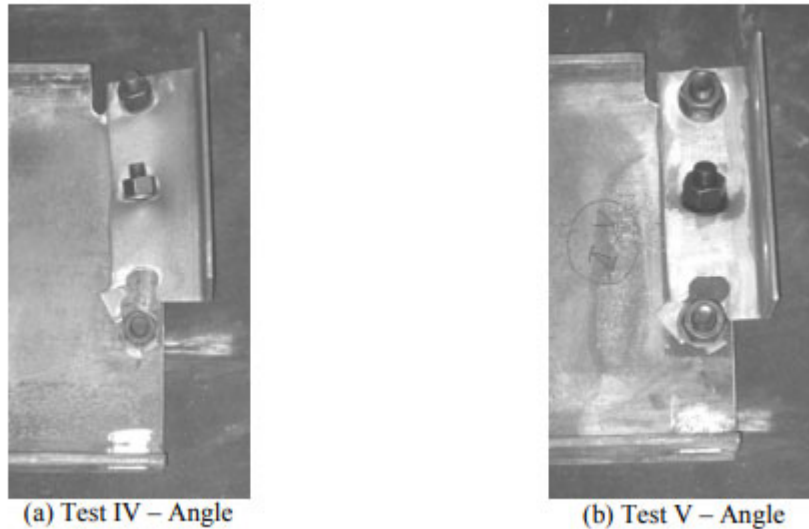
Figure 8: Tests by Franchuk et al. showing tearout of the bottom bolt and bolt tilting

Man et al. (2006) expanded on Franchuk's work of angle connections with slotted holes by testing numerous other conditions, including edge distance, use of plate washers, slot length, pretension, among others. Several specimens used the minimum edge distance of 32 mm (1.25 in.) for a 7/8 in. diameter bolt. Unlike Franchuk et al., Man et al. tested mostly 9.5 mm angle thicknesses (3/8 in.) of 300W steel grade. This is more pertinent to design since the AISC *Specification* (AISC 2016) suggests a minimum of 3/8 in. angle. The bolt tilting and angle bending observed in Franchuk et al. was not precluded with the use of the thicker angle. Nevertheless, tearout of the bottom edge was seen in the tests. The remaining tests by Man et al. demonstrated the potential of horizontal tearout of the beam web using edge distances slightly larger than the minimum, as was seen by Birkemoe and Gilmor.

Alternative Tearout Lengths

Under the current AISC *Specification* (AISC 2016), strength for the limit state of tearout is based on the clear distance, in the direction of force, between the edge of the bolt hole and the edge of the adjacent hole or edge of the material. This distance is denoted as l_c. For the case illustrated in Figure 9, the clear distance is computed as a function of the edge distance, L_e, and the diameter of the hole, d_h:

$$l_c = L_e - \frac{d_h}{2} \tag{11}$$

16

Examination of experimental results has shown that the length of failure planes from specimens that exhibited tearout are somewhat longer than the clear distance. Researchers have proposed various alternative lengths, that when used in lieu of l_c, provide a more accurate assessment of strength. The first alternative tearout length that is investigated in this work, denoted as l_{v1}, was proposed by Kamtekar (2012) and is equal to the clear distance, in the direction of force, between the edge of the bolt hole and the edge of the adjacent hole or edge of the material along lines tangent to the bolt. For the case illustrated in Figure 9, l_{v1} is computed as:

$$l_{v1} = L_e - \frac{\sqrt{d_h^2 - d^2}}{2} \tag{12}$$
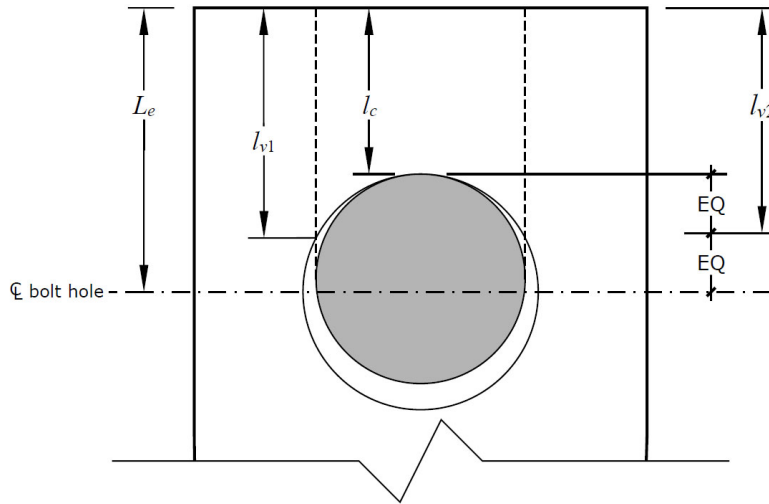
Figure 9: Tearout Length Comparison

The second alternative tearout length, denoted as l_{v2}, was proposed by Clements and Teh (2013) and is equal to the average of the clear distance, l_c, and the edge distance, L_e. For the case illustrated in Figure 9, this is computed as:

$$l_{v2} = L_e - \frac{d_h}{4} \tag{13}$$

Elliot et al. (2019) evaluated the use of l_{v1} and l_{v2} in strength equations for a small set of experiments that failed in tearout. They found them both to provide similarly improved predictions of tearout strength in comparison to current equations. They also evaluated alternative net areas for block shear rupture that are similar in concept to the alternative tearout lengths.

Other tearout lengths have been proposed (e.g., Duerr 2006). However, differences among the lengths are slight. Also, some are more complicated than l_{v1} and l_{v2} to compute for general bolted connections. Therefore, this work focuses on evaluating l_c, l_{v1}, and l_{v2}.

Chapter 3: Evaluation of Published Concentrically Loaded Experiments

Hundreds of physical experimental tests on concentrically loaded bolted connections susceptible to tearout have been performed in past research. This data has been collected and organized into a database for the purpose of evaluating alternative tearout lengths. Only connections categorized as failing in bearing, tearout, or splitting were utilized in this analysis. The limit state of splitting is distinct from the limit state of tearout. Equations have been proposed to predict splitting strength (Duerr 2006) and some standards treat tearout and splitting separately (e.g., ASME 2017). However, splitting is not recognized within the AISC *Specification* (AISC 2016). Therefore, equations for the limit state of tearout are implicitly covering splitting as well. This approach is justified since experimental results have shown the two limit states to have similar strengths and splitting failures are typically included in the evaluation of the tearout equations, as is done in this work. Of the 899 specimens in the concentrically loaded database, 471 failed in bearing, tearout, or splitting, as documented in Table 2. The remaining specimens experienced other failure modes including bolt shear rupture, tensile yielding, tensile rupture, and curling.

Strength of Single-Bolt Specimens

Specimens with a single bolt in the direction of force allow for a direct evaluation of individual limit states. These specimens are evaluated separately from specimens with multiple bolts in the direction of force which may experience multiple limit states (e.g., bearing and tearout). Of the 471 specimens in the database with bearing, tearout, or splitting failures, 313 contained a single bolt in the direction of force. Of these single-bolt specimens, $R_{exp,d}$ was available for 223, $R_{exp,u}$ was available for 301, and both loads were available for 211 of the specimens. The analysis included 265 specimens with one bolt perpendicular to the line of force and 48 with two bolts perpendicular to the line of force. These specimens include many that do not meet the minimum edge distances of Table J3.4 in the AISC *Specification* (AISC 2016). Additionally, not all specimens met the Specification requirement for bolt installation (i.e., installed to a snug-tight condition or pretensioned).

Experimentally obtained strengths are compared to strengths computed from various instances of a generic bearing and tearout strength equation given by Eq. (14).

$$R_n = C_t l_x t F_u \leq C_b d t F_u \tag{14}$$

where, C_t is the coefficient applied to the tearout strength, l_x is the length used for determining tearout strength (i.e., either l_c, l_{v1}, or l_{v2}), and C_b is the coefficient applied to the bearing strength.

The test-to-predicted ratio (TTP) for each specimen is computed as the ratio of the experimentally obtained strength to the strength from Eq. (14) for various selections of C_t, l_x, and, C_b. The mean and coefficient of variation (COV) of the test-to-predicted ratio across the specimens is presented in Table 5 for comparisons to the load at 1/4 in. deformation and Table 6 for comparisons to the ultimate load.

Two values of the mean and COV are presented. The value outside the parentheses includes data from specimens that did not meet the minimum edge distances of Table J3.4 in the AISC *Specification* (AISC 2016). The value inside the parentheses excludes specimens that did not meet the minimum edge distances. Note that Table J3.4 has a footnote that permits lesser edge distances, this footnote was not considered in this work.

Table 5: Test-to-Predicted Ratio Statistics for Various Evaluations of the Load at 1/4 in. Deformation for Single-Bolt Specimens (data from 223 specimens, data from 192 specimens meeting minimum edge distance requirements in parentheses)

	C_t	l_x	C_b	Mean TTP	COV TTP
Current Equations	1.2	l_c	2.4	1.223 (1.180)	0.186 (0.172)
Current Coefficients	1.2	l_{v1}	2.4	0.952 (0.953)	0.137 (0.144)
Current Coefficients	1.2	l_{v2}	2.4	0.992 (0.988)	0.140 (0.147)
Optimized Coefficients	1.63	l_c	2.29	0.957 (0.934)	0.153 (0.144)
Optimized Coefficients	1.17	l_{v1}	2.36	0.975 (0.976)	0.137 (0.144)
Optimized Coefficients	1.23	l_{v2}	2.36	0.975 (0.972)	0.137 (0.144)

Table 6: Test-to-Predicted Ratio Statistics for Various Evaluations of Ultimate Load for Single-Bolt Specimens (data from 301 specimens, data from 234 specimens meeting minimum edge distance requirements in parentheses)

	C_t	l_x	C_b	Mean TTP	COV TTP
Current Equations	1.5	l_c	3	1.065 (1.003)	0.192 (0.140)
Current Coefficients	1.5	l_{v1}	3	0.804 (0.812)	0.139 (0.151)
Current Coefficients	1.5	l_{v2}	3	0.841 (0.842)	0.133 (0.144)
Optimized Coefficients	1.65	l_c	2.95	0.978 (0.921)	0.189 (0.145)
Optimized Coefficients	1.16	l_{v1}	3.21	1.009 (1.010)	0.117 (0.128)
Optimized Coefficients	1.22	l_{v2}	3.23	1.010 (1.005)	0.120 (0.129)
Rounded Coefficients	1.2	l_{v1}	3	0.981 (0.984)	0.119 (0.130)
Rounded Coefficients	1.2	l_{v2}	3	1.030 (1.025)	0.120 (0.129)

The data is also presented in Figure 10 and Figure 11, where the experimentally obtained strength is normalized against the value of dtF_u and plotted against normalized edge distance. Where the specimen included multiple bolts perpendicular to the direction of load, the experimental strengths were divided by the number of bolts in the connection, n, for plotting purposes.

Optimized coefficients are among the instances of Eq. 14 that are compared in Table 5, Table 6, Figure 10, and Figure 11 . Six sets of optimized coefficients were computed, one for each of the three tearout lengths (i.e., l_c, l_{v1}, and l_{v2}) at the ultimate and 1/4 in. deformation levels. The coefficients were obtained using a numerical optimization to minimize the sum of the square of the difference between the test-to-predicted ratio and unity over all specimens. Single-bolt and multiple-bolt specimens were included in the optimization.
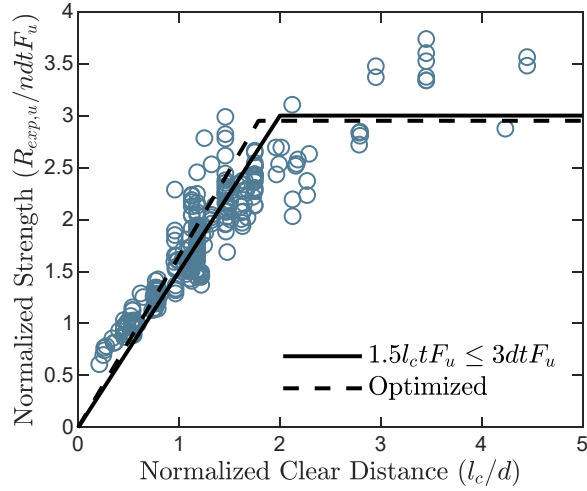
(a) Ultimate Load, l_c
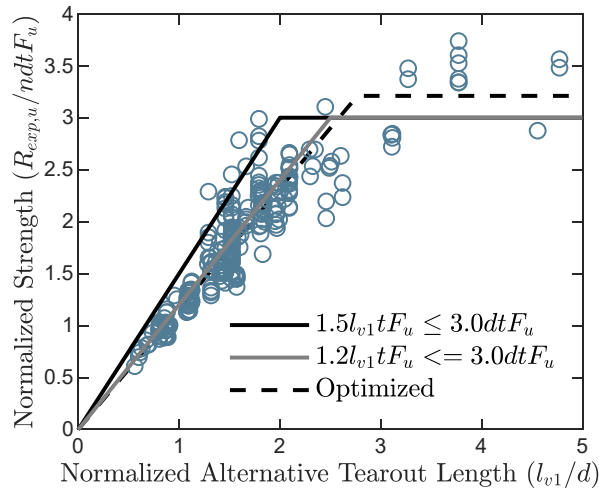
(b) Ultimate Load, l_{v1}
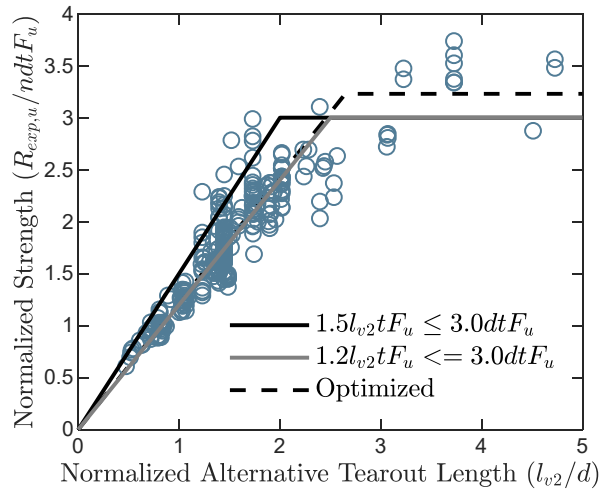
(c) Ultimate Load, l_{v2}

Figure 10: Normalized Strength Comparisons Between Tearout Lengths for Ultimate Load
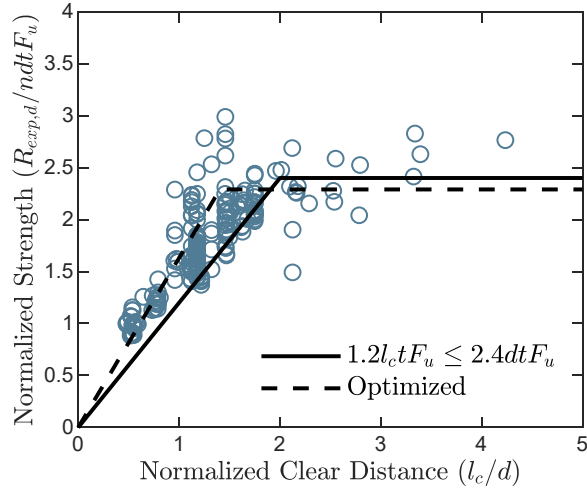
(a) Load at 1/4 in. Deformation, l_c
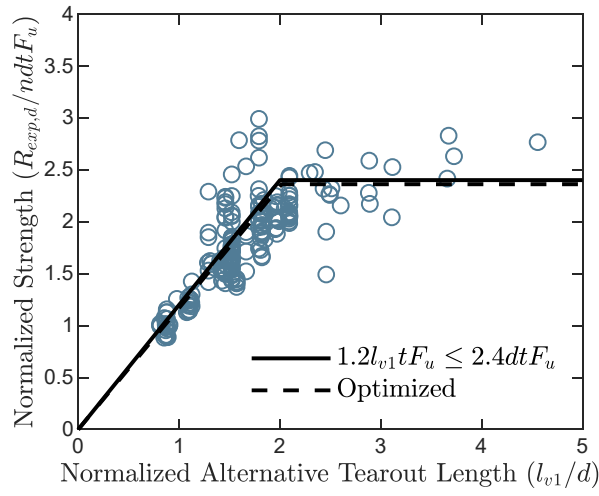
(b) Load at 1/4 in. Deformation, l_{v1}
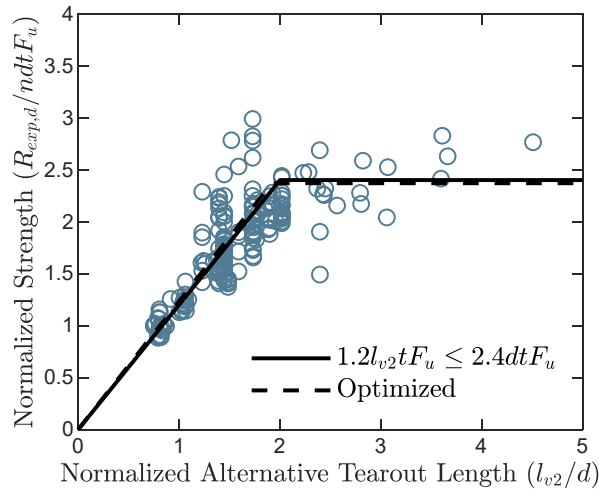
(c) Load at 1/4 in. Deformation, l_{v2}

Figure 11: Normalized Strength Comparisons Between Tearout Lengths for Ultimate Load

The mean test-to-predicted ratio for the current equations is 1.223 for single-bolt specimens and 1.180 for single-bolt specimens meeting minimum edge distance requirements (Table 5), indicating that current provisions for bearing and tearout are conservative in predicting the load at 1/4 in. deformation. This is also seen in Figure 11 (b) where most experimental data are above the line representative of current design equations. This is especially true for specimens with smaller edge distances. Either of the two alternative tearout lengths (i.e., l_{v1} or l_{v2}) provides a more accurate and precise assessment of strength when using the current coefficients as seen in both a mean value of the test-to-predicted ratio that is closer to unity and a COV of the test-to-predicted ratio that is lower than for the current equations. However, the use of l_{v1} with current coefficients somewhat overestimates the strength. Results with the optimized coefficients indicate that current coefficients are generally appropriate for use with l_{v1} or l_{v2}.

Similar trends are seen when comparing to the ultimate load (Table 6). A key difference is that the current coefficients with the alternative tearout lengths result in a significant overestimation of strength. Rather, a coefficient of 1.2, the same as is used in the equations for load at the 1/4 in. deformation limit state, can provide an accurate prediction of strength with less variation than the current equation.

These results suggest that the difference between the load at 1/4 in. deformation and the ultimate load is far smaller than implied by current provisions. Figure 12 shows the ratio $R_{exp,u}/R_{exp,d}$ for single-bolt specimens plotted against the normalized clear distance. The ratio of ultimate load to load at 1/4 in. deformation is 1.25 according to the current AISC *Specification* (AISC 2016) (i.e., the ratio between Eq. 9 and Eq. 10 equals 1.25). However, the experimental ratios are lower, especially for cases with smaller edge distances. The average ratio of the 211 specimens plotted is 1.05 and only 6 of the specimens have a ratio greater than 1.25.
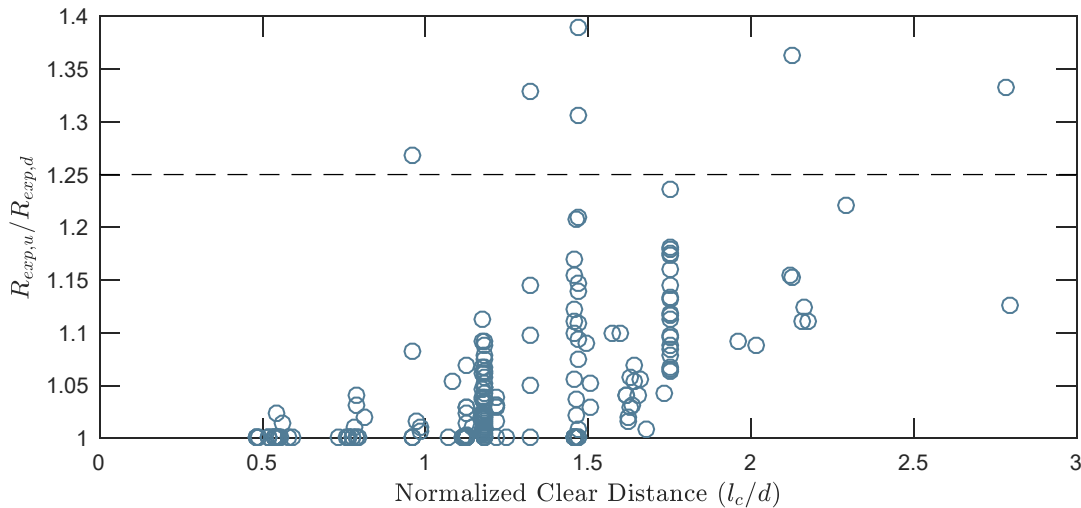
Figure 12: Ratio of Ultimate Load and 1/4 in. Deformation versus Normalized Clear Distance

Strength of Multiple-Bolt Specimens

Of the 471 specimens in the database with bearing, tearout, or splitting failures, 158 have more than one bolt in the direction of force. Of these multiple-bolt specimens, $R_{exp,d}$ was available for 100, $R_{exp,u}$ was available for 136, and both loads were available for 78 of the specimens.

Table 7 and Table 8 provide summary statistics for the test-to-predicted ratios computed using the various instances of Eq. 14 for multiple-bolt specimens. The values of the COV are approximately the same as those for the single-bolt cases, indicating a good fit of the data. At the ultimate load, when including all specimens, and with rounded coefficients, the mean test-to-predicted ratio is 0.927 for l_{v1} and 0.954 for l_{v2}. These values are lower than that for the single-bolt case and lower than is generally acceptable. A possible reason for this is deformation compatibility between bolts. Achieving the full bearing strength of $3.0dtF_u$ requires significant deformation. It is possible, for example, that by the time the full bearing strength of the interior bolts is achieved, the end bolts have passed their peak strength and contribute only a lower post-peak strength. Nonetheless, when specimens not meeting minimum edge distance and spacing requirements are excluded, the mean test-to-predicted ratios are slightly above unity.

Table 7: Test-to-Predicted Ratio Statistics for Various Evaluations of the Load at 1/4 in. Deformation for Multiple-Bolt Specimens (data from 100 specimens, data from 62 specimens meeting minimum edge distance and spacing requirements in parentheses)

	C_t	l_x	C_b	Mean TTP	COV TTP
Current Equations	1.2	l_c	2.4	1.137 (1.106)	0.155 (0.159)
Current Coefficients	1.2	l_{v1}	2.4	0.973 (1.013)	0.127 (0.126)
Current Coefficients	1.2	l_{v2}	2.4	0.992 (1.024)	0.122 (0.127)
Optimized Coefficients	1.63	l_c	2.29	1.032 (1.048)	0.122 (0.129)
Optimized Coefficients	1.17	l_{v1}	2.36	0.992 (1.033)	0.126 (0.126)
Optimized Coefficients	1.23	l_{v2}	2.37	0.995 (1.032)	0.125 (0.127)

Table 8: Test-to-Predicted Ratio Statistics for Various Evaluations of Ultimate Load for Multiple-Bolt Specimens (data from 136 specimens, data from 48 specimens meeting minimum edge distance and spacing requirements in parentheses)

	C_t	l_x	C_b	Mean TTP	COV TTP
Current Equations	1.5	l_c	3	1.011 (1.047)	0.140 (0.172)
Current Coefficients	1.5	l_{v1}	3	0.812 (0.951)	0.188 (0.178)
Current Coefficients	1.5	l_{v2}	3	0.829 (0.961)	0.182 (0.178)
Optimized Coefficients	1.65	l_c	2.95	0.958 (1.029)	0.148 (0.179)
Optimized Coefficients	1.16	l_{v1}	3.21	0.937 (1.003)	0.138 (0.164)
Optimized Coefficients	1.22	l_{v2}	3.23	0.928 (1.000)	0.140 (0.166)
Rounded Coefficients	1.2	l_{v1}	3	0.927 (1.015)	0.145 (0.168)
Rounded Coefficients	1.2	l_{v2}	3	0.954 (1.038)	0.144 (0.168)

Previous editions of the AISC *Specification* included exceptions to tearout provisions when enough bolts were in a line and certain geometric conditions were met. It was theorized that if the interior bolts fail in bearing, the tearout strength of the end bolt would be less critical. To investigate the effect of neglecting tearout, a test-to-predicted ratio equal to the load at 1/4 in. deformation divided by the bearing strength (the result of Eq. 7 times the number of bolts in the connection) is plotted against the normalized clear distance in Figure 13. Only specimens meeting the minimum edge distance and minimum spacing requirements of the current AISC *Specification* (AISC 2016) are plotted. Specimens that meet the criteria for the tearout exception in the 1993

edition of the *Specification* (AISC 1993) (i.e., two or more bolts in a line, edge distance greater than 1.5*d*, and spacing greater than 3*d*) are differentiated with circular markers. The figure shows significant variation; however, many of the specimens have low test-to-predicted ratios, including several that meet the criteria in the 1993 *Specification*. The effect of the exception to the tearout provisions on reliability is investigated in Chapter 5 (e.g., Figure 19b). The effect of the exception on strength is briefly investigated here. The nominal strength of connections for which it was permitted to neglect tearout can be as much as approximately 20% greater when neglecting tearout than when considering tearout using Eq. 15. This maximum difference is for connections with two bolts in the line of force. The maximum difference reduces to approximately 13% for three bolts in the line of force, approximately 9% for four bolts in the line of force, and approximately 7% for five bolts in the line of force.

To summarize, increased accuracy in predicting tearout strength was achieved using either l_{v1} or l_{v2} with a coefficient on the tearout strength of 1.2. This was shown to be true for both the ultimate load and the load at 1/4 in. deformation. Based on these initial results, the remaining analyses are conducted with the following equations for tearout strength:

$$R_n = 1.2 l_{v1} t F_u \tag{15}$$

$$R_n = 1.2 l_{v2} t F_u \tag{16}$$
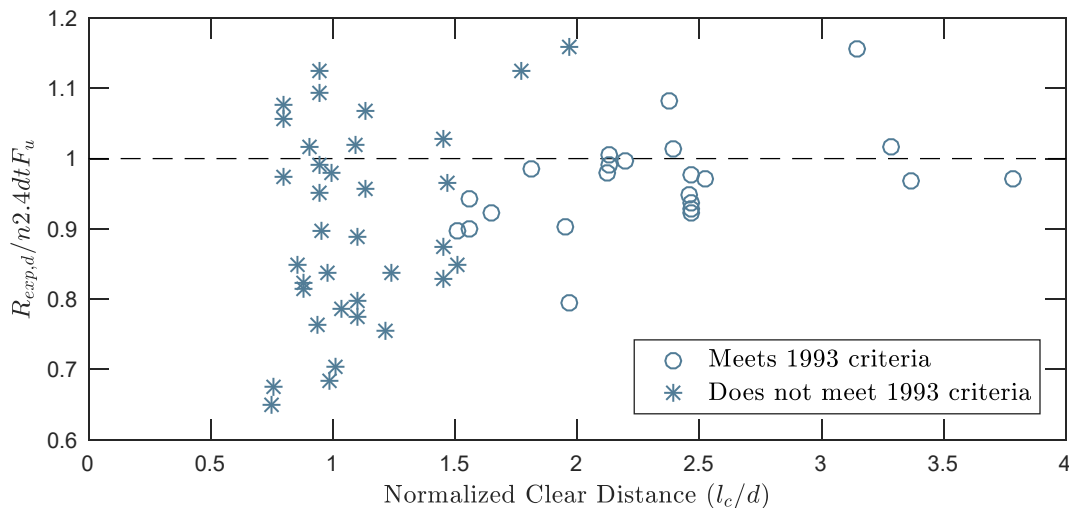
Figure 13: Test-to-Predicted Ratio Excluding Tearout versus Normalized Clear Distance

Effects of Bolt Tightening

The AISC *Specification* (AISC 2016) requires that bolts be installed to a snug-tight condition or pretensioned. Many of the experiments in the database utilize untightened bolts or had a gap between the plates. These loose connections do not satisfy the requirements of the AISC *Specification*, but help minimize the contribution of friction to the strength of the connection and better evaluate the strength of the connected material alone.

Frank and Yura (1981) tested connections with different levels of tightening, although loose connections were not considered. They found that specimens with pretensioned bolts had 10%

higher strength at 1/4 in. deformation when compared to snug-tightened bolts but that the ultimate strength was unaffected by the level of tightening.

Table 9 presents a comparison of experimental strength to strength equations from the current AISC *Specification* (AISC 2016) for all 471 specimens in the database that failed in bearing, tearout, or splitting. No clearly identifiable trend is seen in the mean test-to-predicted ratios at ultimate load. However, as observed by Frank and Yura (1981), the mean test-to-predicted ratios for the load at 1/4 in. deformation tend to increase as the level of tightening increases.

Table 9: Mean values of test-to-predicted ratios based on level of tightening

Load Level	Pretensioned	Snug-Tightened	Untightened/Loose
Ultimate	1.049	1.023	1.067
1/4 in. Deformation	1.246	1.197	1.157

Mixed Failures

Several multiple-bolt specimens tested by Cai and Driver (2008) exhibited mixed failures of bearing or tearout of the end bolts and shear rupture of the interior bolts. This mode of failure is a validation of the premise underlying the use of effective strengths of individual bolts when computing the strength of a bolt group. These specimens were not included in the preceding discussion because they exhibited mixed failures. However, they are examined here to validate the use of the alternative tearout lengths for connections where a mixed failure may occur.

The connected material in which the failures occurred was the web of a wide flange with a measured thickness of 0.36 in. and a measured tensile strength of 74.11 ksi. The connections each had six 3/4 in. diameter bolts (two lines of three) in standard holes. The shear strength of the bolts was measured to be 50.13 kips. Most of these specimens reached their ultimate strength prior to reaching 1/4 in. deformation, so only ultimate load was considered. Table 10 summarizes the specimens along with test-to-predicted ratios calculated using different computed strengths.

The test-to-predicted ratios presented in Table 10 were calculated with tearout strength given by the current equation (i.e., Eq. 10) as well as equations with the alternative tearout lengths (i.e., Eqs. (15) and (16)). Also included in Table 10 are test-to-predicted ratios computed with the predicted strength taken as the lower of the strengths for the bolt group for 1) the limit states of bearing and tearout and 2) the limit state of bolt shear rupture.

The results of these specimens show that it is indeed unconservative to treat bearing and tearout separate from bolt shear rupture, given that doing so results in a 10% overprediction of strength on average. Using this method, specimens C1E1a, C2E1b, and C3E1c were controlled by bearing and tearout strength and the rest were controlled by bolt shear rupture strength. More accurate but still somewhat unconservative results are obtained when considering the potential of mixed failures and summing the effective strengths of each individual bolt to obtain the strength of the bolt group. Little difference is seen between the use of the clear distance and either of the two alternative tearout lengths, all three result in a 4 to 5% overprediction of strength on average. The remaining error may be due to different bolts achieving their peak strength at different levels of deformation, which is not accounted for in the design equations. Further investigation on

deformation compatibility in bolted connections which experience mixed failure is warranted, however, the observed error is small and can be accommodated in the margin of safety.

Table 10: Analysis of specimens tested by Cai and Driver (2008) that exhibited mixed failures

Specimen	L_e (kips)	$R_{exp,u}$ (kips)	Test-to-predicted ratio			
			Using l_c Eq. 10[a]	Using l_c Eq. 10	Using l_{v1} Eq. (15)	Using l_{v2} Eq. (16)
C1E1a	1.00	243.27	0.850	0.981	0.955	0.968
C2E1b	1.00	249.94	0.866	1.005	0.978	0.992
C3E1c	1.00	250.17	0.868	1.007	0.981	0.993
C4E2a	1.25	279.80	0.930	1.044	1.035	1.047
C5E2b	1.26	267.61	0.890	0.993	0.984	0.996
C6E2c	1.26	259.05	0.861	0.965	0.955	0.968
C7E3a	1.50	272.40	0.906	0.946	0.950	0.962
C8E3b	1.50	259.74	0.864	0.903	0.908	0.917
C9E3c	1.51	273.21	0.908	0.947	0.952	0.962
C10E4a	1.76	273.14	0.908	0.908	0.908	0.912
C11E4b	1.75	280.81	0.934	0.934	0.934	0.937
C12E4c	1.75	265.90	0.884	0.884	0.884	0.887
C13E5a	2.00	290.70	0.966	0.966	0.966	0.966
C14E5b	2.00	267.03	0.888	0.888	0.888	0.888
C15E5c	2.01	287.71	0.957	0.957	0.957	0.957
C16E6	2.76	297.49	0.989	0.989	0.989	0.989
		Mean:	0.904	0.957	0.952	0.959

[a] The predicted strengths for these test-to-predicted ratios were computed without considering potential interaction between the limit states of bearing and tearout and the limit state of shear rupture of the bolt.

Chapter 4: Single-Bolt Experiments

The evaluation of published experiments showed that tearout equations using l_{v1} and l_{v2} had similarly improved results in comparison to the current equations. The database contains results from hundreds of experiments across a broad range of parameters. However, it only contains specimens with standard holes because the vast majority of concentrically loaded steel bolted connection tests failing in bearing, tearout, or splitting were performed with standard holes.

For connections with standard holes, l_{v1} is greater than l_{v2}. The difference between the two varies only slightly based on the diameter of the bolt; differing by a maximum of 7% for connections that satisfy minimum edge distance requirements and bolts as large as 1.5 in. diameter. The variation is greater, although still relatively small, over a range of hole types. To address this gap in data, a series of experimental tests was conducted to evaluate tearout strength for connections with different hole types.

Test Matrix

Tension tests of 22 single-bolt butt splice connections with different hole types and edge distances were completed. The specimens consisted of two outer pull plates and a single interior test plate as shown in Figure 14. Specimens were designed to fail in either bearing, tearout, or splitting of the test plate. Specimens included those with standard holes and holes with minimal clearance, where the value of l_{v1} is greater than l_{v2}. Also included were specimens with oversize holes, holes with 1/8 in. more clearance than oversize holes, and short-slotted holes oriented perpendicular to the load, where the value of l_{v2} is greater than l_{v1}.

The test matrix is presented in Table 11. Two main variables are considered: the type of bolt hole and the edge distance. Four edge distances were investigated for each of the five bolt hole types. Nominal values of the edge distances were: 1 in., 1.25 in., 1.5 in., and 2 in. The smallest edge distance (1 in.) is equal to the minimum edge distance permitted by the AISC *Specification* (AISC 2016) for a 3/4 in. bolt in a standard hole. Note that the 1 in. edge distance is not permitted for oversize holes but was used in these tests for consistency. For a 3/4 in. bolt in a standard hole, the transition between tearout and bearing occurs at an edge distance of 1.91 in. per current equations. The largest edge distance (2.0 in.) was selected to be somewhat greater than this length and thus provide a comparison to a bearing-controlled failure. Two additional tests beyond the main set of 20 were also completed. Specimen NC2b was a duplicate of NC2a to investigate repeatability. Specimen STD1g was a duplicate of STD1, but with the test bolt untightened (instead of in a snug-tight condition) and greased plates to investigate the effect of reduced friction.

Materials and Test Setup

The test plates were 1/4 in. thick ASTM A572 Gr. 50 steel and had a yield strength of 54.5 ksi and a tensile strength of 73.7 ksi, based on the mean of three tensile coupon tests conducted in accordance with ASTM E8 (2016). No special preparation was made to the plate surfaces before testing with the exception of specimen STD1g, where grease was applied to the faying surfaces. The test plates were installed in a universal testing machine and subjected to concentric tension load.

Table 11: Experimental Testing Summary

Name	Hole Type	Measured Properties						At 1/4" Deformation				At Ultimate			
		L_e	l_c	l_{v1}	l_{v2}	l_{v1}/l_{v2}	d_h	$R_{exp,d}$	TTP using l_c (Eq. 9)	TTP using l_{v1} (Eq. 15)	TTP using l_{v2} (Eq. 16)	$R_{exp,u}$	TTP using l_c (Eq. 9)	TTP using l_{v1} (Eq. 15)	TTP using l_{v2} (Eq. 16)
---	---	in	in	in	in	---	in	kips	---	---	---	kips	---	---	---
STD1	Standard	1.02	0.615	0.861	0.818	1.052	0.812	19.9*	1.451	1.036	1.091	19.9	1.160	1.036	1.091
STD1g[1]	Standard	0.99	0.578	0.818	0.784	1.044	0.823	17.6	1.359	0.960	1.002	17.8	1.098	0.970	1.012
STD2	Standard	1.16	0.750	0.992	0.954	1.039	0.817	22.9*	1.378	1.042	1.083	22.9	1.103	1.042	1.083
STD3	Standard	1.56	1.157	1.403	1.361	1.031	0.815	31.4*	1.217	1.003	1.034	31.4	0.973	1.003	1.034
STD4	Standard	2.01	1.605	1.846	1.810	1.020	0.818	37.9	1.128	0.912	0.930	43.8	1.042	1.053	1.074
NC1	No Clearance	1.03	0.650	0.983	0.838	1.173	0.753	20.7*	1.412	0.933	1.095	20.7	1.129	0.933	1.095
NC2a	No Clearance	1.32	0.945	1.278	1.133	1.128	0.752	28.9	1.366	1.010	1.139	29.0	1.097	1.014	1.144
NC2b[2]	No Clearance	1.27	0.901	1.240	1.087	1.140	0.744	26.4	1.291	0.939	1.070	27.4	1.070	0.972	1.108
NC3	No Clearance	1.56	1.185	1.527	1.373	1.112	0.752	33.2	1.248	0.969	1.078	34.0	1.021	0.990	1.101
NC4	No Clearance	2.03	1.661	2.015	1.848	1.091	0.747	41.0	1.218	0.974	0.983	42.4	1.009	1.009	1.019
OVS1	Oversize	1.05	0.584	0.769	0.819	0.940	0.938	20.0	1.537	1.167	1.097	20.3	1.246	1.182	1.111
OVS2	Oversize	1.28	0.813	1.000	1.045	0.957	0.928	24.0	1.298	1.055	1.010	24.4	1.053	1.070	1.024
OVS3	Oversize	1.54	1.079	1.266	1.311	0.965	0.929	29.8	1.223	1.042	1.006	31.0	1.018	1.084	1.047
OVS4	Oversize	2.05	1.590	1.781	1.821	0.978	0.923	36.7	1.088	0.914	0.894	42.0	0.995	1.045	1.022
XOVS1	Extra Oversize	0.96	0.427	0.580	0.693	0.838	1.062	14.1*	1.487	1.094	0.917	14.1	1.189	1.094	0.917
XOVS2	Extra Oversize	1.29	0.766	0.920	1.030	0.893	1.056	23.3	1.360	1.132	1.012	24.2	1.131	1.177	1.051
XOVS3	Extra Oversize	1.51	0.983	1.138	1.247	0.913	1.054	26.2	1.198	1.035	0.945	27.1	0.992	1.071	0.977
XOVS4	Extra Oversize	2.04	1.506	1.661	1.771	0.938	1.058	34.7	1.042	0.938	0.880	36.8	0.885	0.996	0.935
SSLT1	Short Slot	1.02	0.616	0.730	0.819	0.891	0.812×0.994	18.1*	1.316	1.110	0.990	18.1	1.053	1.110	0.990
SSLT2	Short Slot	1.31	0.900	1.015	1.104	0.919	0.816×0.997	21.4	1.096	0.974	0.893	21.8	0.894	0.992	0.911
SSLT3	Short Slot	1.56	1.151	1.267	1.353	0.936	0.809×0.990	29.1	1.141	1.038	0.971	29.2	0.917	1.042	0.974
SSLT4	Short Slot	2.10	1.700	1.814	1.901	0.954	0.803×0.992	35.0	1.041	0.858	0.833	40.7	0.971	1.000	0.971

* Ultimate load reached prior to 1/4 in. deformation
1. Duplicate test but bolt was left untightened and plates were greased
2. Duplicate test to verify repeatability

Two linear variable differential transformers (LVDTs) were installed on the test specimen to record movement of the pull plate relative to the test plate over a 4 in. gauge length. The LVDTs recorded the bolt hole deformation as well as elastic deformations of the plates over the gauge length, however elastic deformations were minimal. An Optotrak optical tracking system was used for supplementary deformation measurements. The optical markers were installed on the test plate, pull plates, and the bolt. Measurements from the optical tracking system were used to verify the LVDT measurements as well as measure elastic elongation of the specimen and pull plate.

After applying a preload of 500 lbs to bring the connection into bearing, the test bolt was finger tightened and then brought to a snug-tight condition with a few impacts of an impact wrench. The plies were ensured to be in firm contact. All other bolts were finger tightened. The preload was released prior to applying the main load.

Loading was applied in displacement control at a rate of 0.05 in/min. Most tests were stopped after a near complete loss of load-carrying capacity, typically after one or two loud sounds that likely indicated rupture. To investigate the progression of the failure mechanism, specimens labeled STD1, STD2, STD3, STD4, NC1, NC2b, and SSLT1 were stopped when a steep load drop was seen. Specimen NC2a was stopped even earlier at the first sign of any load drop. All specimens were allowed to achieve their maximum strength.
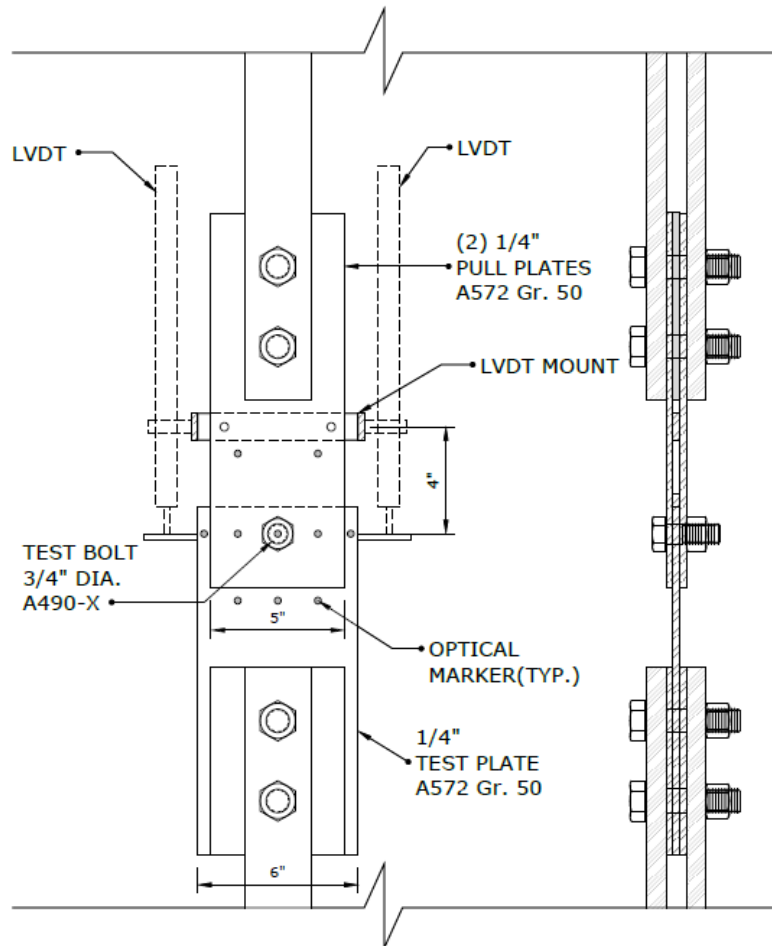
Figure 14: Experimental Test Setup

Results

Load-deformation curves for all specimens are presented in Figure 15. The load at 1/4 in. deformation ($R_{exp,d}$) and the ultimate load ($R_{exp,u}$) are presented in Table 11 along with test-to-predicted ratios computed using the current and proposed equations (Eqs. 15 and 16). Measured values were used in calculating the predicted strengths. For specimens with short-slotted holes, l_{v1} was computed graphically with computer-aided drafting software by drawing the specimen using measured dimensions and measuring the length from the edge of the hole to the edge of the material along lines tangent to the bolt. The difficulty in determining l_{v1} in some cases is a drawback for its use in design equations, however, design tables could be developed to alleviate the problem.
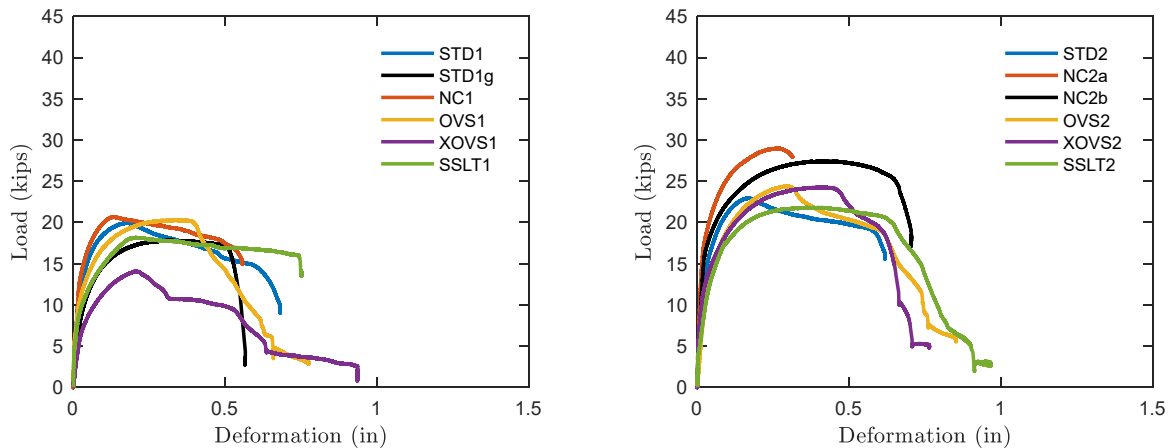
(a) Specimens with nominal edge distance of 1 in.

(b) Specimens with nominal edge distance of 1.25 in.
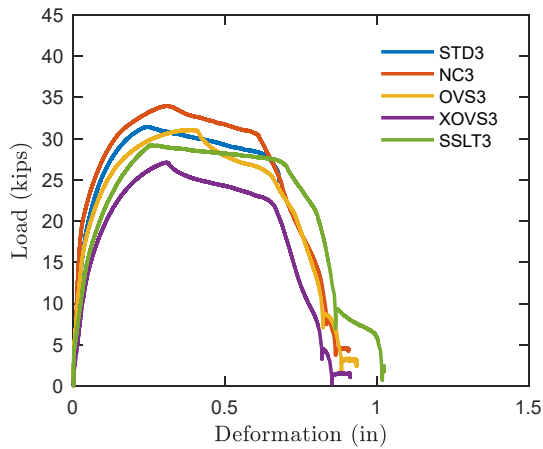
(c) Specimens with nominal edge distance of 1.5 in.
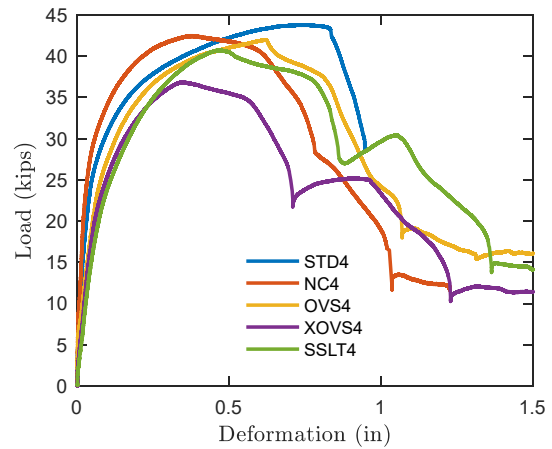
(d) Specimens with nominal edge distance of 2 in.

Figure 15: Load-Deformation Curves for Experimental Tests

Failure Mechanisms

Specimens were disassembled after testing to determine the failure mechanism. Upon disassembly, it was observed that most specimens had a splitting tear as well as shear rupture in the connected material along one or both sides of the bolt hole. For specimens with smaller edge distances (i.e., nominal edge distances of 1 in. and 1.25 in.), the splitting tear extended to the bolt hole, as shown in Figure 16a. For specimens with larger edge distances, the split did not extend all the way to the

bolt hole, as shown in Figure 16b. Specimens STD4, NC4, STD1g, and NC2b did not exhibit any splitting.

For all specimens that exhibited splitting, it is likely that the initiation of splitting occurred prior to shear rupture in the connected material and coincided with the peak load. Testing of specimen NC2a was stopped shortly after the peak load was attained. Upon disassembly, the initiation of a splitting tear was observed, but no initiation of shear rupture in the connected material was observed. Interestingly, the duplicate specimen, NC2b, did not exhibit splitting failure and achieved a 6% lower strength. The initiation of splitting is seen in the load-deformation curves as a dip that occurs after peak load and flattens out prior to the steeper tearout shear rupture, as depicted in Figure 16.

(a) Specimen OVS2

(b) Specimen OVS3
Figure 16: Photograph of specimens after testing

Strength Evaluation

The means of the test-to-predicted ratios were calculated for each hole type to compare the accuracy of each tearout length, shown in Table 12 and Table 13 for the 1/4 in. deformation limit state and ultimate limit state, respectively.

The results of Table 12 and Table 13 verify the trends identified in the analysis of the previously published experiments. The current tearout equation underestimates the load at 1/4 in. deformation,

which is much closer to the ultimate load than the equations imply. For load at 1/4 in. deformation, differences between the equations using l_{v1} and l_{v2} are shown to be minimal for standard and oversize holes and both were more accurate than the current equation. Across all hole types, the proposed equation with l_{v1} showed less variation but was unconservative for holes with minimal clearance. The strength of short-slotted holes was underpredicted by the equation using l_{v2}.

Frank and Yura (1981) tested four specimens with long-slotted holes oriented perpendicular to the load. They observed that the initial stiffness and load at 1/4 in. deformation was reduced when compared to standard holes but that the ultimate strength, which was controlled by bearing for these specimens, was not reduced. As seen in Figure 15, the initial stiffness of the specimens with short-slotted holes was among the lowest of those tested in this work. However, both $R_{exp,d}$ and $R_{exp,u}$ were lower for the specimens with short-slotted holes than for the specimens with standard holes.

Although the mean test-to-predicted ratios for the ultimate limit state appear to be accurate for the current equation (Table 13), the results are not consistent across edge distances. This is seen by plotting the test-to-predicted ratios of all tested specimens using the current equation along with the proposed equation using l_{v1} in Figure 17. The linear best-fit lines depict the inconsistency at the ultimate limit state of the current equation across edge distances in comparison to the proposed equation, evident throughout different hole types.

Table 12: Mean Test-to-Predicted Ratio at the 1/4 in. Deformation Limit State

Hole Type	Using l_c (Eq. 10)	Using l_{v1} (Eq. (15))	Using l_{v2} (Eq. (16))
All	1.264	1.008	0.998
STD	1.293	0.998	1.035
NC	1.307	0.965	1.073
OVS	1.286	1.044	1.002
XOVS	1.272	1.050	0.938
SSLT	1.149	0.994	0.922

Table 13: Mean Test-to-Predicted Ratio at the Ultimate Limit State

Hole Type	Using l_c (Eq. 10)	Using l_{v1} (Eq. (15))	Using l_{v2} (Eq. (16))
All	1.045	1.044	1.032
STD	1.070	1.034	1.071
NC	1.065	0.984	1.093
OVS	1.078	1.095	1.051
XOVS	1.049	1.085	0.970
SSLT	0.958	1.035	0.961

Effect of Bolt Tightening

All but one specimen was tested with the bolt installed to a snug-tight condition. The exception was specimen STD1g, which was nominally identical to STD1 but with the bolt installed loose and grease applied to the faying surfaces so as to investigate the effect of friction. The load-deformation response of specimens STD1g and STD1 is presented in Figure 18.

Several observations can be made from this pair of specimens: 1) the greased specimen was less stiff than the snug-tightened specimens; 2) the load at 1/4 in. deformation was 13% greater for the snug-tightened specimen than for the greased specimen; 3) the ultimate load was 12% greater for the snug-tightened specimen than for the greased specimen; 4) splitting was observed for the snug-tightened specimen, but not the greased specimen.

While these observations were made for a single pair of specimens, the increase in $R_{exp,d}$ corresponds to the increase seen in previous testing data (Table 9). However, the increase in $R_{exp,u}$ was not seen in previous testing data. Also, it is not clear why different failure modes occurred for the two specimens.
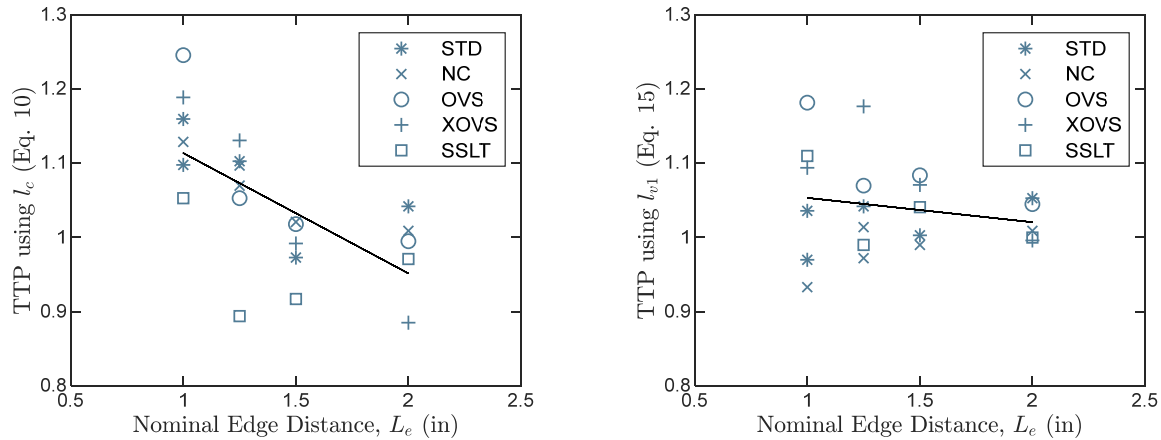
Figure 17: Test-to-Predicted Ratios at Ultimate Limit State with Best Fit Lines
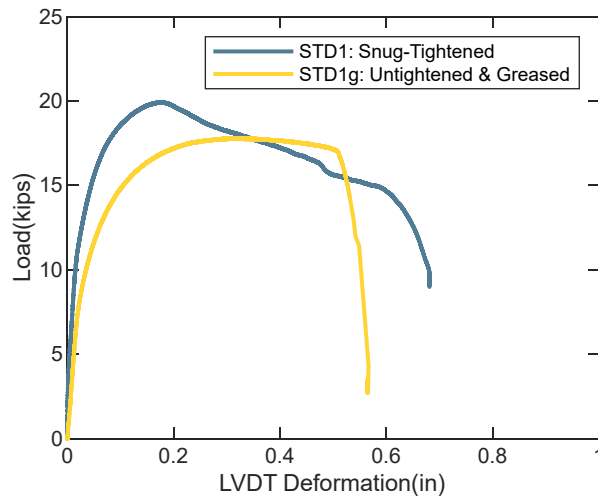
Figure 18: Snug-Tightened Specimen versus Untightened and Greased Specimen

33

Chapter 5: Reliability Analysis for Concentrically Loaded Connections

Through the evaluation of existing and new experimental data presented in the previous chapters, it was determined that 1) the difference between ultimate load and load at 1/4 in. deformation for specimens failing in tearout is less than implied by current equations, 2) current equations for tearout strength underpredict the load at 1/4 in. deformation, and 3) current equations are not consistent across edge distances and tend to underpredict the strengths at smaller edge distances. Accordingly, increased accuracy in design can be achieved by replacing Equations J3-6c and J3-6d in the AISC *Specification* (AISC 2016) with either Eq. 15 or Eq. 16. This chapter presents an analysis to confirm that these equations provide a consistent and sufficient level of reliability.

The Commentary on the AISC *Specification* (AISC 2016) states that the target reliability index for strength limit states is approximately 2.6 for members and 4.0 for connections. The increased target reliability for connections is due to the complexity of modeling them, sensitivity to workmanship, and the benefit that additional strength provides. Previous reliability studies on bearing and tearout in bolted connections used a first-order probabilistic method (Galambos 1985). In this study, noting the nonlinearity arising from multiple possible limit states, a reliability analysis was performed using Monte Carlo simulations.

Methodology

A limit state function, $\tilde{g}$, can be defined as the resistance of a particular connection, $\tilde{R}$, minus the load on that connection, $\tilde{Q}$, all three of which are assumed to be random variables (denoted with a tilde). This is presented in Eq. 17.

$$\tilde{g} = \tilde{R} - \tilde{Q} \tag{17}$$

Failure occurs when $\tilde{Q}$ is greater than $\tilde{R}$, resulting in $\tilde{g} < 0$. The probability of failure, P_f, can be expressed as shown in Eq. 18

$$P_f = P(\tilde{g} < 0) \tag{18}$$

The reliability index is a common method of expressing the probability of failure and is calculated in Eq. 19 as the inverse normal cumulative distribution function of the probability of failure.

$$\beta = -F_X^{-1}(P_f) \tag{19}$$

where, β is the reliability index and F_X^{-1} is the inverse normal cumulative distribution.

The resistance, $\tilde{R}$, should be the best approximation of the true resistance of the connection and can be determined in several ways. For use within Monte Carlo simulations, which require many thousands of trials, code equations offer a good alternative to physical experiments, finite element analyses, or other means of determining the resistance. The proposed equation using the alternative

tearout length l_{v1} (Eq. 15) was used to compute the resistance since this equation resulted in less variation than the current equation when compared to experimental results.

In order to focus on bearing and tearout reliabilities, and reduce the complexity of the problem, it was assumed that shear rupture of the bolt or any other limit state will not control. Therefore, the effective strength of each fastener is the minimum of the strengths computed for the limit states of bearing and tearout. Two sets of equations for $\tilde{R}$ were formulated, one in which deformation at service load is a design consideration and one where it is not.

Eqs. 20 through 24 apply when deformation at service load is a design consideration, denoted as the deformation limit state in this analysis.

$$\tilde{R}_d = \tilde{X}_{Pd} \sum_{i=1}^{n} \tilde{r}_d \tag{20}$$

where $\tilde{X}_{Pd}$ is the professional factor for the deformation limit state and $\tilde{r}_d$ is the effective strength of a fastener at the deformation limit state, computed as shown in Eqs. 21 through 24.

$$\tilde{r}_d = \tilde{r}_{d,tearout} \leq \tilde{r}_{d,bearing} \tag{21}$$

$$\tilde{r}_{d,bearing} = 2.4\tilde{d}\tilde{t}\tilde{F}_u = 2.4\left(\tilde{X}_d d_n\right)\left(\tilde{X}_t t_n\right)\left(\tilde{X}_{F_u} F_{un}\right) \tag{22}$$

For an end bolt:

$$\tilde{r}_{d,tearout} = 1.2\tilde{l}_{v1}\tilde{t}\tilde{F}_u = 1.2\left(\tilde{X}_{l_e}l_{en} - \frac{\sqrt{d_h^2 - \tilde{X}_d d_n^2}}{2}\right)\left(\tilde{X}_t t_n\right)\left(\tilde{X}_{F_u} F_{un}\right) \tag{23}$$

For an interior bolt:

$$\tilde{r}_{d,tearout} = 1.2\tilde{l}_{v1}\tilde{t}\tilde{F}_u = 1.2\left(s - \sqrt{d_h^2 - \tilde{X}_d d_n^2}\right)\left(\tilde{X}_t t_n\right)\left(\tilde{X}_{F_u} F_{un}\right) \tag{24}$$

where d_n is the nominal bolt diameter, d_h is the nominal bolt hole diameter, t_n is the nominal thickness of the connected material, F_{un} is the nominal ultimate tensile strength of the connected material, l_{en} is the nominal center-to-edge distance, and s is the center-to-center spacing of bolts. Most of the nominal values are multiplied by a corresponding random variable (denoted with a tilde) representing the ratio of the actual value to the nominal value of the variable. The random variables are described later and in Table 14.

Eq. 25 applies when deformation at service load is not a design consideration, denoted as the ultimate limit state in this analysis.

$$\tilde{R}_u = \tilde{X}_{Pu} \sum_{i=1}^{n} \tilde{r}_u \tag{25}$$

where $\tilde{X}_{Pu}$ is the professional factor for the ultimate limit state and $\tilde{r}_u$ is the effective strength of a fastener at the ultimate limit state, computed as shown in Eqs. 26 through 28.

$$\tilde{r}_u = \tilde{r}_{u,tearout} \leq \tilde{r}_{u,bearing} \tag{26}$$

$$\tilde{r}_{u,bearing} = 3.0\tilde{d}\tilde{t}\tilde{F}_u = 3.0\left(\tilde{X}_d d_n\right)\left(\tilde{X}_t t_n\right)\left(\tilde{X}_{F_u} F_{un}\right) \tag{27}$$

For an end bolt:

$$\tilde{r}_{u,tearout} = 1.2\tilde{l}_{vl}\tilde{t}\tilde{F}_u = 1.2\left(\tilde{X}_{l_e} l_{en} - \frac{\sqrt{d_h^2 - \tilde{X}_d d_n^2}}{2}\right)\left(\tilde{X}_t t_n\right)\left(\tilde{X}_{F_u} F_{un}\right) \tag{28}$$

For an interior bolt:

$$\tilde{r}_{u,tearout} = 1.2\tilde{l}_{vl}\tilde{t}\tilde{F}_u = 1.2\left(s - \sqrt{d_h^2 - \tilde{X}_d d_n^2}\right)\left(\tilde{X}_t t_n\right)\left(\tilde{X}_{F_u} F_{un}\right) \tag{29}$$

The nominal load effect, $\tilde{Q}$, is equal to the sum of the dead and live load, both of which are expressed as a nominal value multiplied by a random variable representing the actual-to-nominal ratio, as shown in Eqs. 30 through 32. Only dead and live load are considered in this study, as was done in previous reliability studies (Galambos 1983, 1985; Lundberg and Galambos 1996).

$$\tilde{Q} = \tilde{P}_D + \tilde{P}_L \tag{30}$$

$$\tilde{P}_D = \tilde{X}_D P_{Dn} \tag{31}$$

$$\tilde{P}_L = \tilde{X}_L P_{Ln} \tag{32}$$

The nominal values of dead and live load are obtained from current or trial design equations assuming that the connection was designed at the precise limit point as shown in Eq. 33 and assuming a specified ratio of dead load to live load.

$$\phi R_n = R_u \tag{33}$$

The load combinations under consideration are evaluated with Eq. 34.

$$R_u = \max \begin{pmatrix} 1.4P_{Dn} \\ 1.2P_{Dn} + 1.6P_{Ln} \end{pmatrix} \quad (34)$$

Statistical Parameters

The statistical parameters for each of the random variables are described in this section and summarized in Table 14.

Table 14: Summary of Statistical Parameters

Random Variable	Description	Assumed Distribution
$\tilde{X}_{Pd}$	Ratio of actual to predicted strength for bearing and tearout failures when deformation is a design consideration	Normal (mean=1.013, COV=0.126)
$\tilde{X}_{Pu}$	Ratio of actual to predicted strength for bearing and tearout failures when deformation is a not design consideration	Normal (mean=1.015, COV=0.168)
$\tilde{X}_{F_u}$	Ratio of actual to nominal ultimate tensile strength of connected material	Normal (mean=1.12, COV=0.04 for flange) (mean=1.26, COV=0.07 for plate)
$\tilde{X}_t$	Ratio of actual to nominal thickness of connected material	Normal (mean=0.976, COV=0.042 for flange) (mean=1.04, COV=0.025 for plate)
$\tilde{X}_d$	Ratio of actual to nominal bolt diameter	Truncated Normal (mean=1.00, COV=0.02)
$\tilde{X}_{l_e}$	Ratio of actual to nominal edge distance	Normal (mean=0.00, S.D.=0.05 in.)
$\tilde{X}_D$	Ratio of actual to nominal dead load	Normal (mean=1.05, COV=0.10)
$\tilde{X}_L$	Ratio of actual to nominal live load	Type 1 Extreme Value (mean=1.00, COV=0.25)

The professional factors, $\tilde{X}_{Pd}$ and $\tilde{X}_{Pu}$, account for the expected variation between the actual strength of the connection and the computed strength (i.e., the test-to-predicted ratio). The statistical parameters for the professional factors are taken from Table 7 and Table 8 for the deformation and ultimate limit states respectively.

Statistical parameters for material strength ($\tilde{X}_{F_u}$), thickness ($\tilde{X}_t$), bolt diameter ($\tilde{X}_d$), and edge distance ($\tilde{X}_{l_e}$) were explicitly assigned to calculate the expected resistance. The parameters were derived from published literature. Test-to-predicted material strengths were researched by Liu et al. (2007) for various steel strengths and shapes. From this study, data from A992 wide flange shapes as well as A572 plates were used. The random variable for flange thickness was determined from data collected by Kennedy and Aly (1980) of 2768 measurements of flange thicknesses. The random variable for plate thickness was determined from Schmidt and Bartlett (2002) for plates used in welded wide flange plate girders. No previous research on the statistical variation of bolt diameter or bolt placement was found. The variation of bolt diameter was based on manufacturing

tolerances for a heavy hex 3/4 in. diameter bolt per (ASME 2006), and assuming a 99.7% confidence interval (i.e., within three standard deviations). The probability distribution was truncated to be within the ASME tolerances, which guarantees that the bolt diameter does not exceed the hole diameter (a deterministic value). Variation of the bolt edge distance was assumed to follow a normal distribution without bias and with an 99.7% confidence that the bolt is placed within a tolerance of 1/8 in. Spacing of bolts was set as a deterministic value. The random variables for dead and live load are taken as ones proposed by Ellingwood et al. (1980). Dead load is modeled as a normally distributed variable whereas live load is modeled as a Type I extreme value distribution.

Variable Sensitivity Analysis

The reliability index computed as described in this chapter is dependent on many factors, including the number of bolts in a line parallel to load, edge distance, spacing, and specific thicknesses and material strengths for the connected parts. Sensitivity analyses were performed in order to narrow the scope of the reliability analyses.

The configuration selected for analysis was a butt splice connection with the flange of a wide flange on the interior and plates on the exterior. The nominal material strengths were set equal and nominal thickness of the interior connected part was set equal to the sum of the nominal thickness of the exterior parts. This yields the most conservative result since failure can occur in either the flange or the plate. If one of the connected parts was significantly thicker or stronger than the other, then that would effectively eliminate the possibility of failure in that part.

Certain parameters were shown through trial analyses to have minimal effect on the computed reliability index. These include nominal bolt diameter, nominal tensile strength of the connected parts, nominal thickness of the connected parts, and number of bolt lines. Values for these parameters were selected as d_{bn} = 3/4 in., F_{un} = 65 ksi, t_n = 1/4 in. (for the interior part), and one bolt line.

Table 15: Sensitivity of Reliability Index to Live-to-Dead Load Ratio

L/D Ratio	β
1	3.61
2	3.48
3	3.41
4	3.37
5	3.34

The impact of the live-to-dead load ratio (*L/D* ratio) was also investigated. For simplicity, only the current equations and the ultimate limit state were used to determine reliability for the sensitivity analysis. The first stage of the analysis was to perform a sensitivity analysis on these variables by varying them independently on a typical connection with a constant number of bolts in a line (3), edge distance (2*d*), and spacing (3*d*). The effects of changing live-to-dead load ratio are shown in Table 15. As expected, the reliability decreases as the *L/D* ratio increases due to the additional uncertainty inherent in the live load statistical parameter. A *L/D* ratio of 3.0 was chosen for further analysis in this study, as it offers a realistic and conservative approach to calculating reliability and has been previously used in other studies (Galambos 1983, 1985; Lundberg and Galambos 1996).

Reliability Analysis and Results

After determining which variables can be maintained constant, the focus of the reliability study was narrowed to the effects of the number of bolts in a line, edge distance, and spacing. Three combinations of edge distance and spacing were selected to generate plots of reliability versus the number of bolts in a line. Two design methods were also considered: 1) deformation at bolt holes at service load is a design consideration (reliability against deformation limit state) with results shown in Figure 19; and 2) deformation at bolt holes at service load is not a design consideration (reliability against ultimate limit state) with results shown in Figure 20

Each plot includes four lines representing results using 1) the current tearout strength equation, 2) the proposed tearout strength equation using l_{v1}, Eq. (15), 3) the proposed tearout strength equation using l_{v2}, Eq. (16), and 4) neglecting tearout altogether. Results for minimum edge distance ($1^1/_3d$ for a 3/4 in. bolt) and minimum spacing ($2^2/_3d$) are shown in Figure 19a and Figure 20a. Results for a more typical edge distance ($2d$) and spacing ($4d$) are shown in Figure 19b and Figure 20b. Results for a large edge distance ($6d$) and spacing ($12d$) are shown in Figure 19c and Figure 20c. The number of realizations used in the Monte Carlo simulations was 10^6. This number of realizations results in approximately 95% confidence that the computational error of reliability index is less than 0.02 for $\beta \approx 3$ and 0.09 for $\beta \approx 4$.

Based on the results for large edge distance and spacing, the reliability index for bearing is consistent across the number of bolts and between the deformation and ultimate limit state at approximately $\beta = 3$. This value is less than the target reliability index of $\beta = 4$ for connections. This discrepancy may be due to a number of factors, including some conservative choices made in this work. Further investigation is recommended to determine if this lower reliability index is a concern for design; however, for this investigation, the consistent value of $\beta = 3$ is used as the benchmark against which the other results will be compared.

Examining Figure 19a, it is clear that the current tearout strength equations are conservative for the deformation limit state, providing a reliability greater than for the bearing limit state. The proposed equations provide a similar level of reliability that is largely consistent across the number of bolts and with the bearing limit state. As expected, neglecting tearout for connections with minimum edge distance is unsafe, however, as the number of bolts increases, the negative effect of neglecting tearout diminishes. The current tearout strength equations are less conservative for the ultimate limit state. This was seen previously and is also evident comparing Figure 19a to Figure 20a where the reliability index for the ultimate limit state is more consistent with the bearing limit state.

Overall, these results confirm that either of the proposed tearout strength equations provide a sufficient level of reliability that is consistent with the bearing limit state, consistent across a variety of physical connection parameters (e.g., number of bolts, edge distances, and spacing) and consistent across whether or not deformation is a design consideration.
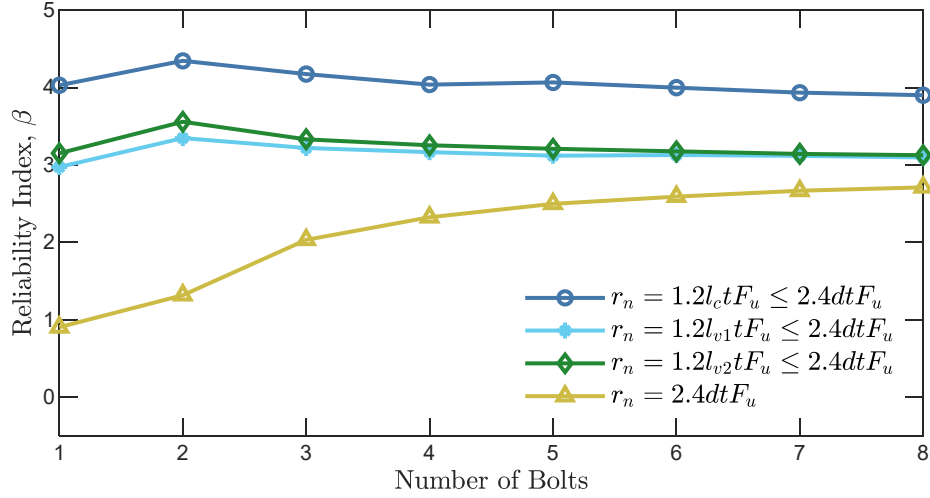
(a) Minimum Edge Distance and Spacing
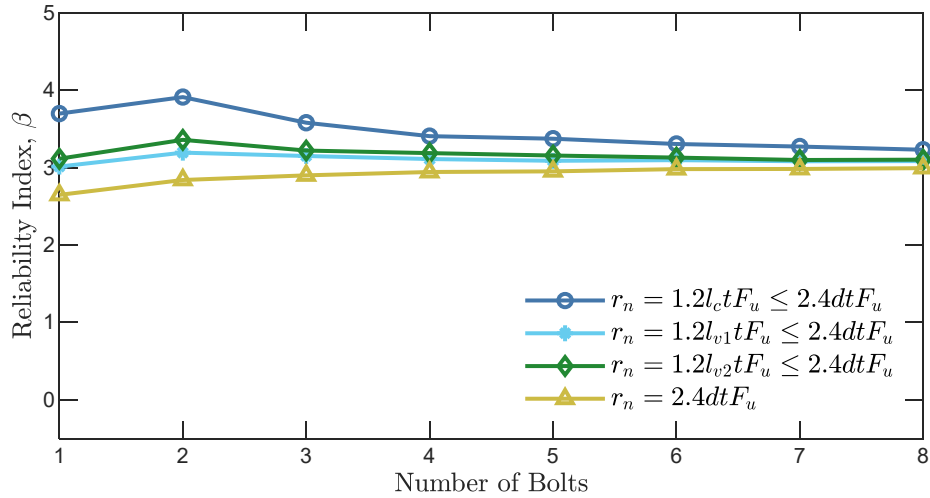
(b) Typical Edge Distance and Spacing
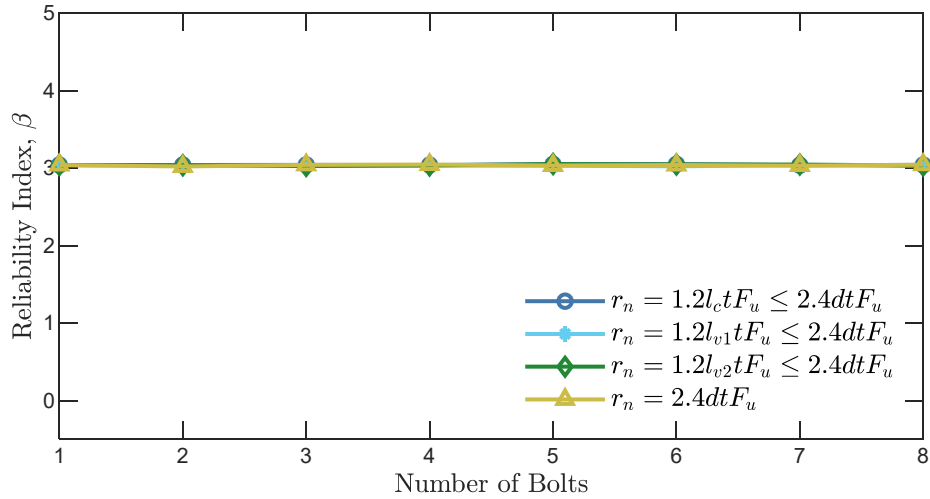
(c) Maximum Edge Distance and Spacing

Figure 19: Reliability Results – Deformation Limit State
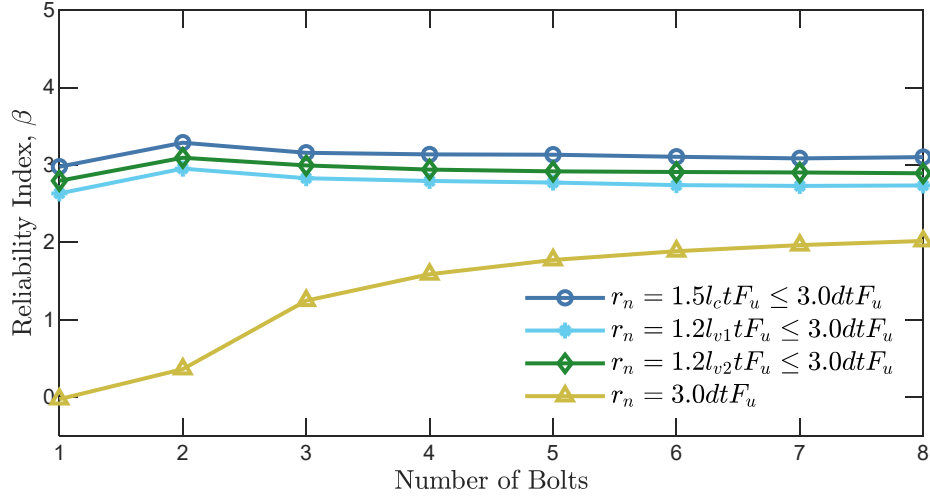
(a) Minimum Edge Distance and Spacing
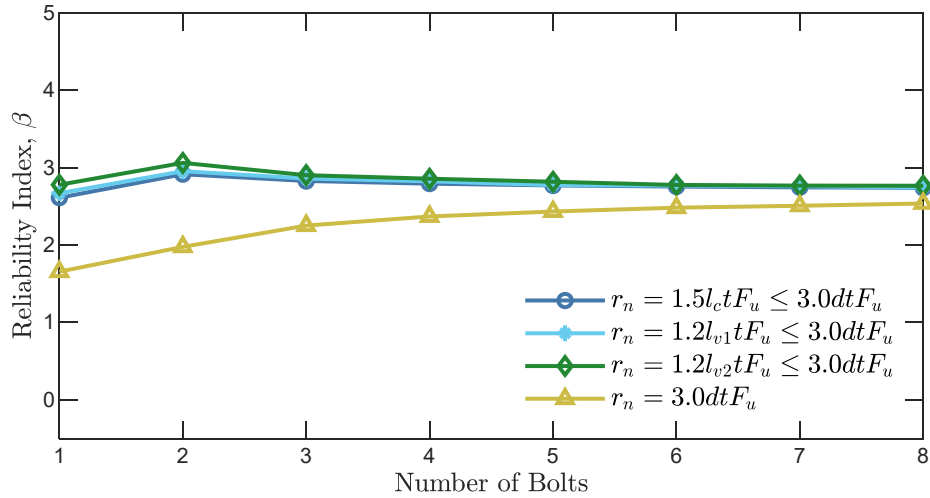
(b) Typical Edge Distance and Spacing
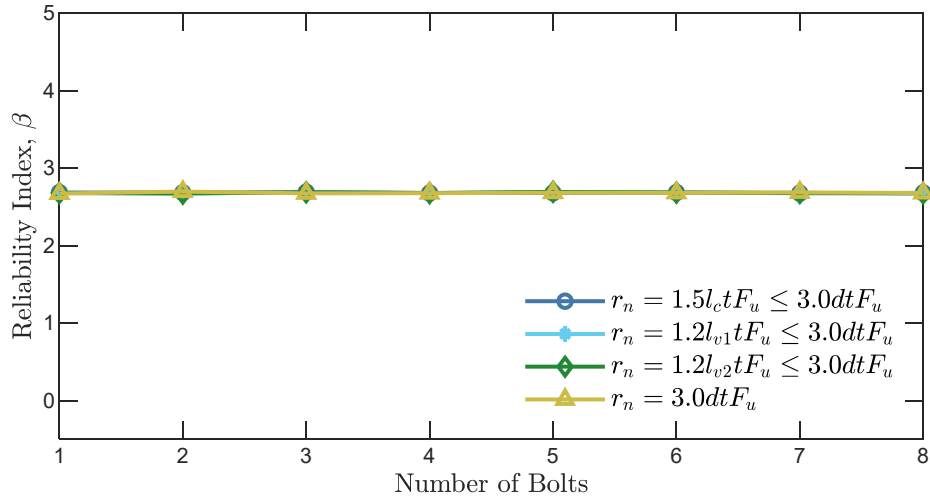
(c) Maximum Edge Distance and Spacing
Figure 20: Reliability Results – Ultimate Limit State

Chapter 6: Alternative Design Approach for Concentrically Loaded Connections

The proposed equations provide improved accuracy over current equations. However, there remains the possibility of different effective strengths for bolts within a group. These different strengths represent physical behavior, but they can be inconvenient for design. It may be convenient to have a uniform effective strength among bolts in a group for design, even if such an evaluation was conservative. In this chapter, an alternative design approach, or rule-of-thumb, where tearout need not be check directly and the strength of each bolt within a group can be taken as the same is developed. For this approach, reduction factors are applied to the bearing and bolt shear rupture strength such that the tearout limit state need not be checked explicitly.

Derivation of the Approach

The strength equations for the limit states of bearing and tearout are similar in that they both include the term tF_u. Accordingly, the ratio between the strength for the two limit states depends only on the bolt diameter, d, and the clear distance, l_c. For the case when deformation at the bolt hole at service load is a design consideration, the ratio of nominal strength for the limit state of tearout for an individual bolt, r_{nt}, to the nominal strength for the limit state of bearing for an individual bolt, r_{nb}, is equal to $l_c/2d$. This ratio is calculated for a range of bolt diameters and for both standard and oversize holes in Table 16 and Table 17. In Table 16, it is assumed that the bolt is adjacent to an edge and the minimum edge distance per Section J3.4 of the AISC *Specification* is provided. In Table 17 , it is assumed that the bolt is adjacent to another bolt and a spacing of $3d$ (as recommended in Section J3.3 of the AISC *Specification*) is provided. From these tables it can be concluded that, for the conditions considered, the tearout strength of an edge bolt is no less than 0.344 times its bearing strength (Eq. 35) and the tearout strength of an interior bolt is no less than 0.850 times its bearing strength (Eq. 36).

$$r_{nt} \geq \alpha r_{nb} = 0.344 r_{nb} \tag{35}$$

$$r_{nt} \geq \beta r_{nb} = 0.850 r_{nb} \tag{36}$$

where, α and β are minimum strength ratios determined from Table 16 and Table 17, respectively (i.e., α = 0.344 and β = 0.850).

Consider the generic connection shown in Figure 21. The strength of the bolt group is the summation of the effective strength of each of the bolts. Assuming that shear rupture of the bolt does not control the effective strength of any of the bolts, the lower bound of the strength of the bolt group can be computed as shown in Eq. (37), noting that there are two bolts adjacent to edges and the remaining bolts are interior.

$$R_n \geq 2\alpha r_{nb} + (n-2)\beta r_{nb} \tag{37}$$

where n is the total number of bolts in the line. Rearranging terms results in Eq. 38:

$$R_n \geq n\left(\frac{2\alpha+(n-2)\beta}{n}\right)r_{nb} = nx_b r_{nb} \qquad (38)$$

where, x_b is a reduction factor applied to the bearing strength.

Table 16: Ratio of tearout strength to bearing strength for edge bolts

d	Standard Holes				Oversize Holes			
	d_h	$L_{e,min}$	$l_{c,min}$	$r_{nt,min}/r_{nb}$	d_h	$L_{e,min}$	$l_{c,min}$	$r_{nt,min}/r_{nb}$
in	In	in	in	---	in	in	in	---
1/2	0.563	0.750	0.469	0.469	0.625	0.813	0.500	0.500
5/8	0.688	0.875	0.531	0.425	0.813	0.938	0.531	0.425
3/4	0.813	1.000	0.594	0.396	0.938	1.063	0.594	0.396
7/8	0.938	1.125	0.656	0.375	1.063	1.188	0.656	0.375
1	1.125	1.250	0.688	0.344	1.250	1.375	0.750	0.375
1 1/8	1.250	1.500	0.875	0.389	1.438	1.625	0.906	0.403
1 1/4	1.375	1.625	0.938	0.375	1.563	1.750	0.969	0.388
1 3/8	1.500	1.719	0.969	0.352	1.688	1.844	1.000	0.364
1 1/2	1.625	1.875	1.063	0.354	1.813	2.000	1.094	0.365

Table 17: Ratio of tearout strength to bearing strength for interior bolts

d	Standard Holes				Oversize Holes			
	d_h	$3d$	$l_{c,3d}$	$r_{nt,3d}/r_{nb}$	d_h	$3d$	$l_{c,3d}$	$r_{nt,3d}/r_{nb}$
in	in	in	in	---	in	in	in	---
1/2	0.563	1.500	0.938	0.938	0.625	1.500	0.875	0.875
5/8	0.688	1.875	1.188	0.950	0.813	1.875	1.063	0.850
3/4	0.813	2.250	1.438	0.958	0.938	2.250	1.313	0.875
7/8	0.938	2.625	1.688	0.964	1.063	2.625	1.563	0.893
1	1.125	3.000	1.875	0.938	1.250	3.000	1.750	0.875
1 1/8	1.250	3.375	2.125	0.944	1.438	3.375	1.938	0.861
1 1/4	1.375	3.750	2.375	0.950	1.563	3.750	2.188	0.875
1 3/8	1.500	4.125	2.625	0.955	1.688	4.125	2.438	0.886
1 1/2	1.625	4.500	2.875	0.958	1.813	4.500	2.688	0.896
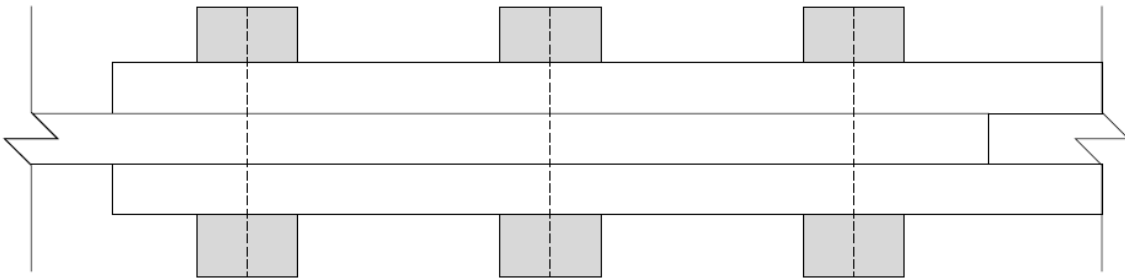
Figure 21: Example Connection for the Alternative Design Method

According to Eq. 38, a lower-bound estimate of the strength can be obtained as the number of bolts times a reduced bearing strength, $x_b r_{nb}$. The reduction factor, x_b, is given by Eq. 39 where a simplified version of the equation assuming the values of α and β determined previously is also presented.

$$x_b = \frac{2\alpha + (n-2)\beta}{n} \approx 0.85 - \frac{1}{n} \tag{39}$$

However, bolt shear rupture cannot be neglected in general. A similar reduction factor applied to the bolt shear rupture strength, r_{ns}, can be determined to address cases where bolt shear rupture and tearout control the effective strength of the various individual bolts. In such a case, a lower-bound estimate of the strength can be computed as Eq. 40.

$$R_n \geq nx_s r_{ns} = 2\alpha r_{nb} + (n-2)r_{ns} \tag{40}$$

The maximum necessary reduction to r_{ns} will occur when the bolt shear rupture strength is equal to the reduced bearing strength for the interior bolts (i.e., $r_{ns} = \beta r_{nb}$):

$$R_n \geq nx_s \beta r_{nb} = 2\alpha r_{nb} + (n-2)\beta r_{nb} \tag{41}$$

Solving for x_s:

$$x_s = \frac{2\alpha + (n-2)\beta}{n\beta} \approx 1 - \frac{1}{0.85n} \tag{42}$$

Accordingly, a lower-bound estimate of the strength of a concentrically loaded bolt group, can be determined using Eq. 43 without the need to directly evaluate the limit state of tearout.

$$R_n \geq n \min\left(x_b r_{nb}, x_s r_{ns}\right) \tag{43}$$

This equation, with x_b defined by Eq. 39 and x_s defined by Eq. 42, is applicable to when deformation at the bolt hole at service load is a design consideration, standard or oversize holes are used, the minimum required edge distances are met, spacing greater than or equal to $3d$ is provided, and strength is computed according to the 2016 AISC *Specification* (i.e., not the proposed equations in this work). However, within these conditions, Eq. 43 applies to any number of bolts, bolt diameter, and bolt grade. Alternative reduction factors for different situations and ranges of parameters can be computed using different values of α and β. However, note that if both the edge distance and bolt spacing are large enough, then tearout does not control and the reduction factors would not be necessary (i.e., $x_b = x_s = 1$). For the equations in the 2016 AISC *Specification*, this would occur when the clear distance is greater than $2d$.

Chapter 7: Single-Plate Shear Connection Experiments

Simple shear connections consisting of a single plate that is welded to the column and bolted to the beam are structurally efficient and easy to build. Connections of this type are not designed to resist bending moments; however, due to the rotation of the beam end and the relative stiffness of components, moments develop and are resisted by the bolt group. This complicates the design of these connections, especially when considering the limit state of tearout since the magnitude and direction of force for each bolt varies from bolt to bolt. Current design recommendations for this type of connection either neglect the eccentricity, which may be unconservative, or utilize approaches, such as the poison bolt method, which may be overly conservative. Most prior experimental tests on single-plate shear connections, and eccentrically loaded bolt groups in general, failed by shear rupture of the bolts or had large enough edge distance that tearout did not control. In this work, a series of physical tests on single-plate shear connections that are susceptible to tearout failures was performed to achieve the following objectives: 1) determine if the existing method of considering bearing and tearout as concentric that is recommended for conventional single-plate shear connections is appropriate, and 2) determine if there are cases in which the bearing and tearout strengths are reduced for extended configurations and what methods best predict these strengths.

Design of Single-Plate Shear Connections

Although single-plate shear connections are often modeled as simple supports and designed only to resist shear forces, they possess rotational stiffness and thus form a statically indeterminate system. Precise modeling of the relative stiffnesses of each component is difficult, thus, the design of these connections often relies on simplifying assumptions and lower bound theory (Muir and Hewitt 2009; Muir and Thornton 2011).

The AISC *Manual* (AISC 2017) recognizes two single-plate shear connection configurations: the extended configuration and the conventional configuration. The extended configuration is general and allows for any number of bolts, any bolt distance from the weld line, and any geometry so long as minimum edge distances are met as required in Table J3.4. For the general method of design for extended-type single-plate shear connections, the weld line (e.g., face of the column or face of the girder web) is assumed to be a point of zero moment. Under this assumption the moment for the bolt group is equal to the reaction times the distance from the weld to the centroid of the bolt group, shown as e in Figure 22. Note that for a single vertical row of bolts, $e = a$, where a is the distance from the weld to the first row of bolts. The bolt group in an extended-type configuration must be checked for bolt shear rupture, bearing, and tearout considering this eccentricity. However, no specific method for determining the strength of the eccentrically-loaded bolt group is provided if the bolt group is susceptible to tearout failures. Additional design checks (e.g., to ensure adequate plate strength) are also required.

The conventional configuration requires that several dimensional limitations be met but simplifies the design checks. The conventional configuration is limited to a single vertical row of 2 to 12 bolts. The distance from the bolt line to the weld line must be less than 3.5 in. The horizontal edge distance is limited to a minimum of two bolt diameters, and maximum limits are placed on the plate and web thickness. A simplified approach is used to evaluate the strength of the bolt group. The bolt group is checked for bolt shear rupture assuming an eccentricity, values for which are

tabulated in Table 10-9 of the AISC *Manual*. The bolt group is checked for bearing and tearout assuming concentric load. This simplified approach allows for hand calculations, but may be unconservative in some situations. Plate strengths should be checked as well, although plate buckling need not be considered for the conventional configuration. The strengths of various conventional connection configurations are listed in Table 10-10 of the AISC *Manual*.
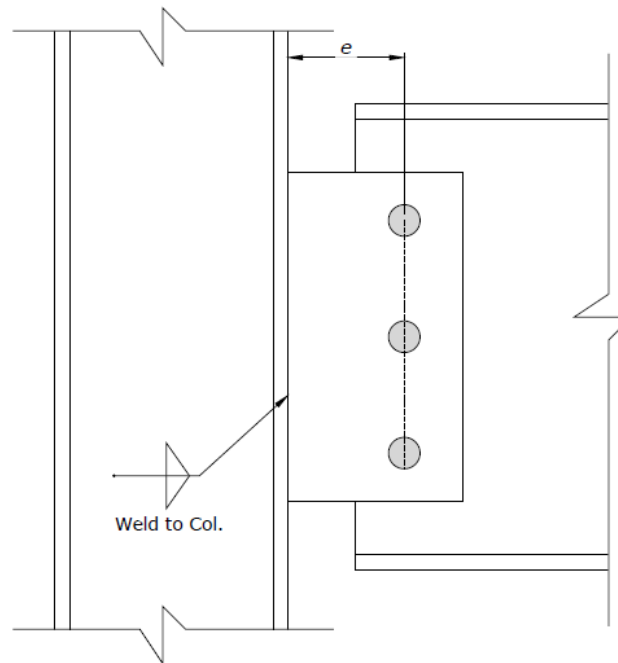
Figure 22. Schematic of typical single-plate shear connection

In an eccentrically loaded bolt group, the magnitude and direction of force in each bolt varies from bolt to bolt. Methods have been developed to consider the effects of eccentricity in bolt groups. The work of Crawford and Kulak (1971) formed the basis of the instantaneous center of rotation method described in the AISC *Manual*. The method involves locating the instantaneous center, typically through an iterative calculation, from which the distance to each bolt can be used to determine the magnitude and direction of force in each bolt. The method has been validated for connections which have been controlled by bolt shear rupture and bearing, but nearly all tests of eccentrically loaded connections included sufficient edge distance to preclude tearout failures.

Modified Instantaneous Center of Rotation Method

A modified version of the instantaneous center of rotation method is proposed in this work. The modified method follows the same general procedure and iterative solution scheme as the standard instantaneous center of rotation method. The difference is that in each iteration, when the load in each bolt is determined, the ultimate strength of the bolt is computed considering the limit state of tearout. The direction of force in each bolt is assumed to be perpendicular to the line from the instantaneous center of rotation to the bolt. If information regarding the geometry of the connected material is provided, the clear distance (from the edge of the bolt hole to the edge of the material or other bolt holes) can be computed for each bolt within each iteration based upon the direction of force. The computed clear distance can be used to calculate the ultimate strength of the bolt,

R_{ult}, which is used in Eq. 44 (Equation 7-1 from the AISC *Manual*) to determine the magnitude of force in the bolt.

$$R = R_{ult}[1 - e^{-10\Delta}]^{0.55}$$ (44)

where, R is the force in the bolt at deformation Δ, R_{ult} is the ultimate strength of the bolt considering bolt shear rupture, bearing, and tearout, and Δ is the deformation of the bolt.

Eq. 44 is representative of a load-deformation curve and is based on the research of Crawford and Kulak (1971) for specimens failing in bolt shear rupture. The equation was subsequently found to be suitable for specimens failing in bearing. In this work, the equation was compared to measured load-deformation response for concentrically loaded specimens failing in tearout (both published and those conducted in this work). Eq. 44 was found to fit the response with reasonable accuracy.

Consider a single-plate shear connection with (2) 3/4 in. diameter A490-X bolts in a single vertical row with standard holes. The plate is 3/8 in. thick and conforms to ASTM A572 Gr. 50 (F_y = 50 ksi and F_u = 65 ksi). The edge distances assumed for Table 10-10b of the AISC *Manual* are l_{eh} = 1.5 in. and l_{ev} = 1.25 in. Combined with a 3 in. bolt spacing, the total depth of the plate is 5.5 in. Note that the distance between the weld line and bolt line is a = 3 in., therefore the connection is designed with an eccentricity of e = a/2 = 1.5 in. per Table 10-9. The design strength of this connection per Table 10-10b is 39.1 kips with a controlling limit state of bolt shear rupture.

The instantaneous center of rotation and forces applied by the bolt on the plate for this case are depicted in Figure 23(a). The solid lines in this figure represent the bolt forces, the dashed lines connect the instantaneous center to the center of the bolt. Results from both the standard and modified version of the instantaneous center of rotation method are shown in Figure 23(a), however, the results are identical since the clear distance for both bolts is sufficient to ensure the design strength for tearout is greater than that for bolt shear rupture (ϕr_n = 27.8 kips) or bearing.

If minimum edge distances per Table J3.4 (i.e., l_{eh} = l_{ev} = 1 in.) were used in lieu of those assumed in Table 10-10, several things would be different about the design of this connection. The total depth of the plate would be 5 in. The connection would be considered as extended since the horizontal edge distance is less than two times the bolt diameter. The connection would need to be designed for an eccentricity of e = a = 3 in. since it is extended. The results for both the standard and modified instantaneous center of rotation method are shown in Figure 23(b) for the smaller edge distances and larger eccentricity. In this condition, the clear distance for the bottom bolt is small enough that tearout controls. The standard instantaneous center of rotation method does not capture this effect, but the modified version does. The lower strength of the bottom bolt results in an upward shift of the instantaneous center and a lower strength overall. The design strength of this connection is 16.1 kips with the controlling limit state being the effective strength of the bolt group. Note deformation at the bolt hole at service load was not a design consideration for this example.
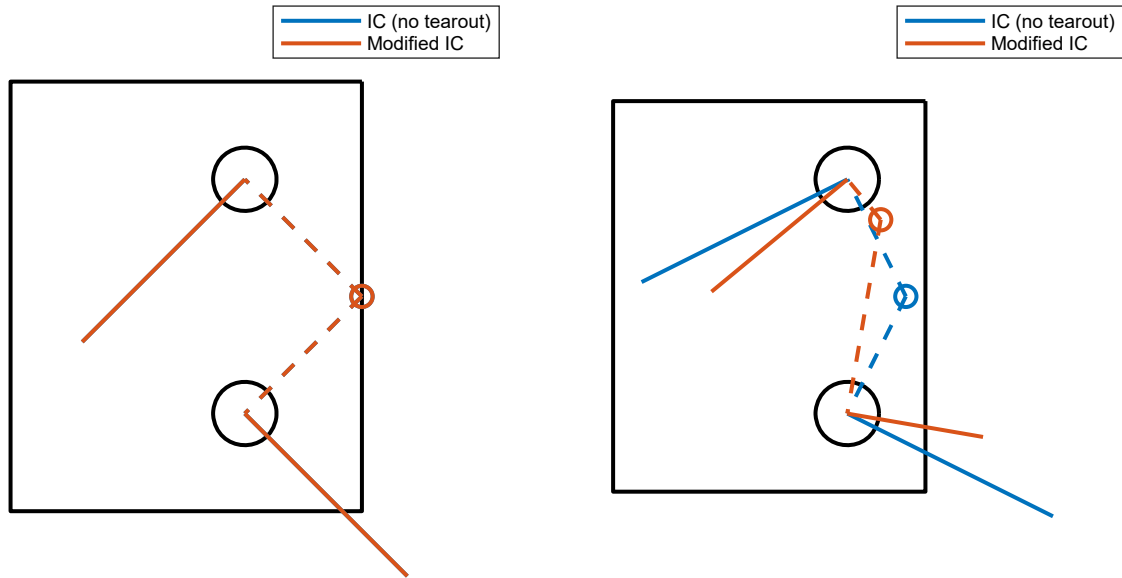
(a) Edge distance per Table 10-10   (b) Minimum edge distance per Table J3.4
   (l_{eh} = 1.5 in. and l_{ev} = 1.25 in.)   (l_{eh} = 1 in. and l_{ev} = 1 in.)
Figure 23. Instantaneous center of rotation method for 2-bolt single-plate shear connection

The impact of tearout on the strength of an eccentrically loaded bolt group can be seen more generally in a plot of moment vs. reaction, as shown in Figure 24 for the two single-plate shear connections considered above. These plots are generated by performing the instantaneous center of rotation method many times for many different values of eccentricity and serve as a sort of interaction diagram for the bolt group.

Three different interaction curves are shown in Figure 24. The blue line is computed using the standard instantaneous center of rotation method neglecting tearout. A blue horizontal dashed line is also shown, which is at the design strength for the connection assuming the reaction is applied concentrically. Reducing the interaction diagram by neglecting strength above that line is consistent with the recommended design method for conventional single-plate shear connections. However, current recommendations can be interpreted such that only the limit states of bearing and tearout need to be considered for this cap on the strength of the connection. The red line is computed using the modified instantaneous center of rotation method. The yellow line is computed using the poison bolt method. For this method, the tearout strength for the smallest clear distance for any bolt in any direction is taken as R_{ult} within the standard instantaneous center of rotation method. Also shown in the plot is a black dashed line which has a slope of the inverse of the eccentricity (i.e., $1/e$) for the connections. The intersection of the black dashed line with the interaction curves represents the strength for the bolt group (e.g., in Figure 24(a) the intersection of the black dashed line and the blue curve occurs at 39.1 kips).
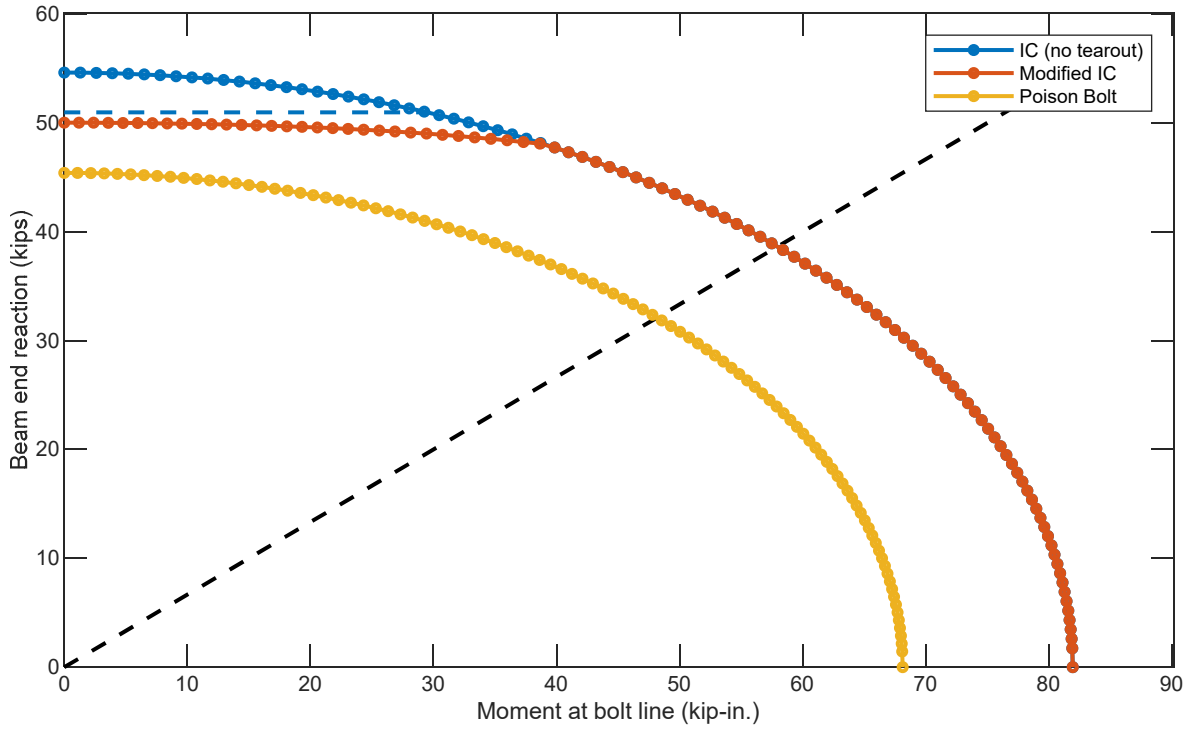
(a) Edge distance per Table 10-10 ($l_{eh} = 1.5$ in. and $l_{ev} = 1.25$ in.)
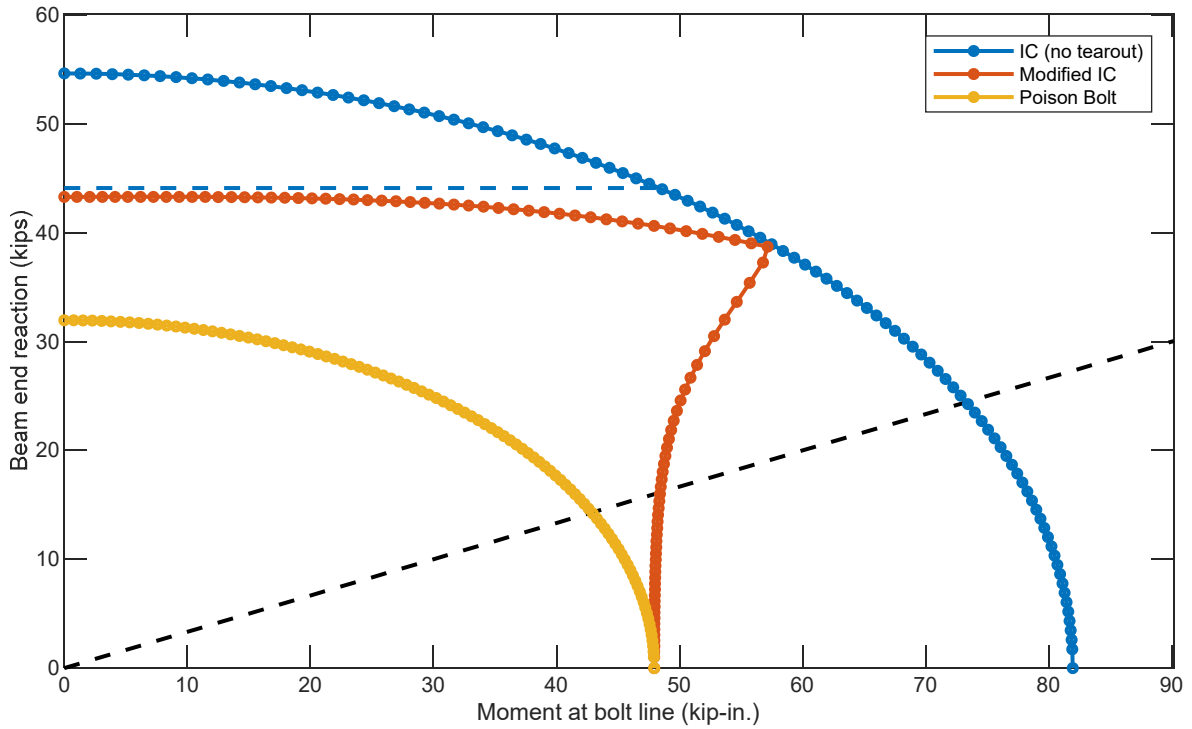
(b) Minimum edge distance per Table J3.4 ($l_{eh} = 1$ in. and $l_{ev} = 1$ in.)
Figure 24. Bolt group interaction strength for 2-bolt single-plate shear connection

Several interesting observations can be made from Figure 24. First, for the connection with larger edge distances, the modified instantaneous center of rotation curve is well-represented by the standard instantaneous center of rotation curve with the reaction capped at strength of the connection assuming the load is applied concentrically and considering all applicable limit states. Note that the small difference between the strength for the modified instantaneous center of rotation method (i.e., red line) at zero eccentricity and the capping strength (i.e., blue dashed line) is due to the strength of individual bolts being capped at a deformation of $\Delta = 0.34$ in. in the load deformation relationship Eq. 44. For the connection with minimum edge distances, the modified and standard instantaneous center of rotation methods diverge for greater eccentricities. As expected, the poison bolt method provides the lowest strength. However, for very large eccentricities the poison bolt method and the modified instantaneous center of rotation method converge for the connection with minimum edge distances.

The results of Figure 24(a) indicate the current method of handling tearout for the conventional configuration may be appropriate. To explore this further, the strength of all connections in Table 10-10 with standard holes was recomputed using the modified instantaneous center of rotation method. The resulting strengths were identical to those currently listed in the table, indicating that the edge distances are sufficiently large to preclude tearout failures.

Overall, the modified instantaneous center of rotation method presented in this work is a promising approach for accounting for tearout in the strength of eccentrically loaded bolt groups. It is based upon the solid foundation of the instantaneous center of rotation method and includes a rational extension for tearout failures which is compliant with the AISC *Specification*. However, experimental validation is necessary to confirm its accuracy.

Test Matrix

A total of 10 single-plate shear connection specimens were selected for testing as shown in Table 18. The tests include a variety of conventional and extended configurations which were selected, based on current design methods, as those which would highlight the greatest potential impact of the tearout limit state as well as the greatest potential difference between the simplified approach for handling bearing and tearout for conventional connections, the modified instantaneous center of rotation method, and the poison bolt method. The vertical edge distance, l_{ev}, was taken as the minimum value from Table J3.4 in the AISC *Specification* (AISC 2016) for all specimens. Two conventional connections were included with the horizontal edge distance, l_{eh}, taken as two times the bolt diameter. The horizontal edge distance for the remaining eight specimens was taken as the minimum value from Table J3.4. The distance from the weld line to the bolt line, a, was 3 in. for some specimens and 9 in. for others.

The specimens consisted of a beam, connection, and column in a sub-assembly. This allowed beam end rotations to form as they would in a practical structure. A beam rotation target of 0.03 radians has been used in previous research for shear connection strength (Baldwin Metzger 2006; Creech 2005). This target rotation is unlikely to occur in most cases but has been adopted as the upper bound rotation for a wide range of applicability (Muir and Thornton 2011). Many previous tests designed for this target rotation failed in beam bending rather than bolt or connection failure, including 4 of 10 tested by Creech (2005) and 4 of 8 tested by Baldwin Metzger (2006). Other specimens that failed in bolt shear first experienced some degree of beam yielding. In the development of the test matrix, a factor of safety of 1.25 for beam bending was applied against the

expected failure load of the connection based on current design methods. This was done to reduce the possibility of beam failures, however, as a result, the beam rotation target of 0.03 radians was not able to be achieved. The location of the concentrated load away from midspan was selected to maximize the end rotation. Two beam lengths of 18 ft. and 26 ft. were chosen to simplify the test setup. The beam sections and span are listed in Table 19.

Table 18: Single-Plate Shear Connection Test Matrix

Specimen	Bolts	a	l_{eh}	l_{ev}	t_p	d_p	Type
---	---	in	in	in	in	in	---
2A	(2) 3/4" DIA. A490-X	3	1 1/2	1	3/8	5	Conventional
2B	(2) 3/4" DIA. A490-X	3	1	1	3/8	5	Extended[1]
2C	(2) 1" DIA. A490-X	3	1 1/4	1 1/4	1/2	5.5	Extended[1]
2D	(2) 3/4" DIA. A490-X	9	1	1	3/8	5	Extended[2]
2E	(2) 1" DIA. A490-X	9	1 1/4	1 1/4	1/2	5.5	Extended[2]
5A	(5) 3/4" DIA. A490-X	3	1 1/2	1	3/8	14	Conventional
5B	(5) 3/4" DIA. A490-X	3	1	1	3/8	14	Extended[1]
5C	(5) 1" DIA. A490-X	3	1 1/4	1 1/4	1/2	14.5	Extended[1]
5D	(5) 3/4" DIA. A490-X	9	1	1	3/8	14	Extended[2]
5E	(5) 1" DIA. A490-X	9	1 1/4	1 1/4	1/2	14.5	Extended[2]

[1] Extended because $l_{eh} < 2d$
[2] Extended because $l_{eh} < 2d$ and $a > 3.5"$

Table 19: Beam Data for the Single-Plate Shear Connection Experiments

Specimen	Section	t_w	Span
---	---	in	ft
2A	W10×77	0.53	18
2B	W8×58	0.51	18
2C	---	---	---
2D	W8×21[1]	0.625[1]	18
2E	W10×77	0.53	18
5A	W18×130	0.67	26
5B	W18×130	0.67	26
5C	W18×143	0.73	26
5D	W18×143	0.73	26
5E	W18×76	0.425	26

[1] 3/8 in. cheek plate installed on beam web

Materials and Test Setup

Figure 25 shows the general test-setup. Each column was used for two specimens with a connection plate welded to each flange. The columns were bolted to a fixture that was tied to the strong floor and secured laterally with diagonal braces.

The welds between the column and the connection plate were sized as $(^5/_8)t_p$ per the AISC *Manual*. Specifically, a 1/4 in. fillet weld was specified for the specimens with 3/8 in. thick plate and a 5/16 in. fillet weld was specified for the specimens with a 1/2 in. thick plate. However, after specimens 2A and 2B failed by weld shear, the welds on the remaining specimens with 3/8 in. thick plate (i.e., 2D, 5A, 5B, and 5D) were reinforced with two additional lines of weld on each side. The cause of the failure by weld shear was not determined. Several explanations are possible including

problems related to the welding process, problems related to the model that has been adopted to develop the plate strength, or inconsistent overstrength between the plate and weld.
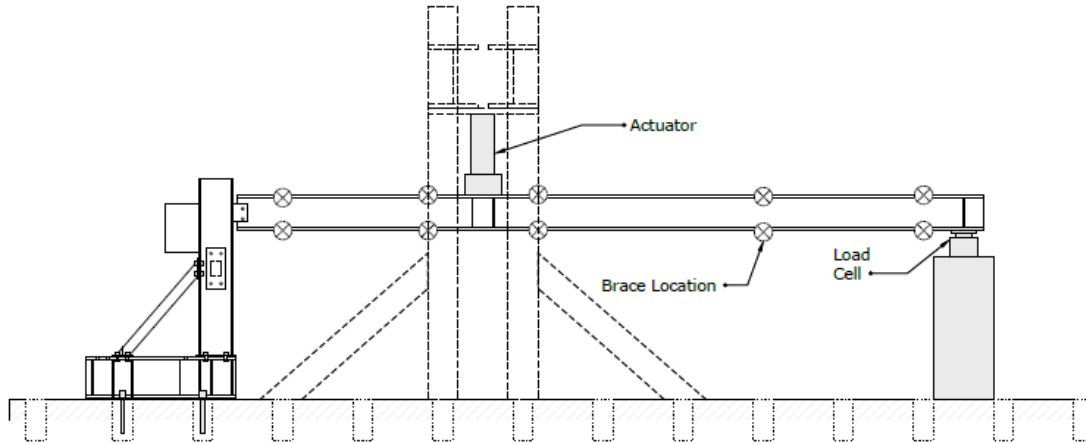
Figure 25: Test Setup

Lateral bracing was provided at a maximum of 6 ft. spacing using rods with ball-bearing ends on both sides of the beam's top and bottom flange as shown in Figure 26. The bracing rods were fastened to support frames that are anchored to the strong floor. The bracing rods allow the beam to deflect downwards but not laterally as described by Yarimci et al. (1967). The braces, however, were not strong enough to handle the large demands placed upon them after buckling of the plate. Two specimens (2E and 5C) exhibited a failure mode than included beam twist. In the subsequent tests of specimens 5A, 5B, 5D and 5E, the lateral brace nearest the connection was replaced with a pair of vertically oriented wide flange steel shapes which provided more substantial bracing (Figure 27). A minor stick-slip response due to friction at this brace is seen in the behavior of these specimens.

The beam was loaded at 6 ft. from the bolt line for all tests using an actuator installed on a reaction frame anchored to the floor. The other end of the beam was supported on a pedestal and load cell. A pair of stiffeners was welded to the beam at the point of load application and another pair was welded at the end reaction. All wide flange sections were specified as A992. Some of the specimens were designed to use the same beam, with one connection on either end of the beam. However, yielding of the beam occurred in some specimens preventing further use of the beam. New holes were drilled in the opposite end of beams designed for only one specimen to complete some tests. However, no available beam was suitable for specimen 2C and thus that connection was not tested. Table 19 lists the beams that were used in the experiment.

Figure 26: View from tail end of beam showing lateral bracing (Specimen 5A)

All bolts were specified as ASTM F3125 Gr. A490. The faying surfaces were cleaned with a wire brush prior to assembly and the bolts were installed to a snug-tight condition with a few impacts of an impact wrench.

The material used for the connection plates was specified as A572 Gr. 50 and sourced from two heats of steel, one for each plate thickness. Extra plate material of each thickness was supplied for tensile coupon testing. The yield strength and ultimate strength were determined in accordance with ASTM E8 (ASTM E8 / E8M-16ae1 2016) based on the average of three coupon tests and are reported in Table 20. Note that the tensile strength of the 1/2 in. thick plate was slightly lower than the minimum specified value of 65 ksi.

Table 20: Tensile Coupon Testing Results for the Single-Plate Shear Connections

Nominal Plate Thickness (in.)	Measured Plate Thickness (in.)	F_y (ksi)	F_u (ksi)
3/8	0.373	56.9	78.9
1/2	0.502	56.7	63.5

The bolts used for the single-plate shear connection in the experiments were sourced from two batches, one for each diameter. Extra bolts were tested in shear (threads excluded from the shear plane) at the University of Cincinnati. The shear strength of the bolts is reported in Table 21 based on the average of two tests.

Table 21: Bolt Shear Testing Results

Nominal Bolt Diameter (in.)	Nominal Shear Strength, $F_{nv}A_b$ (kips)	Measured Shear Strength (kips)
3/4	37.1	46.8
1	66.0	81.1

Instrumentation included: 1) load cell and LVDT installed in line with the actuator, 2) load cell supporting the tail end of the beam, 3) two LVDTs at the connection, and 4) 12 optical tracking markers at the connection. The instrumentation at the connection is shown in Figure 27. The LVDTs at the connection were separated by 6 in. with the LVDT nearer the column located directly above the bolt line. These two displacement measurements allow for calculation of beam rotation. The optical tracking markers served as a supplementary measurement of beam rotation as well as other connection deformations.

Additional data was computed from the recorded data. The additional data includes: reaction at the connection, Eq. (45); moment at the bolt line, Eq. (46); and moment at the column face (weld), Eq. (47). These equations were derived from statics. Horizontal distances and beam weights are listed in Table 22. The beam weight was estimated based on data recorded from the load cell located at the tail when the beam was let down from cribbing and thus includes the weight of all attached bracing. Note that R_{tail} is the total reaction, including that due to the weight of the beam and that a positive value of moment indicates that the point of zero moment is located in the direction of the column face, while a negative value of moment indicates that the point of zero moment is located in the direction of the beam tail.

$$R = P_{actuator} + W_{beam} - R_{tail} \tag{45}$$

$$M_{bolts} = P_{actuator}\left(x_{actuator} - x_{bolts}\right) + W_{beam}\left(x_{beam} - x_{bolts}\right) - R_{tail}\left(x_{tail} - x_{bolts}\right) \tag{46}$$

$$M_{weld} = P_{actuator}\left(x_{actuator} - x_{column\ face}\right) + W_{beam}\left(x_{beam} - x_{column\ face}\right) - R_{tail}\left(x_{tail} - x_{column\ face}\right) \tag{47}$$

Table 22: Horizontal distances and beam weights

Specimen	$x_{column\ face}$	x_{bolts}	$x_{actuator}$	x_{beam}	x_{tail}	W_{beam}
---	in.	in.	in.	in.	in.	kips
2A	9	12	84	122.25	228	2.2
2B	9	12	84	130.25	228	1.8
2C	---	---	---	---	---	---
2D	3	12	84	130.25	228	1.0
2E	3	12	84	122.5	228	2.2
5A	9	12	84	177.25	324	3.9
5B	9	12	84	177.75	324	3.9
5C	9	12	84	170.375	324	4.4
5D	3	12	84	170.5	324	4.4
5E	3	12	84	170.375	324	2.3

Note: distances measured from a fixed point on the strong floor

At the start of each test, the specimen was initially loaded with two cycles up to 2 kips applied load. Instruments were checked during the first cycle. The second cycle was used to confirm the synchronization of data recorded by separate devices. Following these initial cycles, the specimen was loaded in displacement control at a rate of 0.1 in./min (of the actuator) until failure.

Figure 27: Instrumentation at the connection (Specimen 5D)

Results

Plots of results are presented in Appendix A, plots include:
- Beam deflection at bolt line versus beam end reaction
- Beam end rotation versus beam end reaction
- Moment at the bolt line and column face versus beam end rotation
- Eccentricity at the bolt line (M_{bolts}/R) versus beam end reaction
- Moment at the bolt line versus beam end reaction (constructed as described previously but without resistance factors and using measured material properties).

A wide variety of behavior was observed during testing of the specimens. The types of damage observed for each specimen are listed in Table 23. Note that minor damage (e.g., bearing deformation on only one side of the connected material) and damage that clearly occurred after a loss of load carrying capacity was not included. Some damage resulted in loss of load carrying capacity, while others did not. For example, the first observed damage for specimen 2E was flexural yielding of the plate at the column face, which occurred at approximately half the peak load achieved during the experiment. Subsequent damage, including additional yielding of the plate near the bolt group, plate buckling, bolt hole ovalization, and necking of the top of the plate at the column face occurred as the load continued to rise. The test of specimen 2E was halted after approximately 3 in. of deflection due an overstressing of the lateral bracing.

Table 23: Observed damage in single-plate shear connection tests

Specimen	Observed Damage[a]
2A	**Weld rupture**, plate yielding, bolt hole ovalization (plate)
2B	**Weld rupture**, **bolt shear rupture**[b], plate yielding, bolt hole ovalization (plate), flexural yielding (beam)
2C	---
2D	**Flange local buckling (beam)**, flexural yielding (beam and plate), plate buckling
2E	Plate yielding, plate buckling, plate necking, bolt hole ovalization (plate and beam web)
5A	**Bolt shear rupture**, **tearout (plate)**, plate yielding, bolt hole ovalization (plate)
5B	**Bolt shear rupture**, **tearout (plate)**, plate yielding, bolt hole ovalization (plate)
5C	**Beam twist**, bolt hole ovalization (plate), plate yielding, **weld rupture**
5D	**Bolt shear rupture**, **tearout (plate)**, plate yielding, plate buckling, bolt hole ovalization (plate)
5E	Flexural yielding (beam)

[a] Bolded items occurred at specimen failure (i.e., loss of load carrying capacity)
[b] Only one of the two bolts ruptured

Strength Evaluation

Few specimens failed in the expected manner based on the design procedure. The reason for this is evident in the observed progression of damage and measurements of the eccentricity at the bolt line. The design method presented in the AISC *Manual* for extended single-plate shear connection relies on lower bound theory and specifically an assumption that the point of zero moment is located at the face of the support. This is a logical simplifying assumption since it matches the typical assumption for design of the supporting member (Muir and Hewitt 2009). However, the assumption will not be accurate when the supporting member is able to provide rotational restraint, such as was the case for these specimens. Significant moment built up at the column face shifting the location of the point of zero moment towards the bolt line. The effect was to reduce the eccentricity on the bolt group from what was assumed in design. As a result, the connections were stronger than anticipated in addition to not failing the in expected manner.

The design strength computed using nominal properties is listed for each specimen in Table 24 along with the peak reaction from the experiment, R_{exp}. For these calculations, deformation at the bolt hole at service load was not a design consideration. The conventional specimens were treated as conventional with $e = a/2$ and the extended specimens were treated as extended with $e = a$ and the strength of the bolt group was computed using the modified instantaneous center of rotation method. Similarly, the nominal strength computed using measured properties is listed for each specimen in Table 25.

The ratio of experimental strength to design strength using nominal properties ranges from 1.71 to 6.11 (Table 24). The ratio of experimental strength to nominal strength using measured properties ranges from 1.06 to 4.67 (Table 25). This indicates that the design methods are conservative, especially since some of the specimens did not experience a connection failure. For example, the experimental strengths of specimens 2B, 2D, and 5E was limited by flexural yielding of the beam, yet these specimens still exceeded their predicted strength by a margin.

For cases where the support is able to provide rotational restraint a more efficient design approach may be to identify the location of the point of zero moment that provides the greatest connection design strength and assume the location there. For cases where the support is unable to provide

rotational restraint (e.g., a beam framing into a girder), the current design method may remain appropriate.

Table 24: Comparison on design strength using nominal properties to experimental strength.

Specimen	Design Strength, ϕR_n	Controlling Limit State	Experimental Strength, R_{exp}	$R_{exp}/\phi R_n$
	kips	---	kips	---
2A	35.7	Shear Rupture of the Plate	61.0	1.71
2B	16.1	Modified IC	49.2	3.05
2C	24.8	Modified IC	---	---
2D	5.3	Modified IC	17.5	3.28
2E	8.2	Modified IC	50.3	6.11
5A	105.6	Shear Rupture of the Plate	224.7	2.13
5B	105.0	Modified IC	223.3	2.13
5C	125.2	Shear Rupture of the Plate	237.0	1.89
5D	39.4	Modified IC	163.1	4.14
5E	62.9	Modified IC	131.5	2.09

Table 25: Comparison of nominal strength using measured properties to experimental strength.

Specimen	Nominal Strength, R_n	Controlling Limit State	Experimental Strength, R_{exp}	R_{exp}/R_n
	kips	---	kips	---
2A	57.4	Shear Rupture of the Plate	61.0	1.06
2B	25.9	Modified IC	49.2	1.90
2C	32.5	Modified IC	---	---
2D	8.6	Modified IC	17.5	2.04
2E	10.8	Modified IC	50.3	4.67
5A	170.0	Shear Rupture of the Plate	224.7	1.32
5B	158.5	Interaction Strength of the Plate	223.3	1.41
5C	163.8	Shear Rupture of the Plate	237.0	1.45
5D	64.4	Modified IC	163.1	2.53
5E	82.5	Modified IC	131.5	1.59

However, not all of the conservativeness is due to the assumption regarding the point of zero moment. Specimens 2A, 5A, and 5C were predicted to fail by shear rupture of the plate. This limit state is not affected by the assumption of the point of zero moment, yet these connections also exceeded their predicted strength, albeit by a lower margin than some of the others. Conservativeness in the evaluation of the shear rupture limit state may be related to the difference between the net area and physical failure paths, a discrepancy similar to that addressed by the alternative tearout lengths investigated in this work.

Since the eccentricity that the bolt groups experienced was less than expected, the experiments did not provide strong validation of the modified instantaneous center of rotation method. However, some observations regarding the strength of the bolt group can be made. The poison bolt method was shown to be conservative with all specimens except 5E (which failed in flexural yielding of the beam) exhibiting pairs of beam end reaction and moment at the bolt line outside of the poison bolt interaction strength. The beam end reaction and moment at the bolt line for specimen 2D also exceeded the interaction strength computed from the modified instantaneous center of rotation method. This observation may indicate that the modified instantaneous center of rotation method is also conservative.

Specimens 5A and 5B failed at a similar load and in a similar manner, clearing indicating that small edge distances do not necessarily reduced the strength of the connection. Both of these specimens failed in tearout of the bottom bolt and shear rupture of the other bolts. This confirms that such mixed failures are possible. It also highlights a potential issue with the recommended design checks for conventional type connections. Current recommendations in the AISC *Manual* state that plate bearing and tearout are to be checked in accordance with AISC *Specification* section J3.10 assuming the reaction is applied concentrically. It may be interpreted that only bearing and tearout need to be considered for this check. However, based on the results of specimens 5A and 5B, the strength of the connection should not exceed the strength of the bolt group assuming the reaction is applied concentrically and considering all applicable limit states (bearing, tearout, and bolt shear rupture). A comparison of strength for specimens 5A and 5B is presented in Table 26. The experimental strength was less than that calculated assuming only bolt shear rupture and far less than that calculated assuming only bearing and tearout. Computing the strength for all applicable limits, however, gives an accurate and safe estimate of the experimental strength. Note that for these calculations, bearing and tearout were computed assuming deformation at the bolt hole at service load is not a design consideration.

Table 26: Comparison of strength for specimens 5A and 5B.

Condition	Strength
	kips
Experimental strength, specimen 5A	224.7
Experimental strength, specimen 5B	223.3
Calculated strength assuming concentric load and only bolt shear rupture	234.0
Calculated strength assuming concentric load and only bearing and tearout	291.0
Calculated strength assuming concentric load and bolt shear rupture, bearing, and tearout	213.4

Specimen 5D also failed in a combination of tearout of the bottom bolt and bolt shear rupture of the remaining bolts. However, specimen 5D differs in that the experimental strength was less than that for a concentrically loaded bolt group, the measured eccentricity at the bolt group was large enough to induce significant moment into the bolt group (albeit less than that assumed in design) and the direction of tearout of the bottom bolt was at a diagonal as opposed to straight down for specimens 5A and 5B. The experimental strength for this connection was in between that for the standard and modified instantaneous center of rotation methods, but at an eccentricity where the strength per the two methods was relatively similar. So, while this specimen exhibited a failure that combined bolt shear rupture and tearout in an eccentrically loaded bolt group, it provided limited information on the validity of the modified instantaneous center of rotation method. Further testing on eccentrically loaded bolt groups with small edge distances is recommended to provide the necessary data. Such testing should consider large eccentricities where the impact of tearout is likely to be greater and different experimental setups where the eccentricity can be controlled directly.

Chapter 8: Conclusions and Recommendations

A multifaceted investigation of the limit state of tearout and its impact on the design of steel bolted connections has been conducted. Previously published experimental data was evaluated and supplemented with new experimental data to assess the accuracy of current provisions as well as potential alternative provisions.

Through the evaluation of existing and new experimental data on concentrically loaded connections, it was determined that 1) the difference between ultimate load and load at 1/4 in. deformation for specimens failing in tearout is less than implied by current equations, 2) current equations for tearout strength underpredict the load at 1/4 in. deformation, and 3) current equations are not consistent across edge distances and tend to underpredict the strengths at smaller edge distances. Accordingly, increased accuracy in design can be achieved by replacing Equations J3-6c and J3-6d in the AISC *Specification* (AISC 2016) with Eq. 15, which utilizes l_{v1}. The equation with l_{v1} is selected since it provides somewhat better results over a wider range of bolt hole types, particularly short-slotted holes. The same equation but with l_{v2} in lieu of l_{v1} (i.e., Eq. 16) would provide similar benefits, and the relative simplicity of calculating l_{v2} may be preferable. A reliability analysis described in Chapter 5 confirmed that both Eq. 15 and Eq. 16 provide a consistent and sufficient level of reliability.

An example of the difference between the current and proposed equations is seen in Figure 28. The plotted case is for a single 3/4 in. diameter bolt in a standard hole. The minimum edge distance permitted by the AISC *Specification* (1 in.) is shown with a dashed vertical line. Figure 28(a) demonstrates that the equations with the alternative tearout lengths (i.e., Eq. 15 and 16) offer additional strength compared to the current equation when deformation at the bolt hole at service load is a design consideration. The difference in strength when deformation at the bolt hole at service load is not a design consideration is less.

(a) when deformation at the bolt hole at service load is a design consideration

(b) when deformation at the bolt hole at service load is not a design consideration
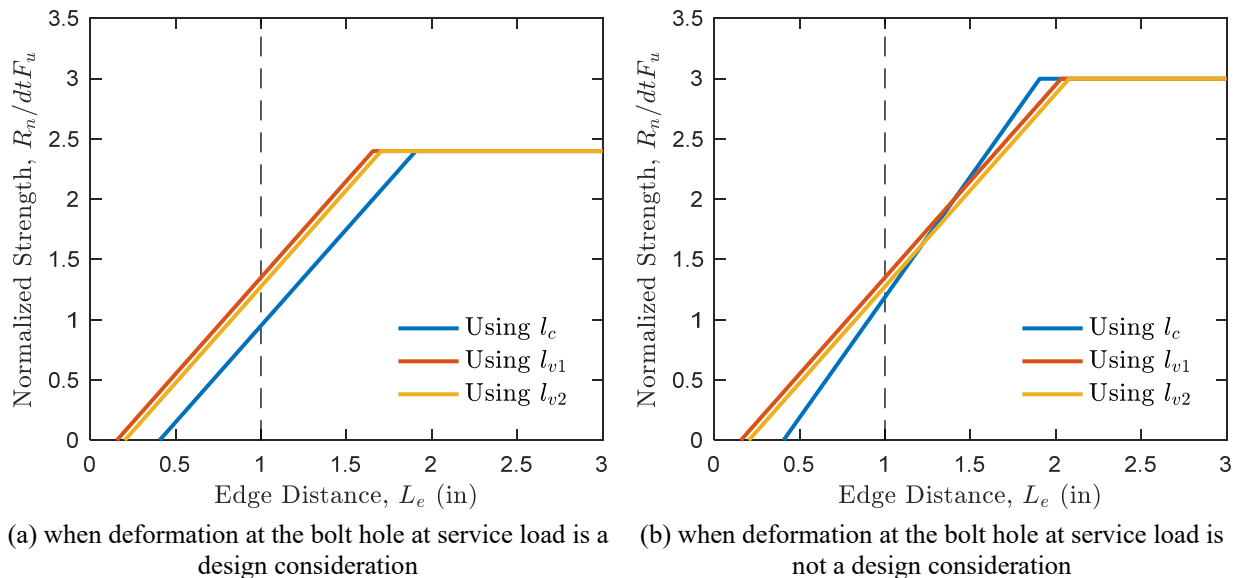
Figure 28. Comparison of bearing and tearout strength equations for a 3/4 in. diameter bolt in a standard hole

While Eq. 15 provides increased accuracy over current equations, the computation of the alternative tearout lengths is somewhat more complicated than the computation of the clear distance. This is especially true for eccentrically loaded bolt groups which pose an additional challenge since the direction of force varies from bolt to bolt. Neither of the alternative tearout lengths are well defined nor have they been validated for loads at an angle. Additional development and validation are necessary for eccentrically loaded connections and the simplicity of the clear distance may continue to be desirable for these situations.

The following additional conclusions regarding concentrically loaded bolt groups can be made from this work:

- Tearout impacts the strength of bolt groups, even for cases of multiple bolts in a row.

- The current equation for tearout strength when deformation at the bolt hole at service load is a design consideration (i.e., load at 1/4 in. deformation) is conservative, especially for shorter edge distances. On average, the current equation underestimates the experimental strength by 20-25%.

- The ultimate load for the limit state of tearout is approximately 5% larger than the load at 1/4 in. deformation, significantly less than the 25% implied by current provisions.

- Bolt tightening increases the load at 1/4 in. deformation by an average of 8% for a pretensioned bolt condition over an untightened bolt condition. No clear effect of bolt tightening was found at the ultimate load.

- Two alternative tearout lengths, l_{v1} and l_{v2}, were investigated for their potential to improve the accuracy of design equations. Strength equations using these alternative tearout lengths were found to be more accurate than the current equations which use the clear distance, l_c, with a mean test-to-predicted ratio closer to unity and a smaller coefficient of variation for all examined cases.

- Design equations with l_{v1} and l_{v2} are similarly accurate for connections with standard and oversize holes. The design equation using l_{v2} was found to be somewhat unconservative for short-slotted holes and holes with clearance greater than oversize. The design equation using l_{v1} was found to be accurate over the entire range of hole types investigated.

- The proposed equations provide a sufficient and consistent level of reliability across a wide range of parameters.

- An alternative design method in which reduction factors are used on bearing and bolt shear rupture strength was developed. The method allows the tearout check to be removed by reducing strength, which can be beneficial in some design cases.

Experimental testing on nine single-plate shear connections was also conducted. The specimens included those with minimum edge distances were the impact of tearout was expected to be most pronounced per current design methods. These tests demonstrated the conservativeness of the current design methods for conditions where the supporting member is able to provide rotational restraint to the connection plate. They also showed that small edge distances do not necessarily reduce the strength of a single-plate shear connections. However, the impact of tearout is expected to be greater for configurations that behave more like the design assumption (i.e., large bolt group

eccentricity). It is noted that larger than minimum edge distances may be necessary to meet design requirements for structural integrity such as those in Section B3.9 of the AISC *Specification*.

The following additional conclusions regarding single-plate shear connections and eccentrically loaded bolt groups can be made from this work:

- A modified version of the instantaneous center of rotation method that considers the effect of tearout was developed. The results indicate that this method is promising, but further experimental testing is necessary to confirm its accuracy.

- It is recommended that the design method for conventional single-plate shear connections be clarified such that the reaction be no greater than the strength of the bolt group assuming the reaction is applied concentrically and considering all applicable limit states.

Acknowledgements

References

AISC. (1923). *Standard Specification for Structural Steel Buildings*. American Institute of Steel Construction, New York, NY.

AISC. (1936). *Specification for the Design, Fabrication and Erection of Structural Steel for Buildings*. American Institute of Steel Construction, New York, NY.

AISC. (1961). *Specification for the Design, Fabrication and Erection of Structural Steel for Buildings*. American Institute of Steel Construction, New York, NY.

AISC. (1978). *Specification for the Design, Fabrication and Erection of Structural Steel for Buildings*. American Institute of Steel Construction, Chicago, IL.

AISC. (1986). *Load and Resistance Factor Design Specification for Structural Steel Buildings*. American Institute of Steel Construction, Chicago, IL.

AISC. (1993). *Load and Resistance Factor Design Specification for Structural Steel Buildings*. American Institute of Steel Construction, Chicago, IL.

AISC. (1999). *Load and Resistance Factor Design Specification for Structural Steel Buildings*. American Institute of Steel Construction, Chicago, IL.

AISC. (2010). *Specification for Structural Steel Buildings*. American Institute of Steel Construction, Chicago, IL.

AISC. (2016). *Specification for Structural Steel Buildings*. American Institute of Steel Construction, Chicago, IL.

AISC. (2017). *Steel Construction Manual, 15th Edition*. American Institute of Steel Construction, Chicago, Illinois.

ASME. (2006). *Fasteners for Use in Structural Applications*. The American Society of Mechanical Engineers.

ASME. (2017). *Design of Below-the-Hook Lifting Devices*. American Society of Mechanical Engineers.

Astaneh, A., McMullin, K. M., and Call, S. M. (1988). *Design of Single Plate Shear Connections*. University of California, Berkeley, California.

ASTM E8 / E8M-16ae1. (2016). *Standard Test Methods for Tension Testing of Metallic Materials*. ASTM International, West Conshohocken, PA.

Badawi, H. E.-D. S. (1983). "Behaviour of eccentric bolted shear connections." Master Thesis, McGill University, Montreal, Quebec.

Baldwin Metzger, K. A. (2006). "Experimental Verification of a New Single Plate Shear Connection Design Model." Master Thesis, Virginia Polytechnic Institute and State University, Blacksburg, VA.

Birkemoe, P. C., and Gilmor, M. I. (1978). "Behavior of Bearing Critical Double-Angle Beam Connections." *Engineering Journal*, 15(4), 7.

Brown, J. D., Lubitz, D. J., Yavor, C. C., Frank, K. H., and Keating, P. B. (2007). *Evaluation of Influence of Hole Making Upon the Performance of Structural Steel Plates and Connections*. Center for Transportation Research, The University of Texas, Austin, TX.

Cai, Q., and Driver, R. G. (2008). *End tear-out failures of bolted tension members*. Structural Engineering Report, University of Alberta, Edmonton, Alberta.

Carter, C. J., Tide, R. H. R., and Yura, J. A. (1997). "A Summary of Changes and Derivation of LRFD Bolt Design Provisions." *Engineering Journal*, 70–81.

Clements, D. D. A., and Teh, L. H. (2013). "Active Shear Planes of Bolted Connections Failing in Block Shear." *Journal of Structural Engineering*, 139(3), 320–327.

Crawford, S. F., and Kulak, G. L. (1971). "Eccentrically Loaded Bolted Connections." *Journal of the Structural Division*, Proceedings of the American Society of Civil Engineers, 97(3), 765–783.

Creech, D. D. (2005). "Behavior of Single Plate Shear Connections with Rigid and Flexible Supports." Master Thesis, North Carolina State University, Raleigh, NC.

Draganić, H., Dokšanović, T., and Markulak, D. (2014). "Investigation of bearing failure in steel single bolt lap connections." *Journal of Constructional Steel Research*, 98, 59–72.

Duerr, D. (2006). "Pinned Connection Strength and Behavior." *Journal of Structural Engineering*, 132(2), 182–194.

Ellingwood, B., Galambos, T. V., MacGregor, J. G., and Cornell, C. A. (1980). *Development of a probability based load criterion for American National Standard A58*. NBS Special Publication, National Bureau of Standards, Washington D.C.

Elliott, M. D., Teh, L. H., and Ahmed, A. (2019). "Behaviour and strength of bolted connections failing in shear." *Journal of Constructional Steel Research*, 153, 320–329.

Fisher, J. W., and Struik, J. H. A. (1974). *Guide to Design Criteria for Bolted and Riveted Joints*. Wiley, New York.

Franchuk, C. R., Driver, R. G., and Grondin, G. Y. (2002). *Block Shear Behavior of Coped Steel Beams*. Structural Engineering Report, University of Alberta, Alberta, Canada.

Frank, K. H., and Yura, J. (1981). *An Experimental Study of Bolted Shear Connections*. Department of Transportation, Washington, D.C.

Freitas, S. T. D. (2005). "Experimental research project on bolted connections in bearing for high strength steel." Thesis, Delft University of Technology, Delft.

Galambos, T. V. (1983). "Reliability of axially loaded columns." *Engineering Structures*, 5(1), 73–78.

Galambos, T. V. (1985). *Reliability of Connections, Joints and Fasteners*. Structural Engineering Report, University of Minnesota, Minneapolis, MN.

Gillett, P. E. (1978). "Ductility and Strength of Single Plate Connections." PhD Dissertation, The University of Arizona, Tucson, AZ.

Hertz, J. (2014). "Testing of Extended Shear Tab Connections Subjected to Shear." Master Thesis, McGill University, Montreal, Quebec.

Kamtekar, A. G. (2012). "On the bearing strength of bolts in clearance holes." *Journal of Constructional Steel Research*, 79, 48–55.

Karsu, B. (1995). "The load deformation response of single bolt connections." M.S. Thesis, Virginia Polytechnic Institute and State University, Blacksburg, VA.

Kennedy, D. J. L., and Aly, M. G. (1980). "Limit states design of steel structures—performance factors." *Canadian Journal of Civil Engineering*, 7(1), 45–77.

Kim, H. J., and Yura, J. A. (1999). "The effect of ultimate-to-yield ratio on the bearing strength of bolted connections." *Journal of Constructional Steel Research*, 49(3), 255–269.

Lewis, B. E., and Zwerneman, F. J. (1996). *Edge Distance, Spacing, and Bearing in Bolted Connections*. Oklahoma State University, Stillwater, OK.

Liu, J., Sabelli, R., Brockenbrough, R. L., and Fraser, T. P. (2007). "Expected Yield Stress and Tensile Strength Ratios for Determination of Expected Member Capacity in the 2005 AISC Seismic Provisions." *Engineering Journal*, AISC, 44, 15–26.

Lundberg, J. E., and Galambos, T. V. (1996). "Load and resistance factor design of composite columns." *Structural Safety*, 18(2–3), 169–177.

Man, J. C. Y., Grondin, G. Y., and Driver, R. G. (2006). *Beam-to-Column Shear Connections with Slotted Holes*. Structural Engineering Report, University of Alberta, Edmonton, Alberta.

Marosi, M. (2011). "Behaviour of Single and Double Row Bolted Shear Tab Connections and Weld Retrofits." Master Thesis, McGill University, Montreal, Quebec.

Može, P., and Beg, D. (2010). "High strength steel tension splices with one or two bolts." *Journal of Constructional Steel Research*, 66(8–9), 1000–1010.

Može, P., and Beg, D. (2011). "Investigation of high strength steel connections with several bolts in double shear." *Journal of Constructional Steel Research*, 67(3), 333–347.

Može, P., and Beg, D. (2014). "A complete study of bearing stress in single bolt connections." *Journal of Constructional Steel Research*, 95, 126–140.

Muir, L. S., and Hewitt, C. M. (2009). "Design of Unstiffened Extended Single-Plate Shear Connections." *AISC Engineering Journal*, 46(2), 67–80.

Muir, L. S., and Thornton, W. A. (2011). "The Development of a New Design Procedure for Conventional Single-Plate Shear Connections." *AISC Engineering Journal*, 48(2), 141–152.

Nissen, J. S. (2014). "Test of gusset plate connections." BEng Thesis, Technical University of Denmark, Kgs. Lyngby, Denmark.

Porter, K. A., and Astaneh-Asl, A. (1990). *Design of single plate shear connections with snug-tight bolts in short slotted holes*. Structural Engineering Materials and Mechanics, University of California at Berkeley, Berkeley, CA.

Puthli, R., and Fleischer, O. (2001). "Investigations on bolted connections for high strength steel members." *Journal of Constructional Steel Research*, 57(3), 313–326.

Research Council on Structural Connections. (1994). *Load and Resistance Factor Design Specification for Structural Joints Using ASTM A325 or A490*.

Rex, C. O., and Easterling, W. S. (2003). "Behavior and Modeling of a Bolt Bearing on a Single Plate." *Journal of Structural Engineering*, 129(6), 792–800.

Salmon, C. G., Johnson, J. E., and Malhas, F. A. (2009). *Steel Structures: Design and Behavior*. Pearson Education International.

Sarkar, D. (1992). "Design of Single Plate Framing Connections." Thesis, University of Oklahoma, Norman, OK.

Schmidt, B. J., and Bartlett, F. M. (2002). "Review of resistance factor for steel: data collection." *Canadian Journal of Civil Engineering*, 29(1), 98–108.

Segui, W. T. (2013). *Steel Design, Fifth Edition*. Cengage Learning.

Sherman, D. R., and Ghorbanpoor, A. (2002). *Design of Extended Shear Tabs*. Final Report, University of Wisconsin, Milwaukee, WI.

Teh, L. H., and Uz, M. E. (2016). "Combined Bearing and Shear-Out Capacity of Structural Steel Bolted Connections." *Journal of Structural Engineering*, 142(11).

Udagawa K., and Yamada T. (1998). "Failure Modes and Ultimate Tensile Strength of Steel Plates Jointed with High-Strength Bolts." *Journal of Structural and Construction Engineering (Transactions of AIJ)*, 63(505), 115–122.

Udagawa, K., and Yamada, T. (2004). "Ultimate Strength and Failure Modes of Tension Channels Jointed with High-Strength Bolts." Vancouver, British Columbia.

Wang, Y.-B., Lyu, Y.-F., Li, G.-Q., and Liew, J. Y. R. (2017). "Behavior of single bolt bearing on high strength steel plate." *Journal of Constructional Steel Research*, 137, 19–30.

Wing, P. C., and Harris, P. J. (1983). "Eccentrically loaded bolted beam connections." *Canadian Journal of Civil Engineering*, 10(2), 295–305.

Yarimci, E., Pura, J. A., and Lu, L. W. (1967). "Techniques for testing structures permitted to sway." *Experimental Mechanics*, 7(8), 321–331.

Appendix A: Single-Plate Shear Connection Test Results

This appendix consists of a series of figures with photographs and plots of results from the nine single-plate shear connections that were tested.

(a) Connection before testing

(b) Connection after testing
Figure 29. Photographs and Results for Specimen 2A
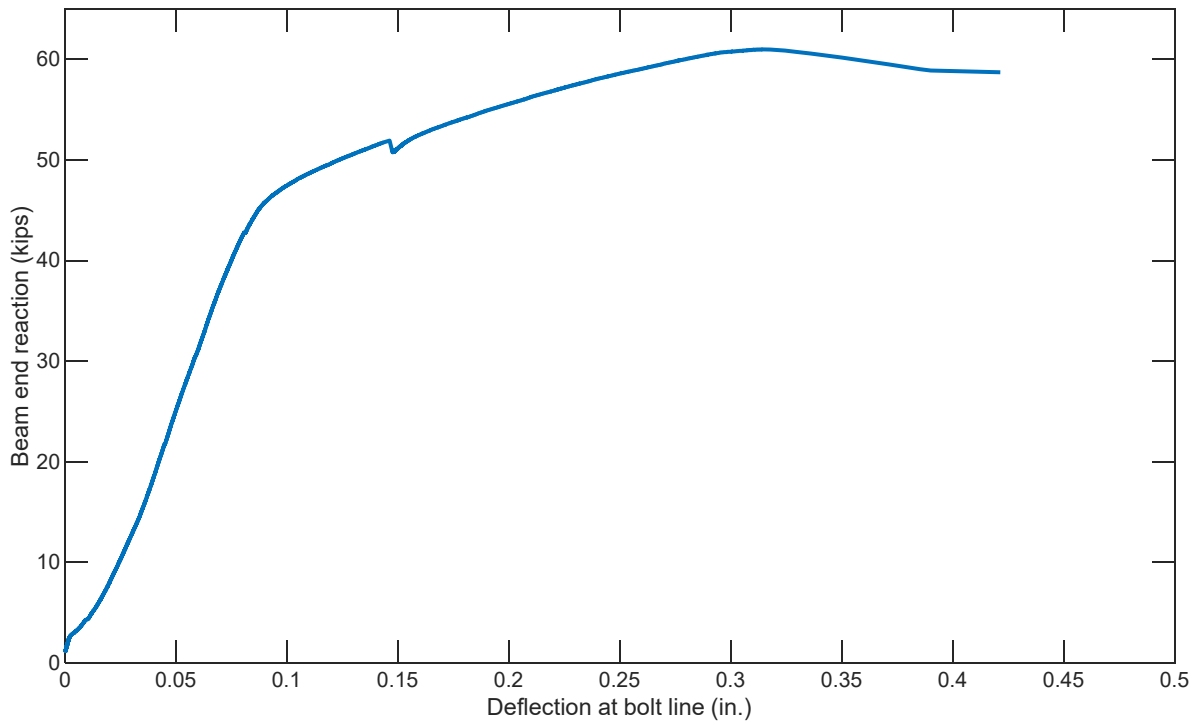
(c) Deflection at bolt line vs beam end reaction
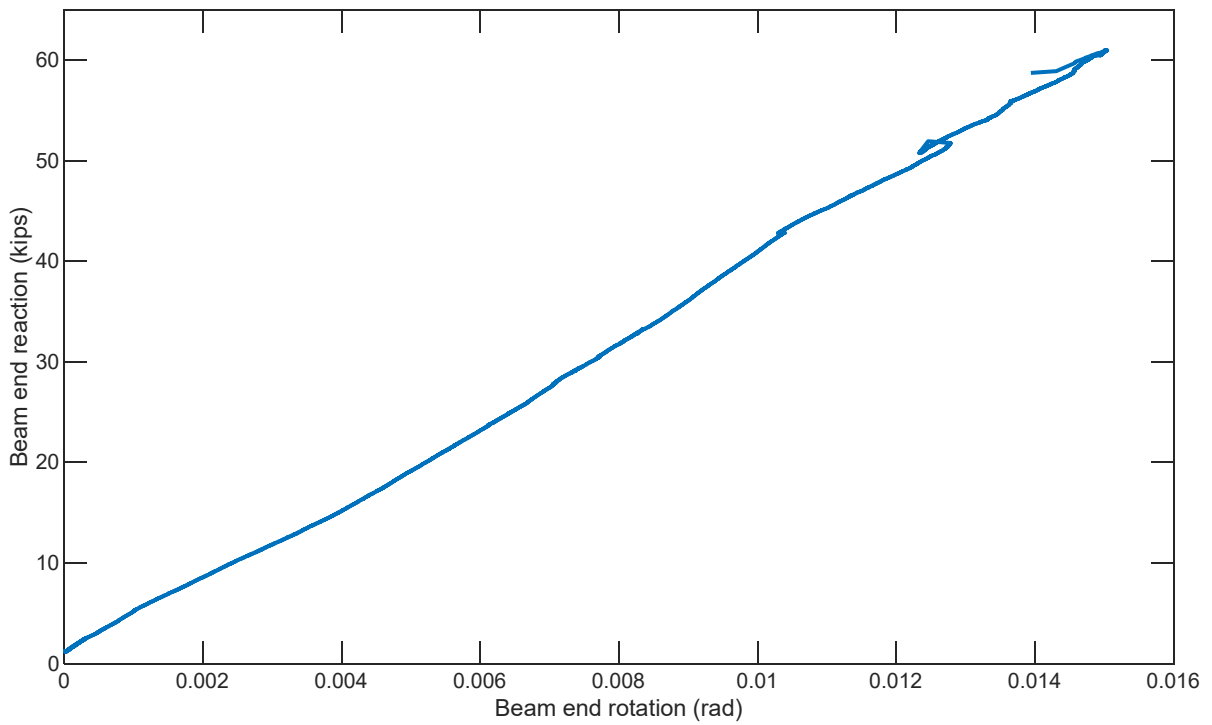
(d) Beam end rotation vs. beam end reaction
Figure 29. Photographs and Results for Specimen 2A (continued)
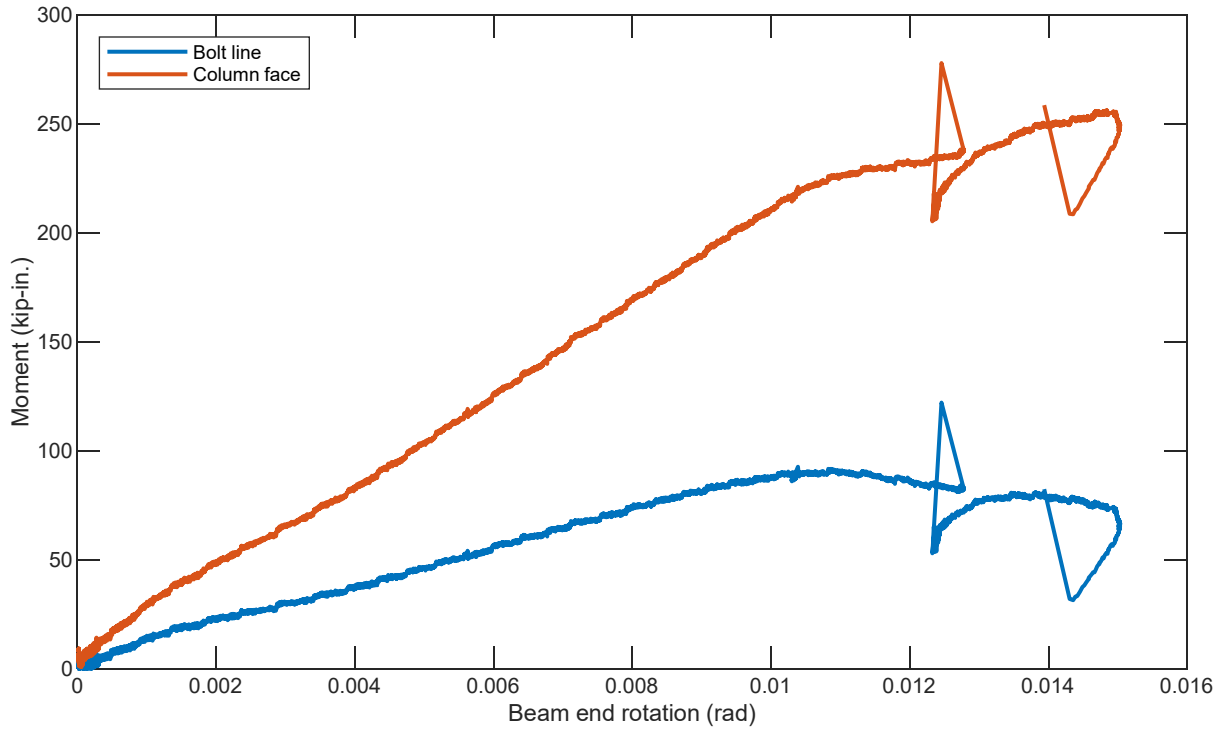
(e) Beam end rotation vs. moment at bolt line and column face
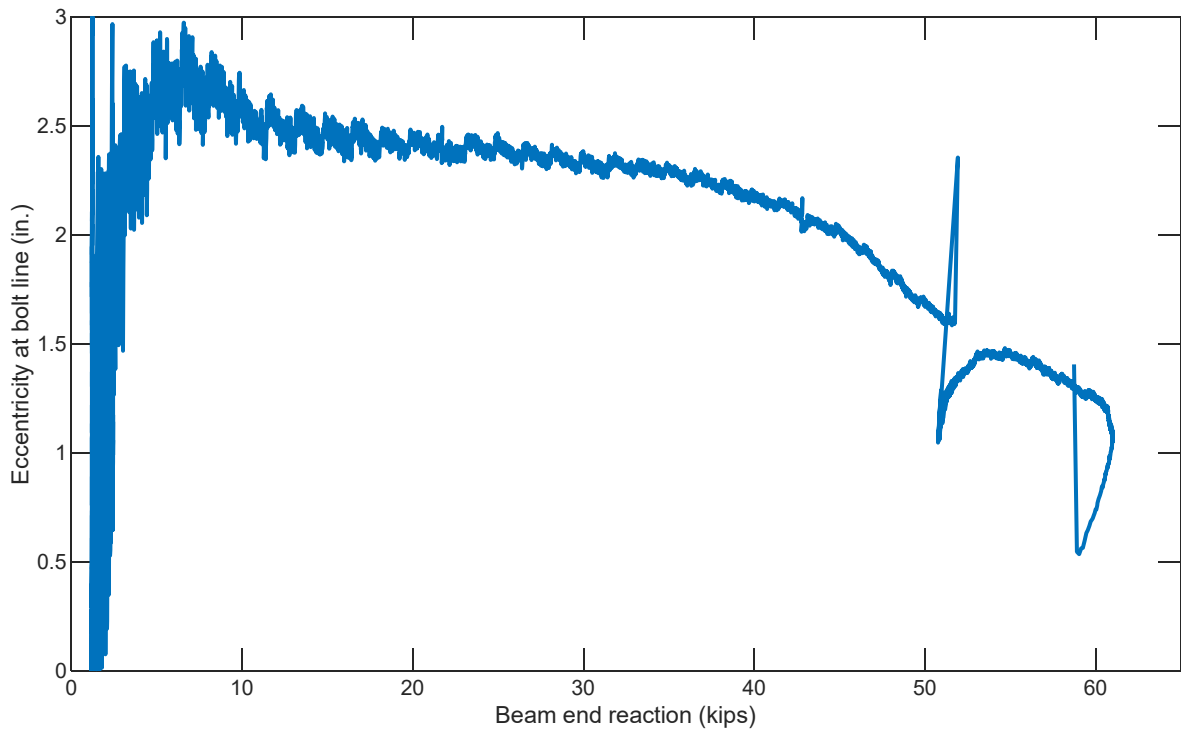
(f) Beam end reaction vs. eccentricity at bolt line
Figure 29. Photographs and Results for Specimen 2A (continued)
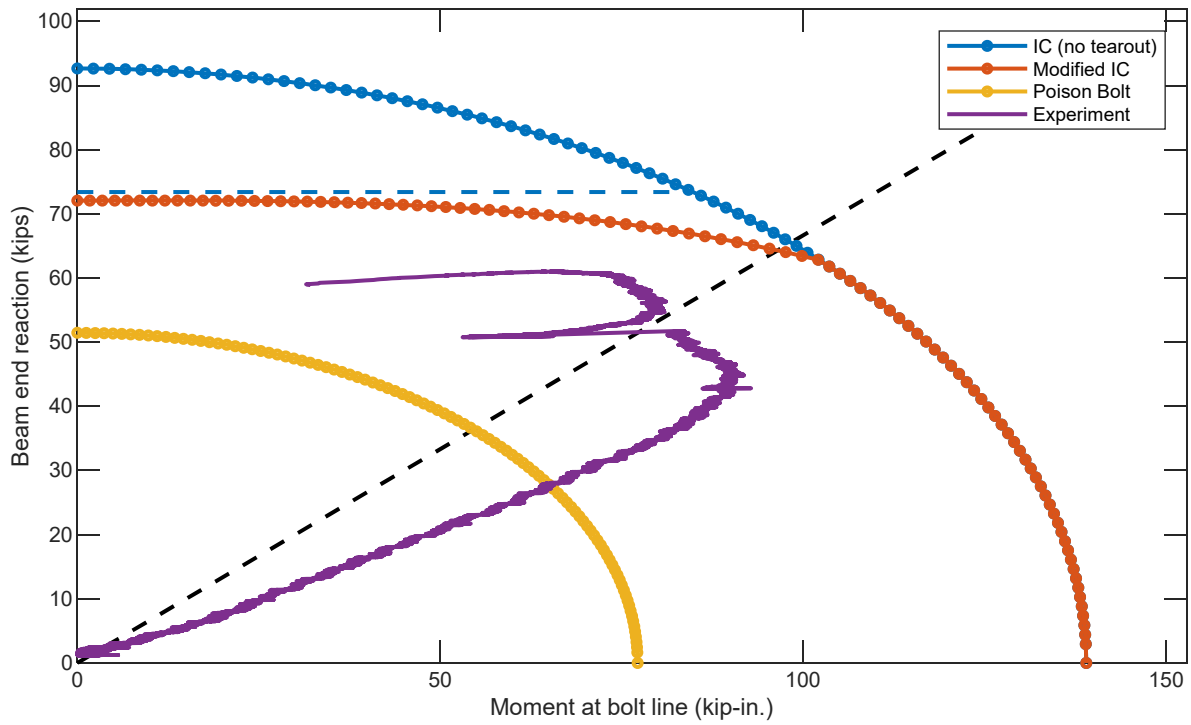
(g) Moment at bolt line vs. beam end reaction
Figure 29. Photographs and Results for Specimen 2A (continued)

(a) Connection before testing

(b) Connection after testing
Figure 30. Photographs and Results for Specimen 2B
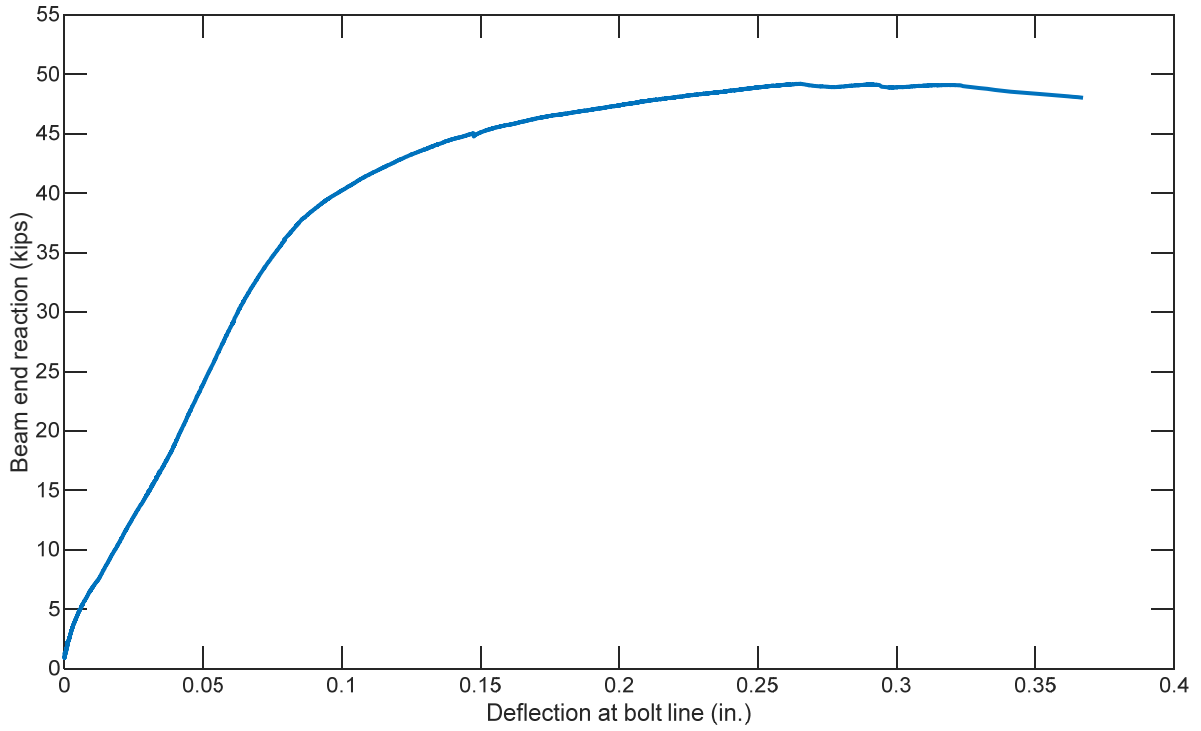
(c) Deflection at bolt line vs beam end reaction
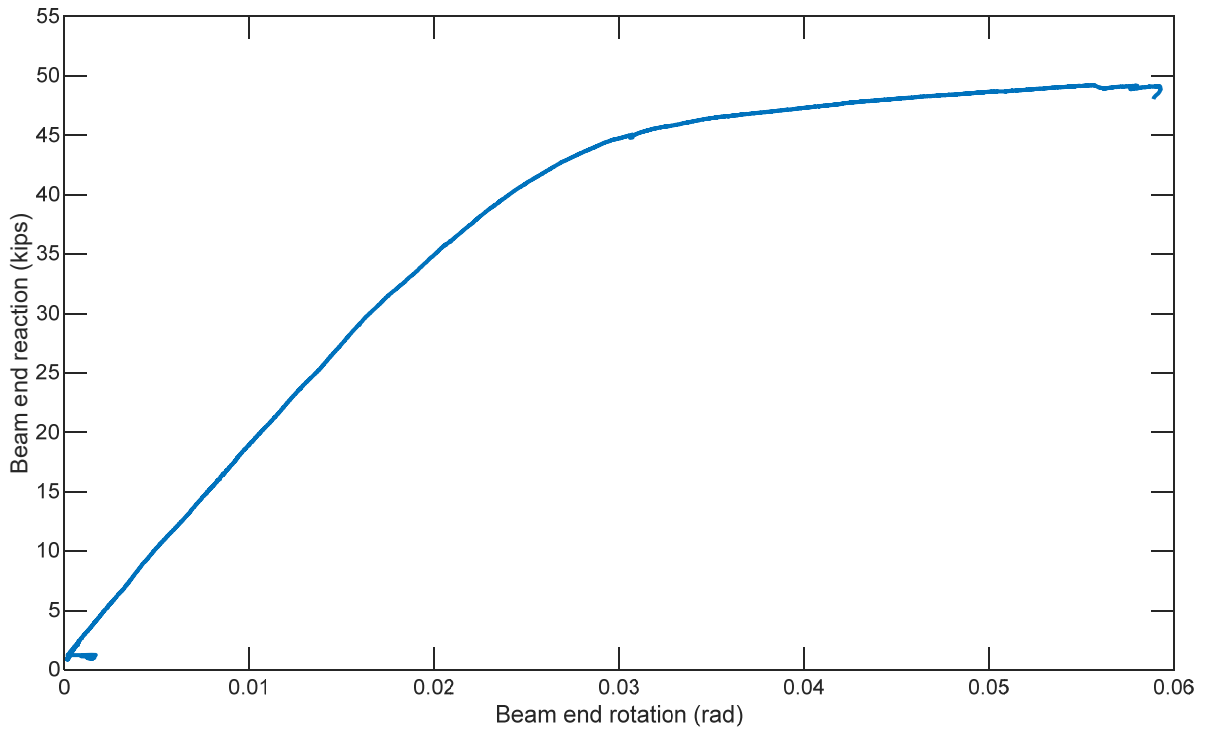
(d) Beam end rotation vs. beam end reaction

Figure 30. Photographs and Results for Specimen 2B (continued)
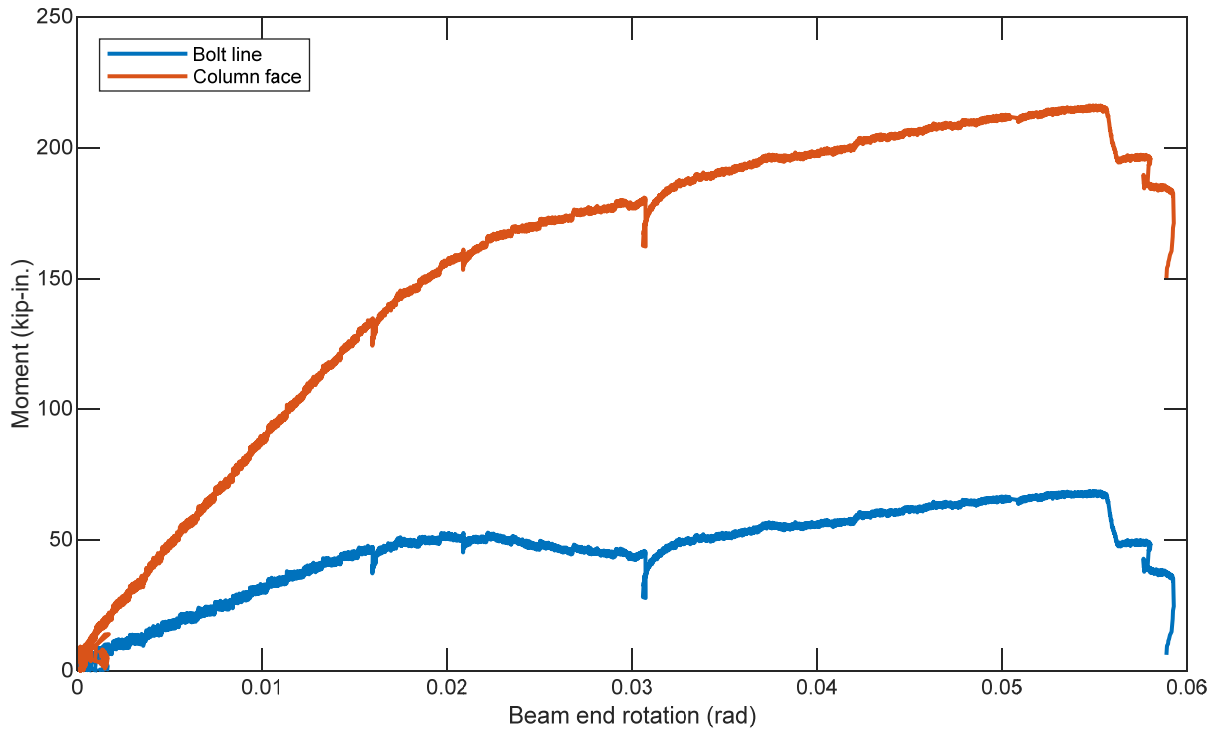
(e) Beam end rotation vs. moment at bolt line and column face
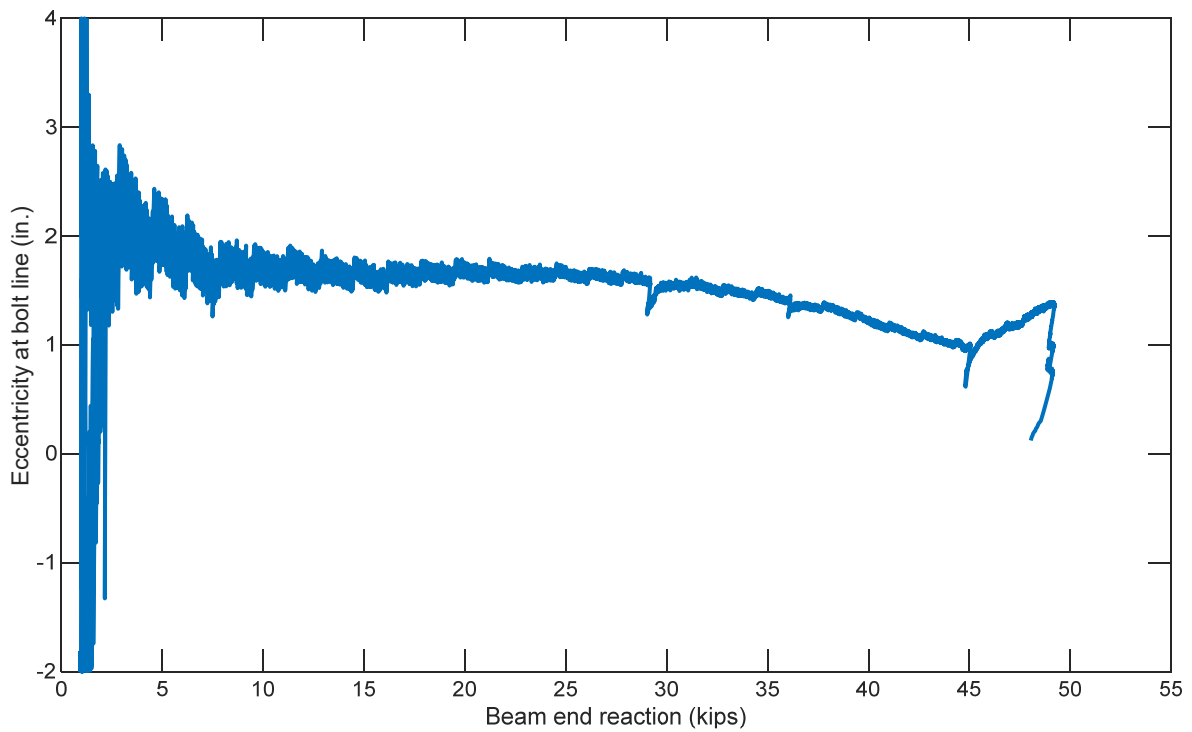
(f) Beam end reaction vs. eccentricity at bolt line
Figure 30. Photographs and Results for Specimen 2B (continued)
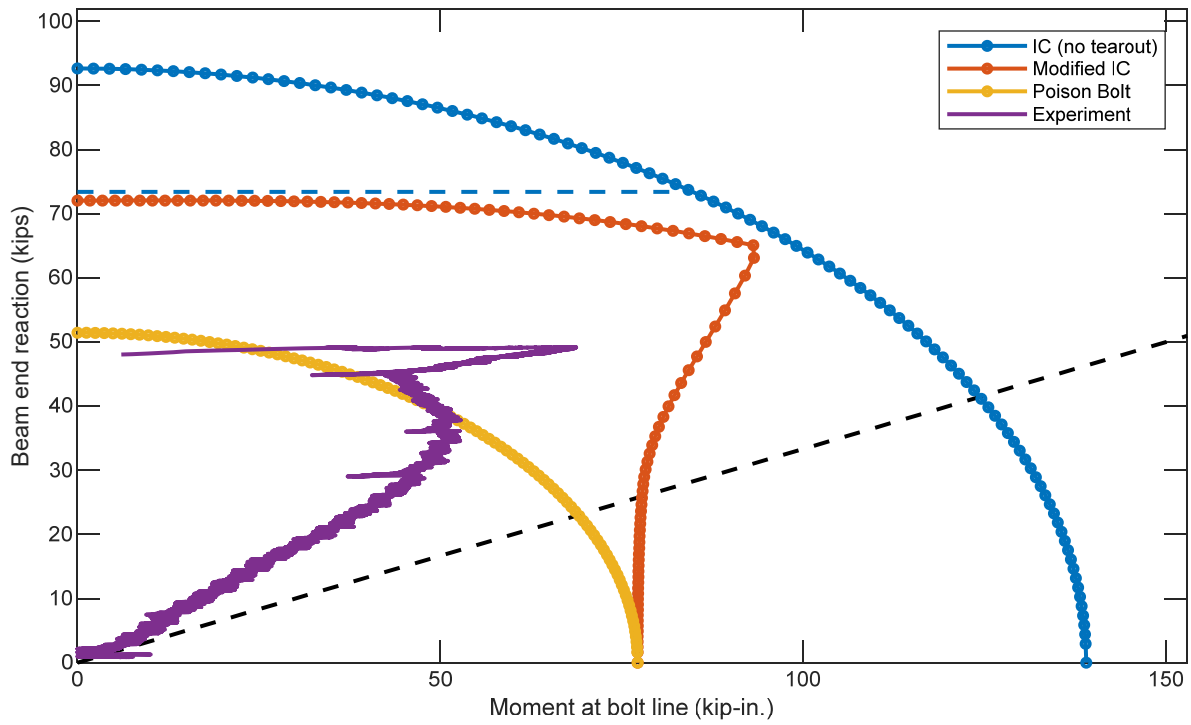
(g) Moment at bolt line vs. beam end reaction
Figure 30. Photographs and Results for Specimen 2B (continued)
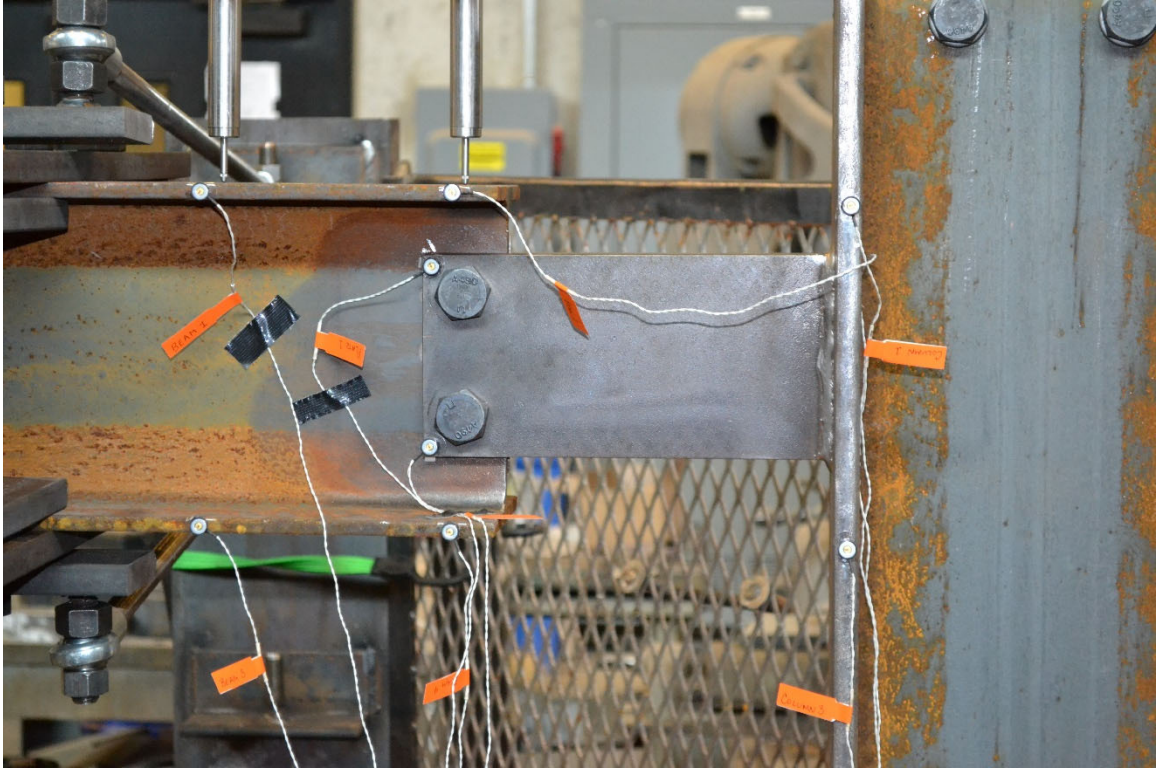
(a) Connection before testing

(b) Connection after testing
Figure 31. Photographs and Results for Specimen 2D
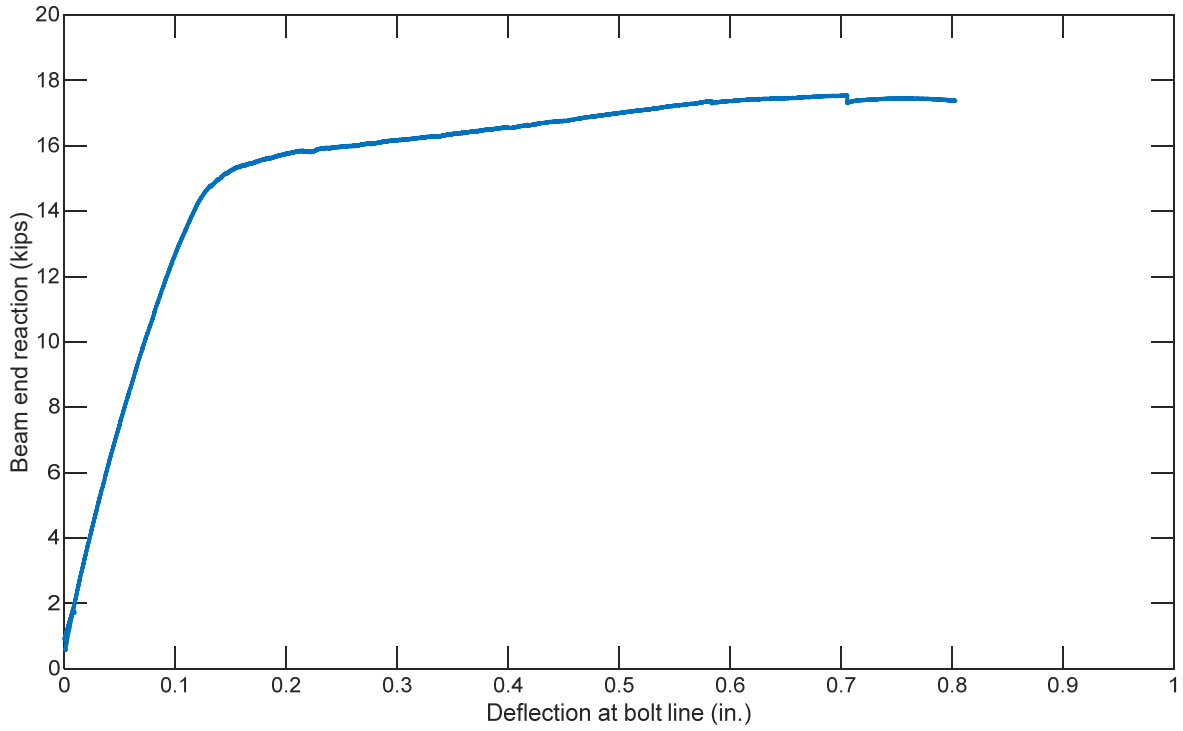
(c) Deflection at bolt line vs beam end reaction
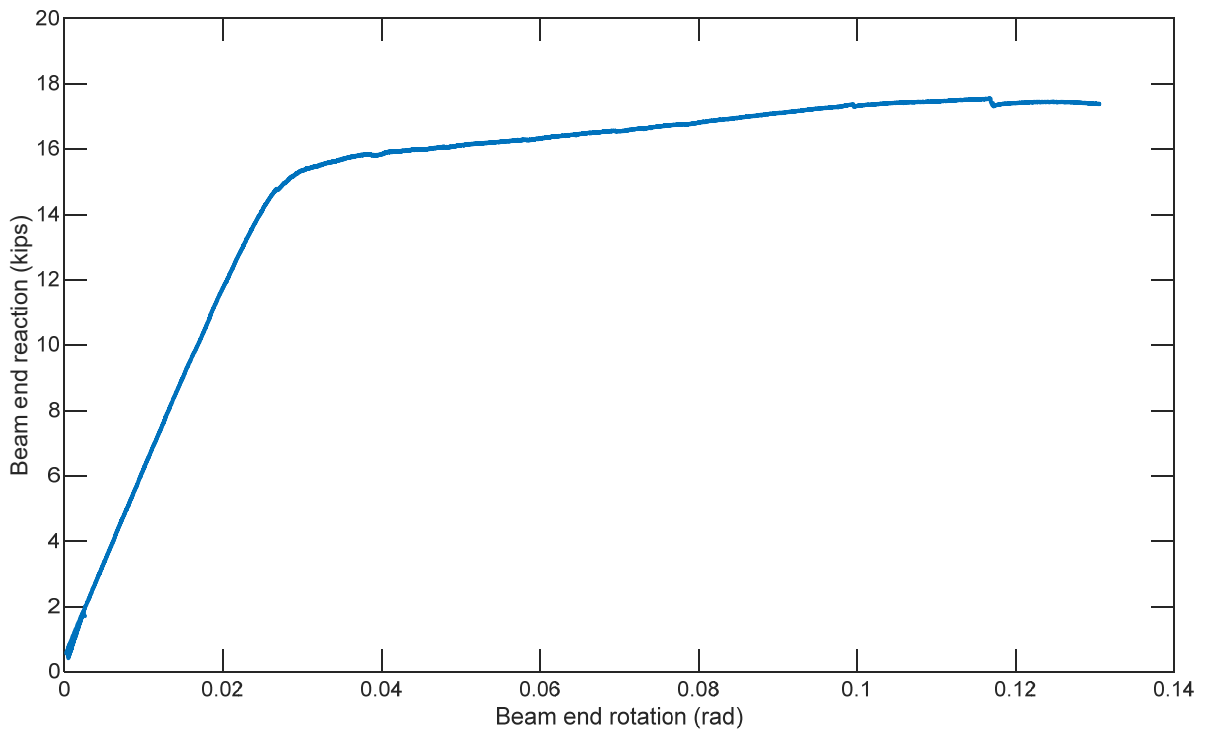
(d) Beam end rotation vs. beam end reaction
Figure 31. Photographs and Results for Specimen 2D (continued)
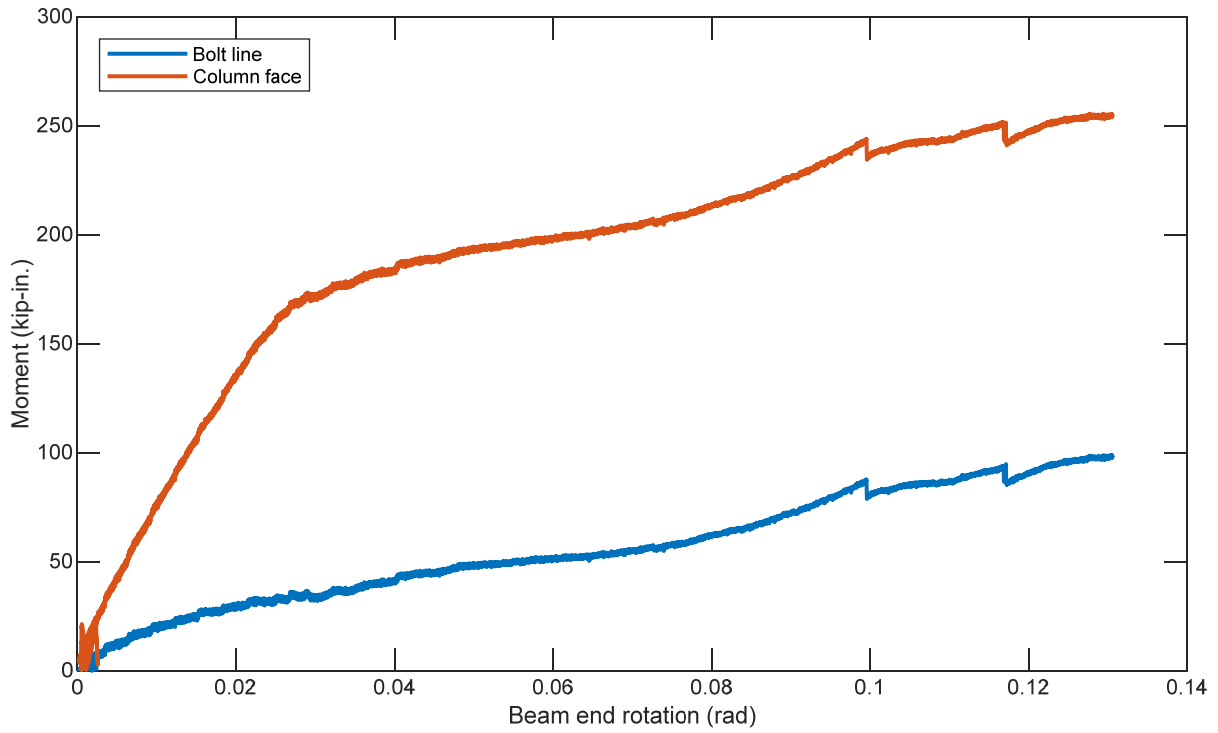
(e) Beam end rotation vs. moment at bolt line and column face
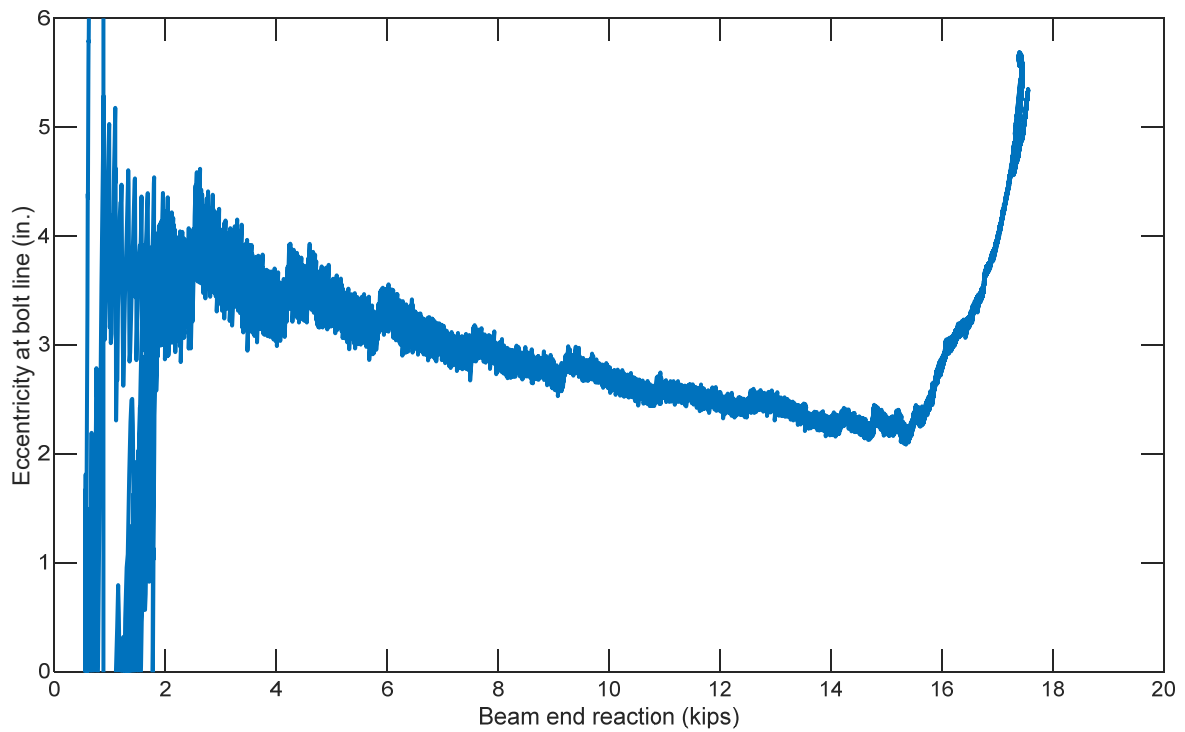
(f) Beam end reaction vs. eccentricity at bolt line

Figure 31. Photographs and Results for Specimen 2D (continued)
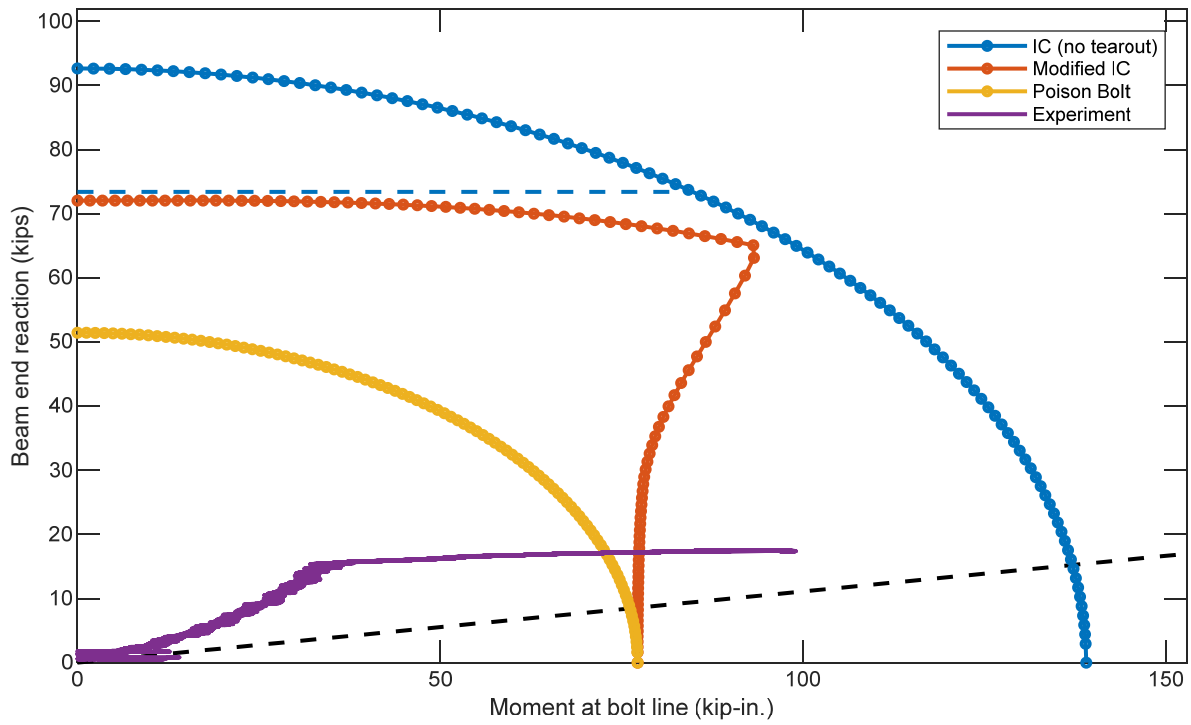
(g) Moment at bolt line vs. beam end reaction
Figure 31. Photographs and Results for Specimen 2D (continued)
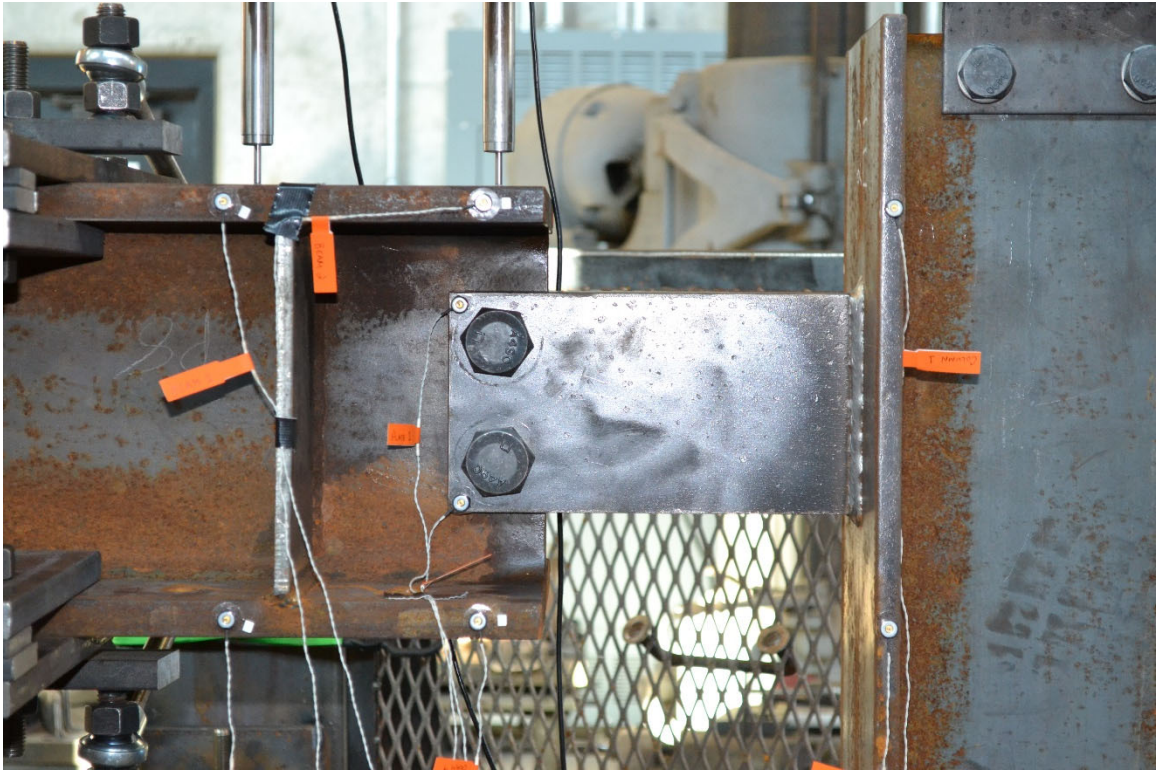
(a) Connection before testing

(b) Connection after testing
Figure 32. Photographs and Results for Specimen 2E
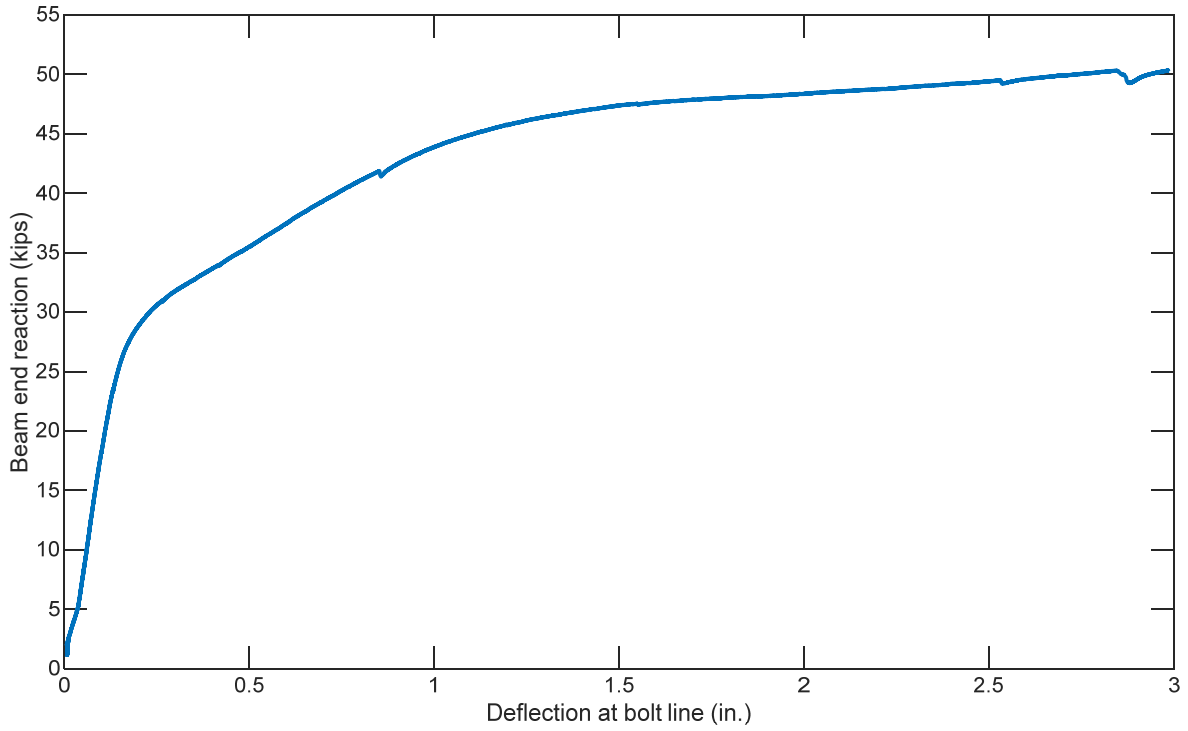
(c) Deflection at bolt line vs beam end reaction
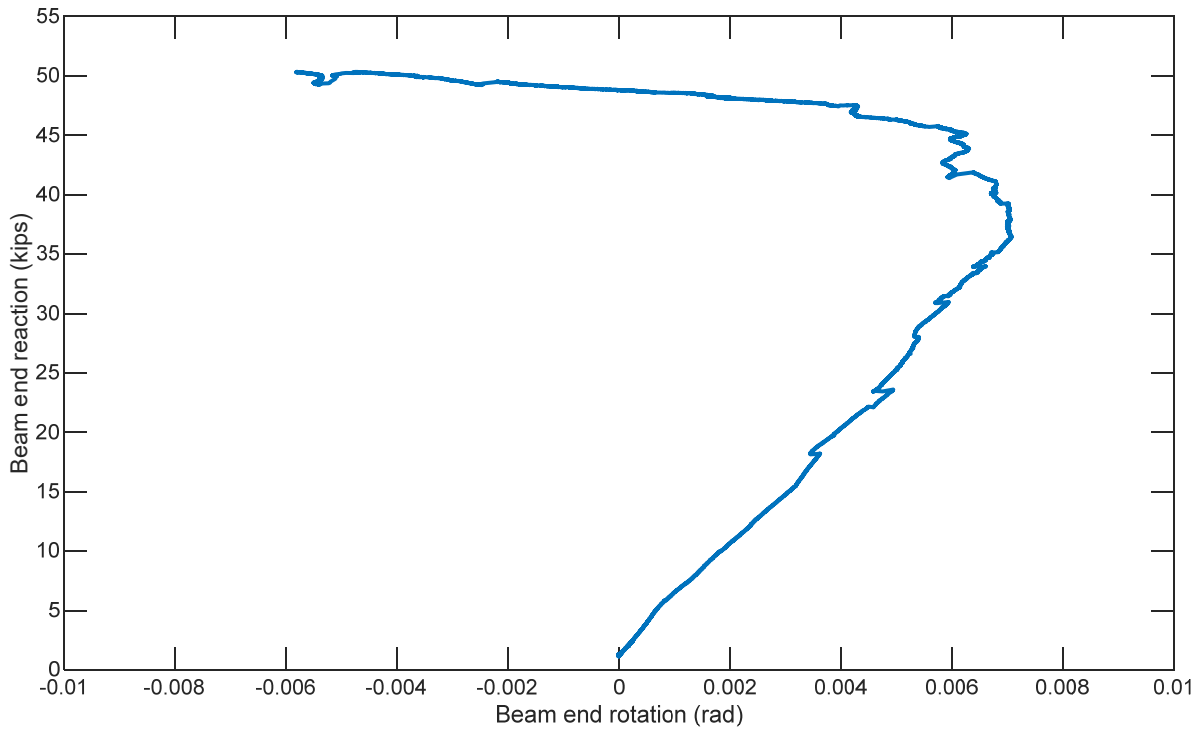
(d) Beam end rotation vs. beam end reaction
Figure 32. Photographs and Results for Specimen 2E (continued)
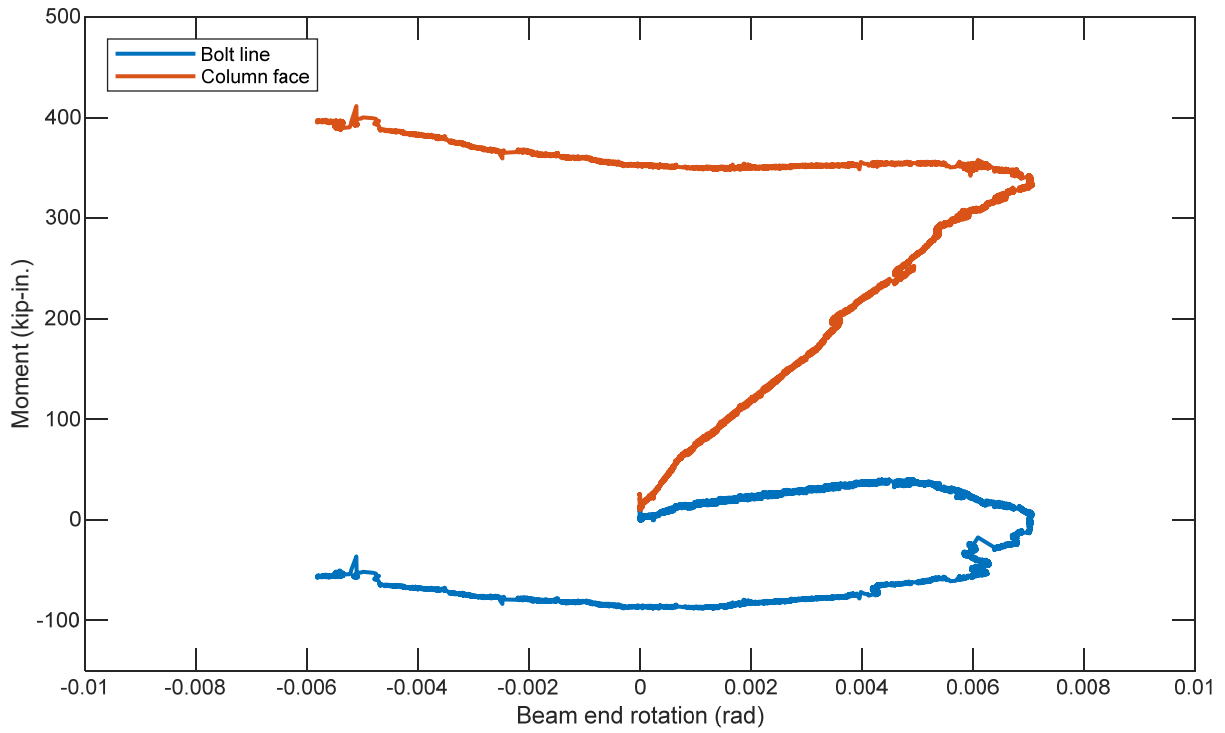
(e) Beam end rotation vs. moment at bolt line and column face
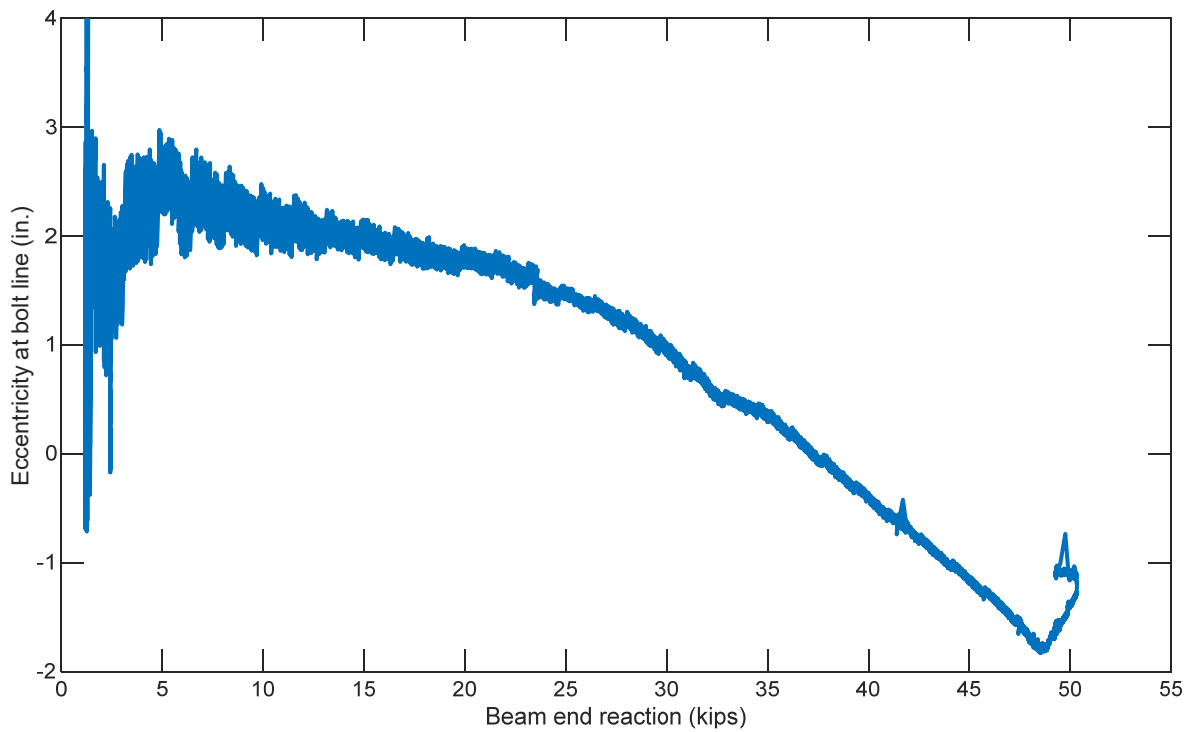
(f) Beam end reaction vs. eccentricity at bolt line
Figure 32. Photographs and Results for Specimen 2E (continued)
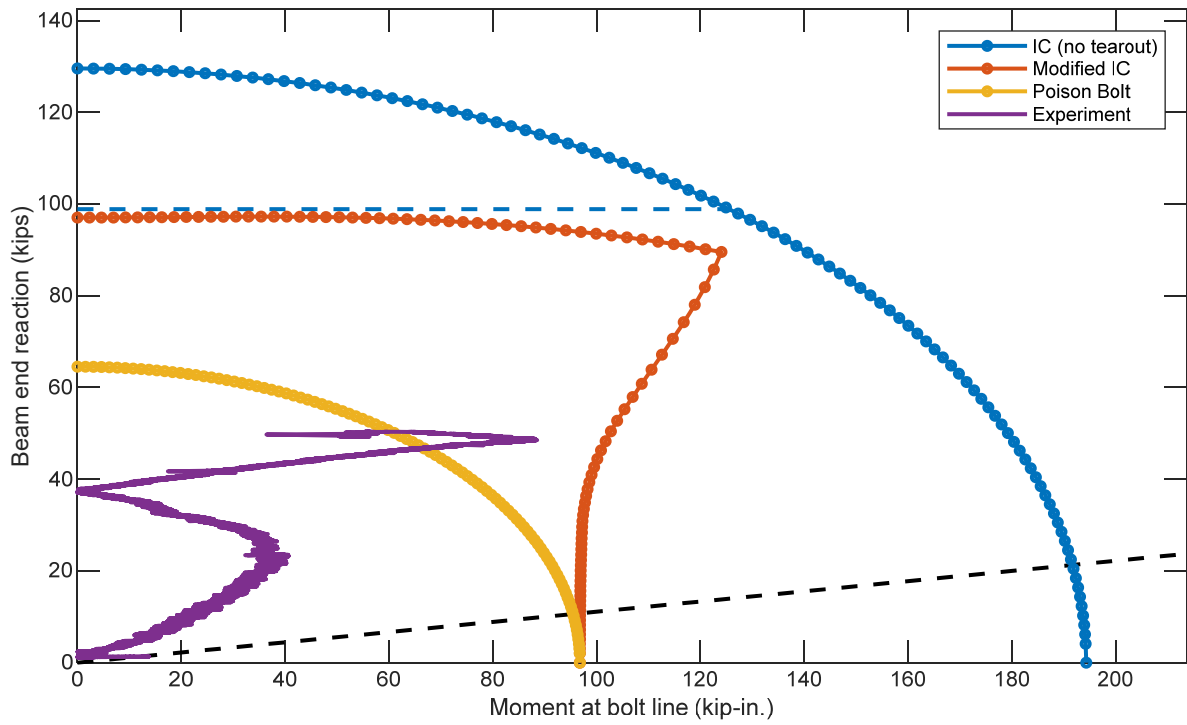
(g) Moment at bolt line vs. beam end reaction
Figure 32. Photographs and Results for Specimen 2E (continued)

(a) Connection before testing

(b) Connection after testing
Figure 33. Photographs and Results for Specimen 5A
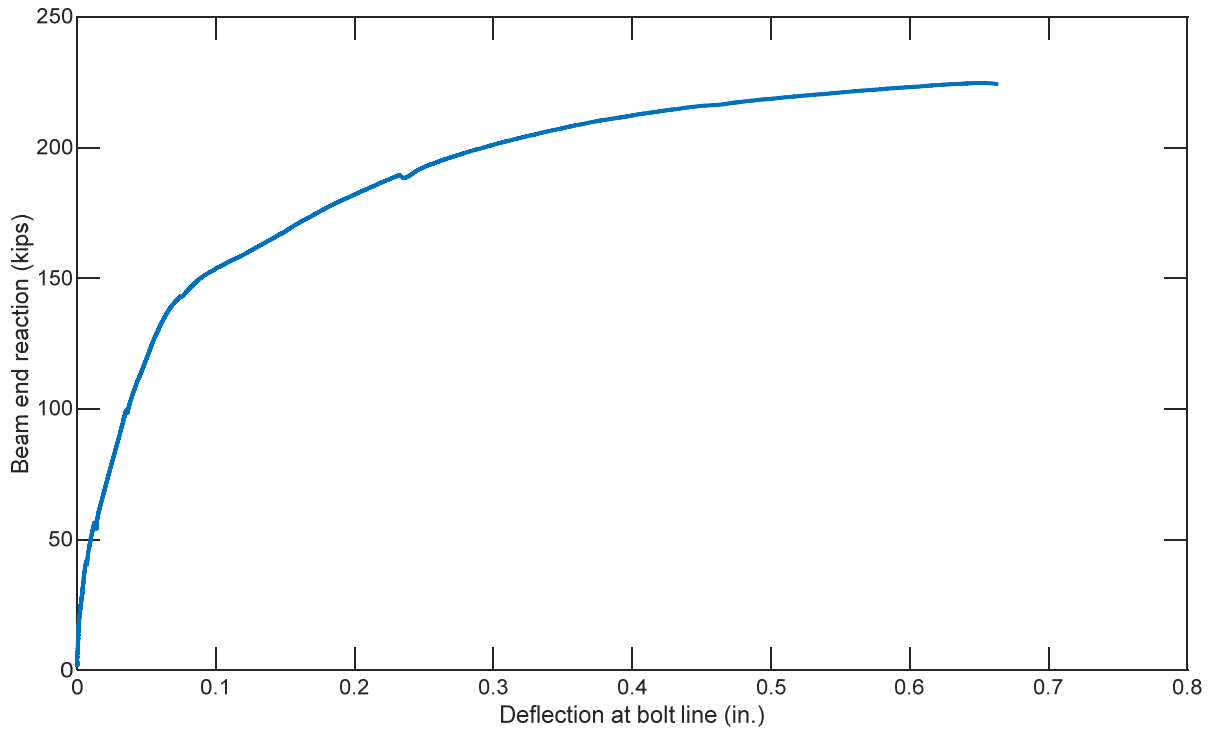
(c) Deflection at bolt line vs beam end reaction
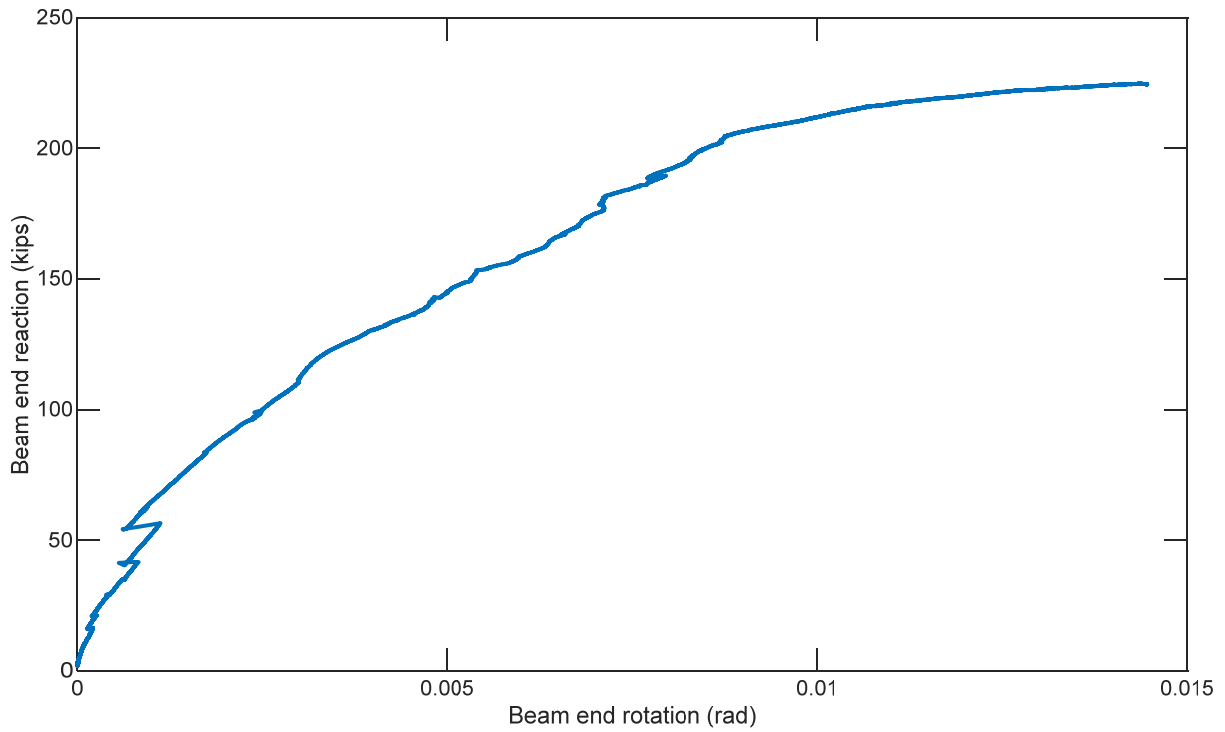
(d) Beam end rotation vs. beam end reaction
Figure 33. Photographs and Results for Specimen 5A (continued)
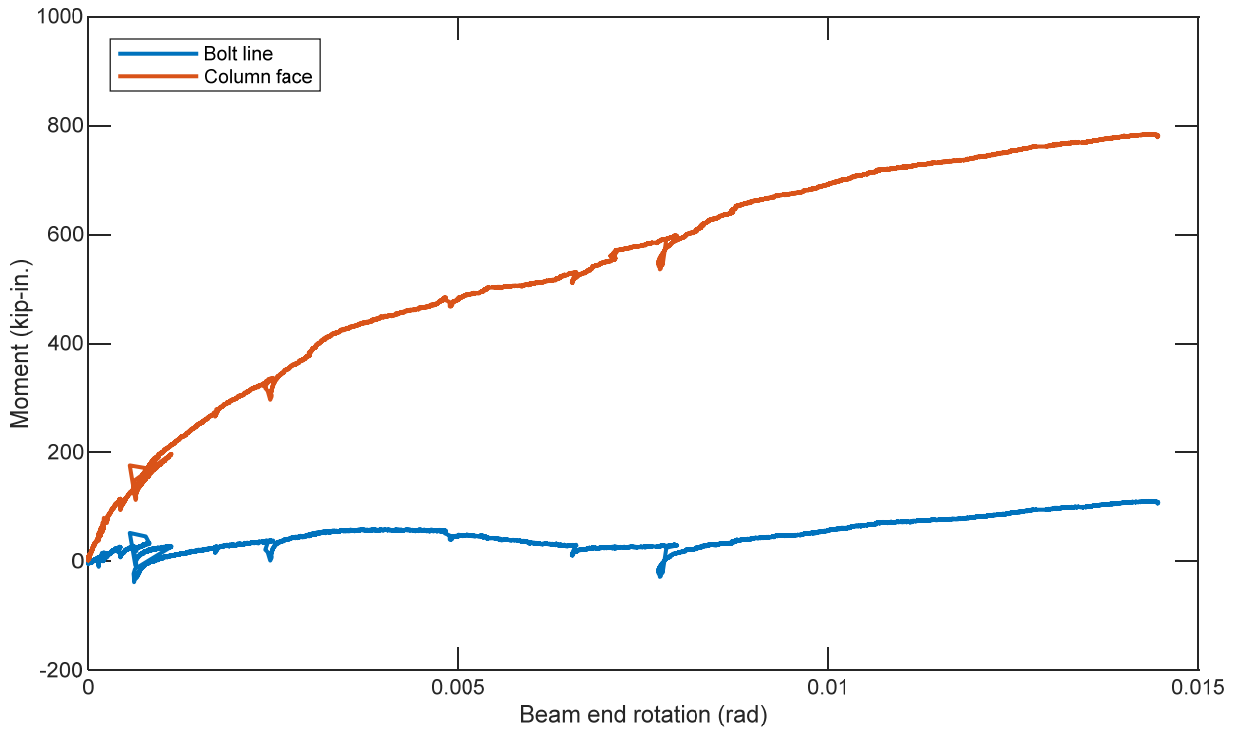
(e) Beam end rotation vs. moment at bolt line and column face
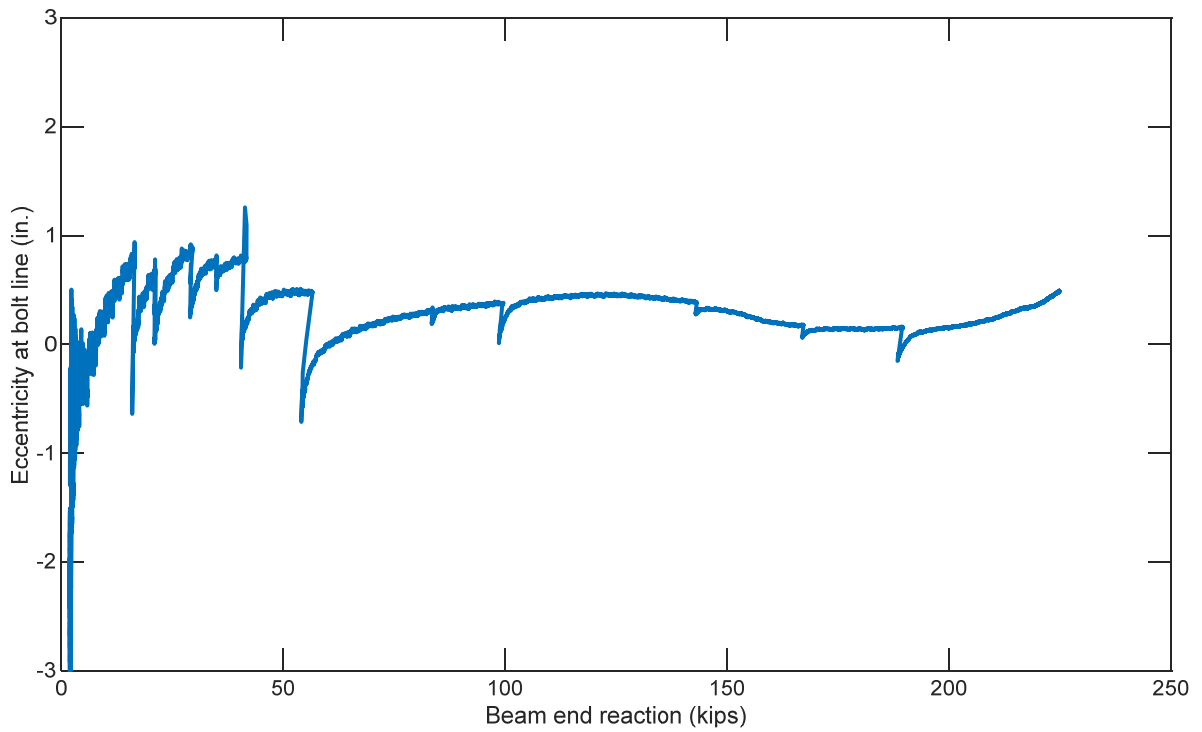
(f) Beam end reaction vs. eccentricity at bolt line

Figure 33. Photographs and Results for Specimen 5A (continued)
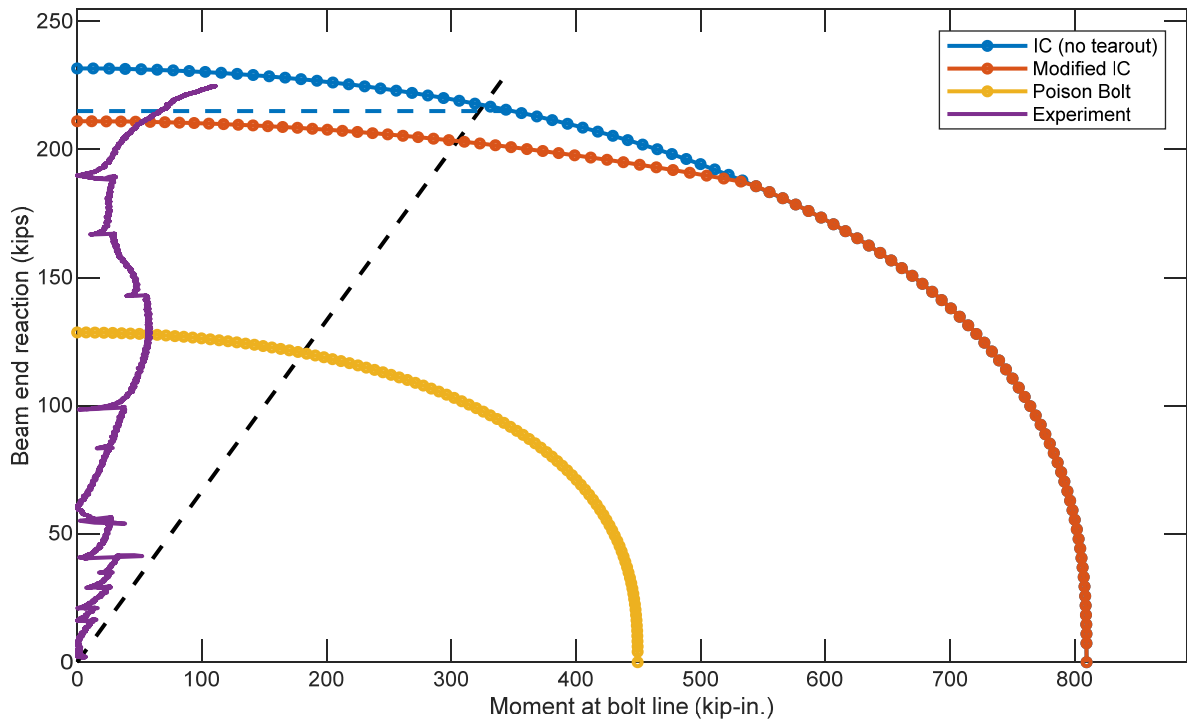
(g) Moment at bolt line vs. beam end reaction
Figure 33. Photographs and Results for Specimen 5A (continued)

(a) Connection before testing

(b) Connection after testing
Figure 34. Photographs and Results for Specimen 5B
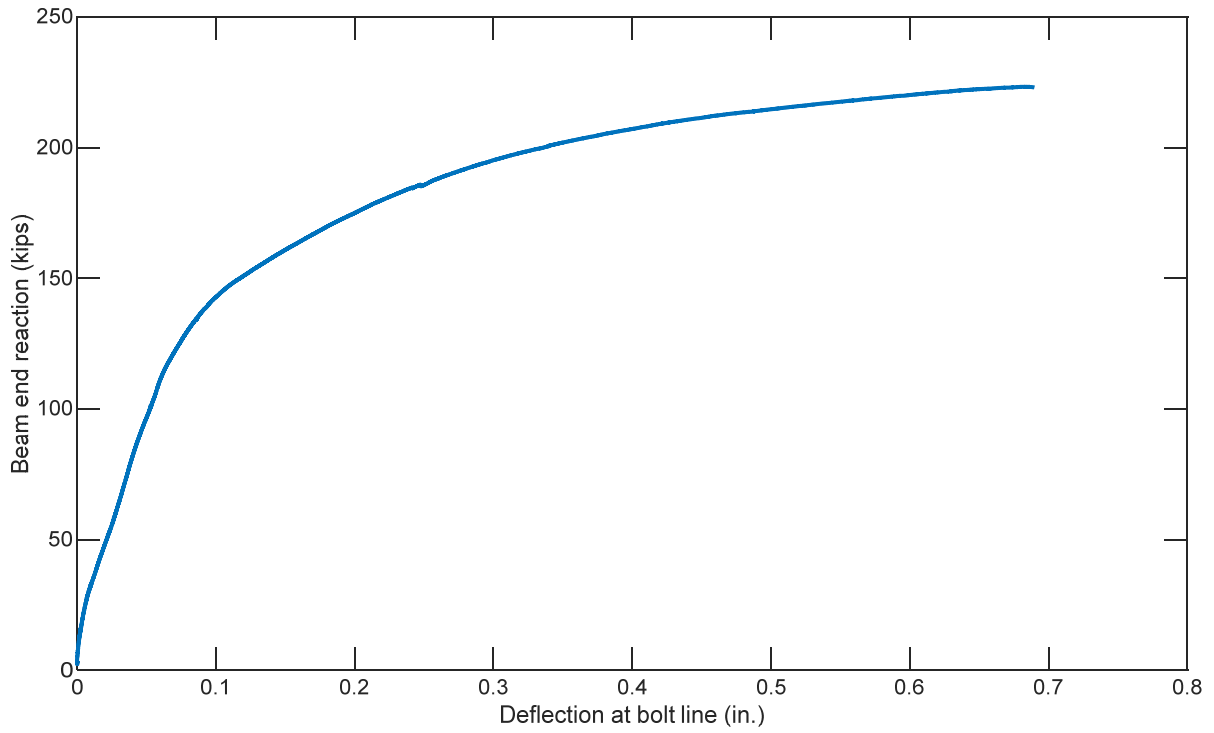
(c) Deflection at bolt line vs beam end reaction
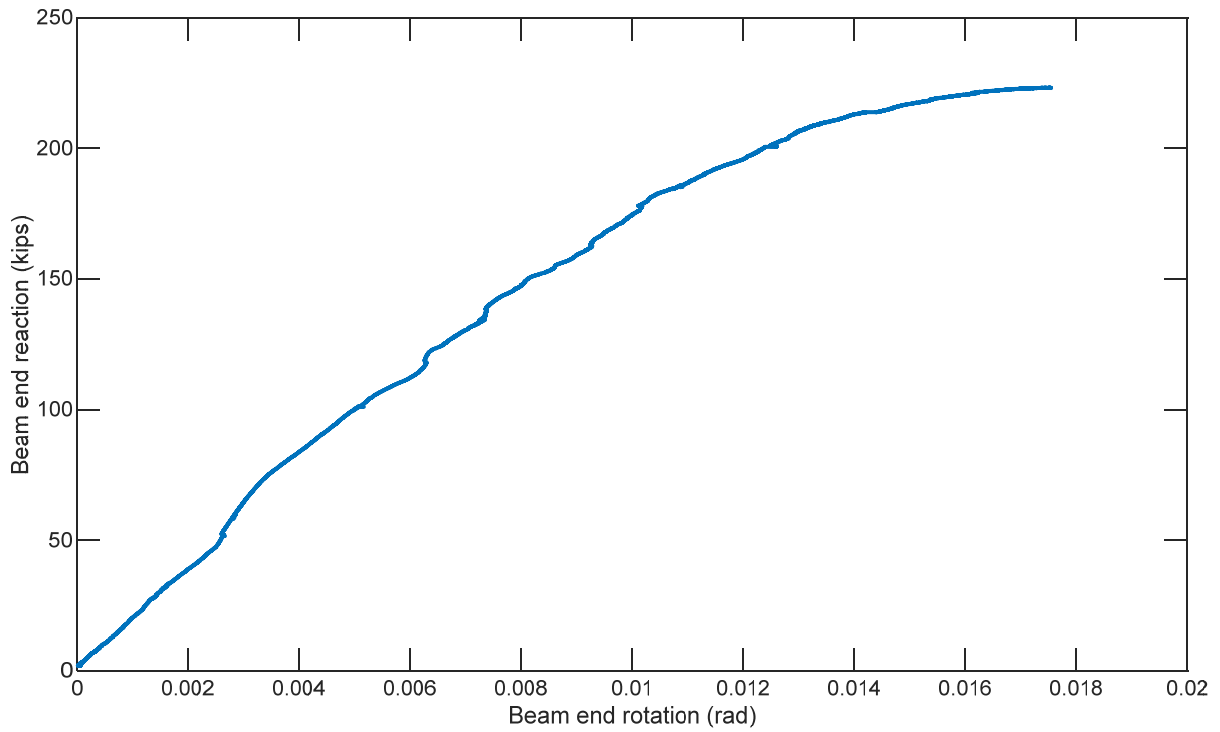
(d) Beam end rotation vs. beam end reaction
Figure 34. Photographs and Results for Specimen 5B (continued)
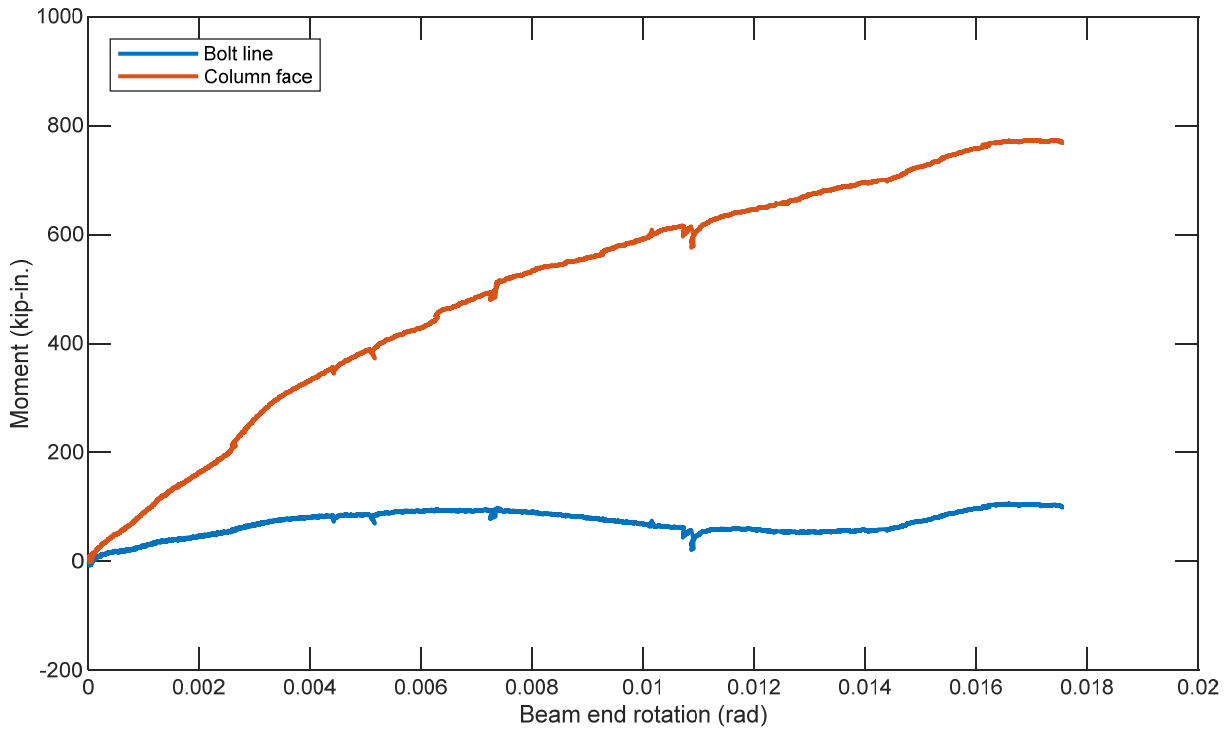
(e) Beam end rotation vs. moment at bolt line and column face
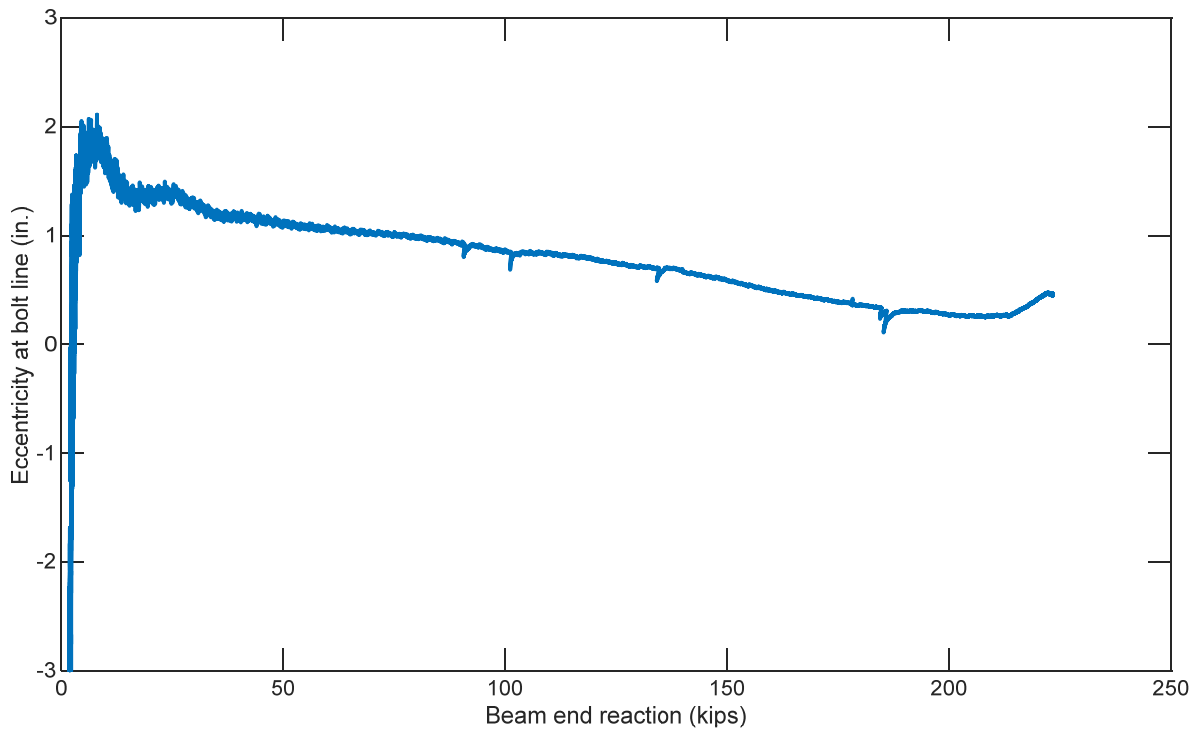
(f) Beam end reaction vs. eccentricity at bolt line
Figure 34. Photographs and Results for Specimen 5B (continued)
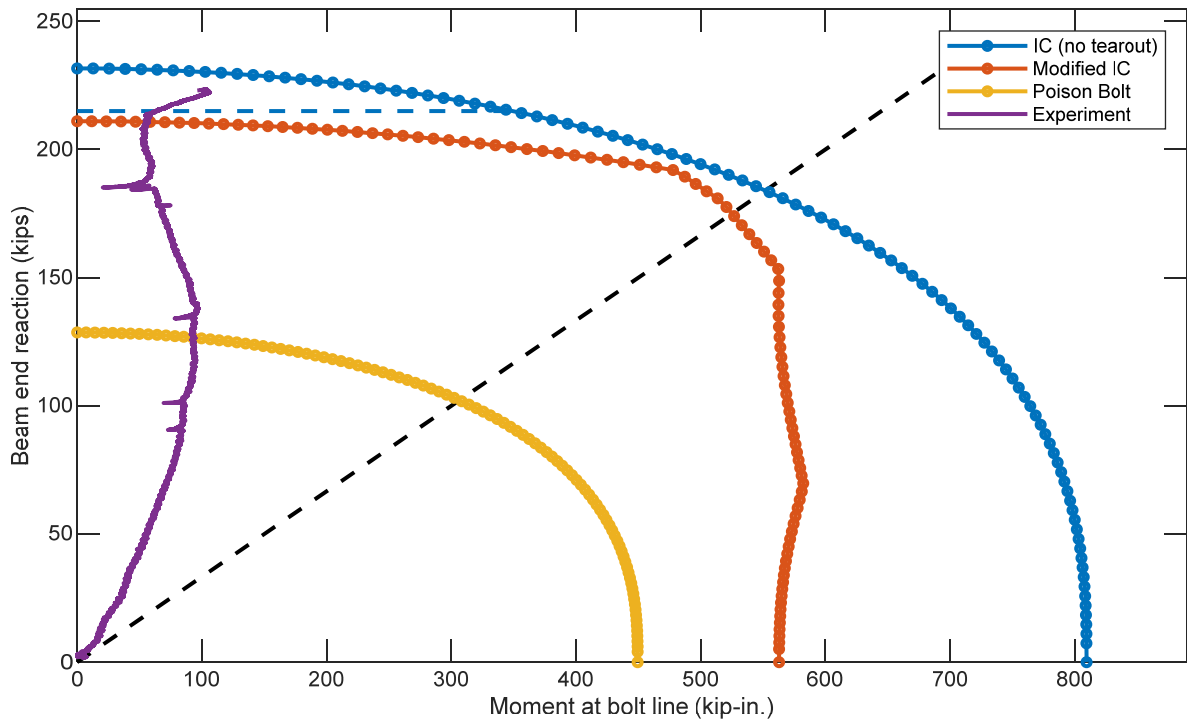
90

(g) Moment at bolt line vs. beam end reaction
Figure 34. Photographs and Results for Specimen 5B (continued)

(a) Connection before testing

(b) Connection after testing
Figure 35. Photographs and Results for Specimen 5C
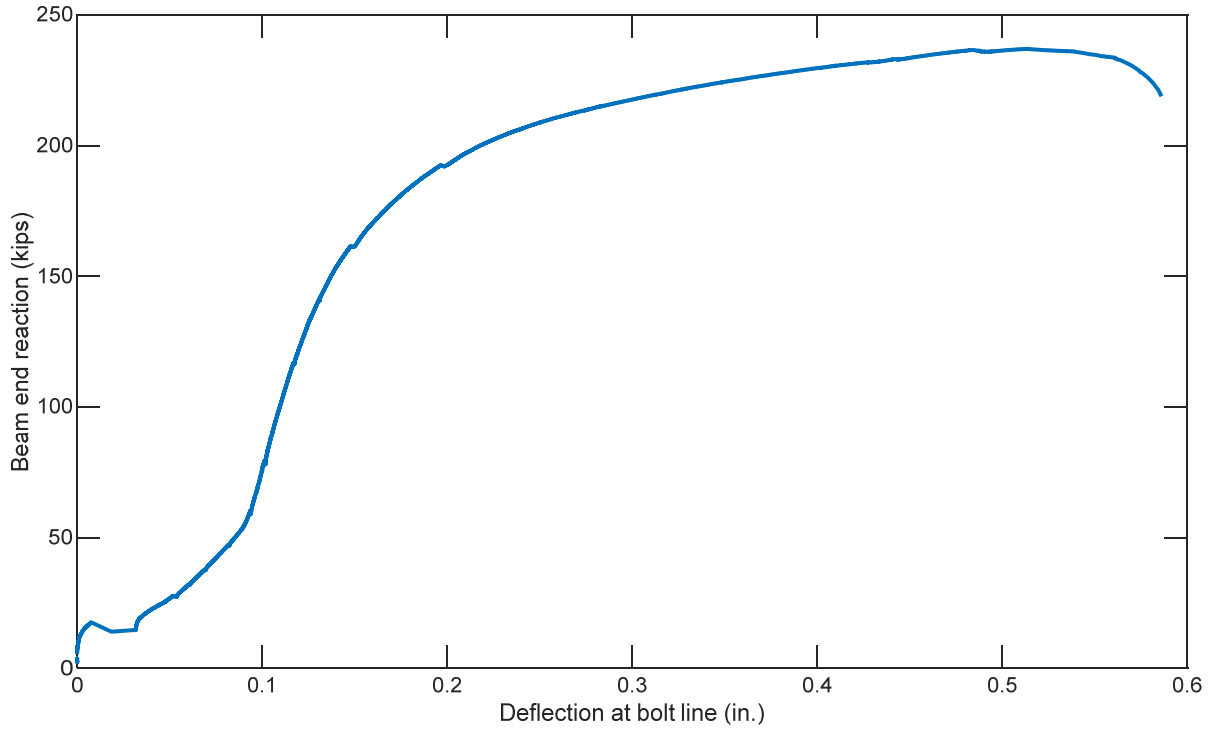
(c) Deflection at bolt line vs beam end reaction
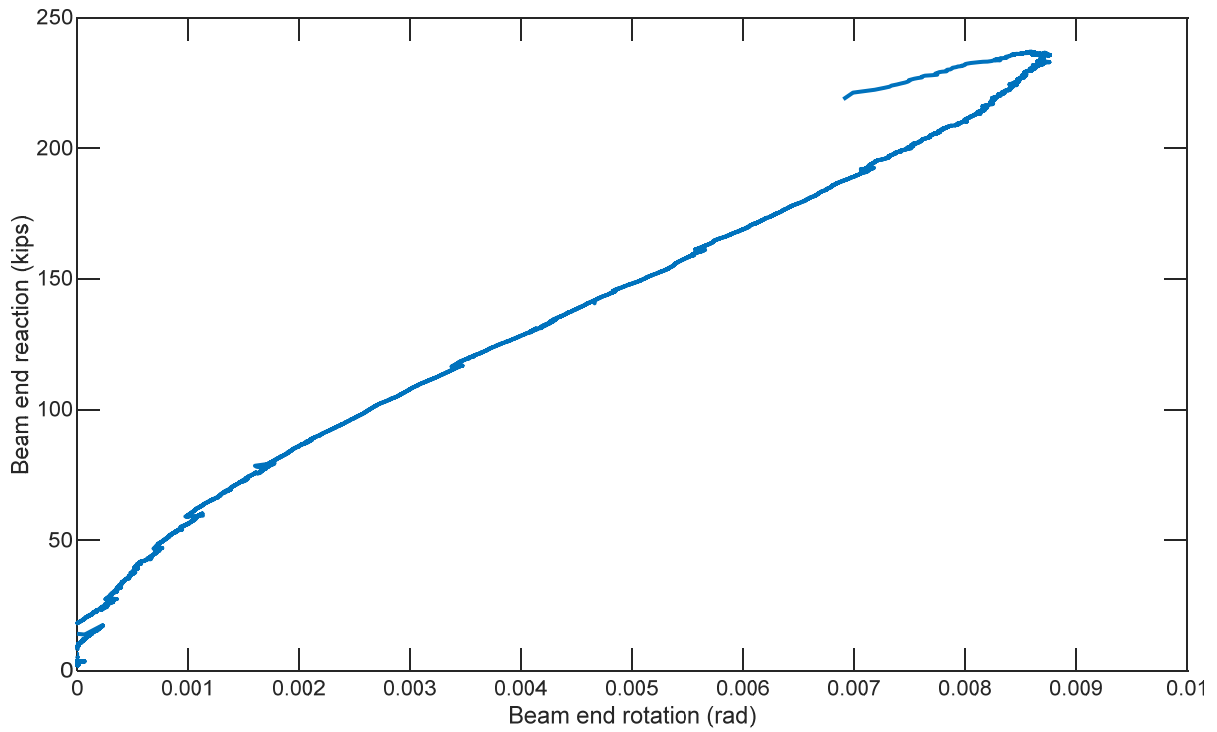
(d) Beam end rotation vs. beam end reaction
Figure 35. Photographs and Results for Specimen 5C (continued)
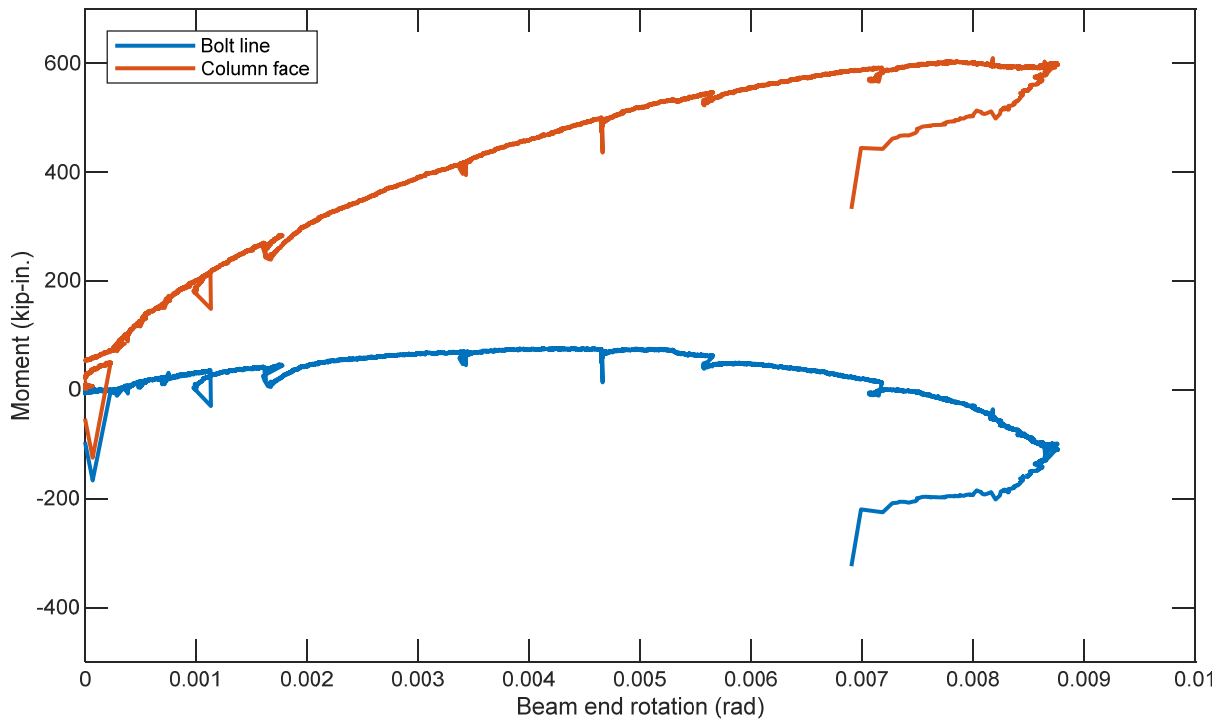
(e) Beam end rotation vs. moment at bolt line and column face
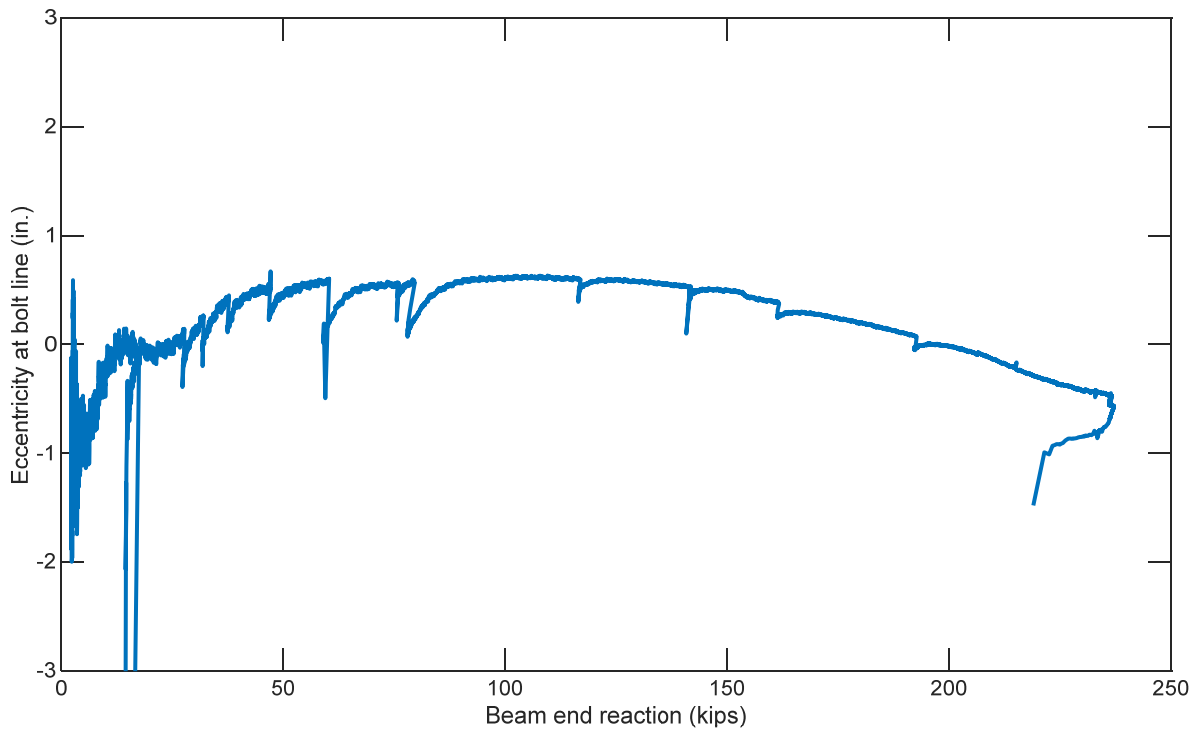
(f) Beam end reaction vs. eccentricity at bolt line
Figure 35. Photographs and Results for Specimen 5C (continued)
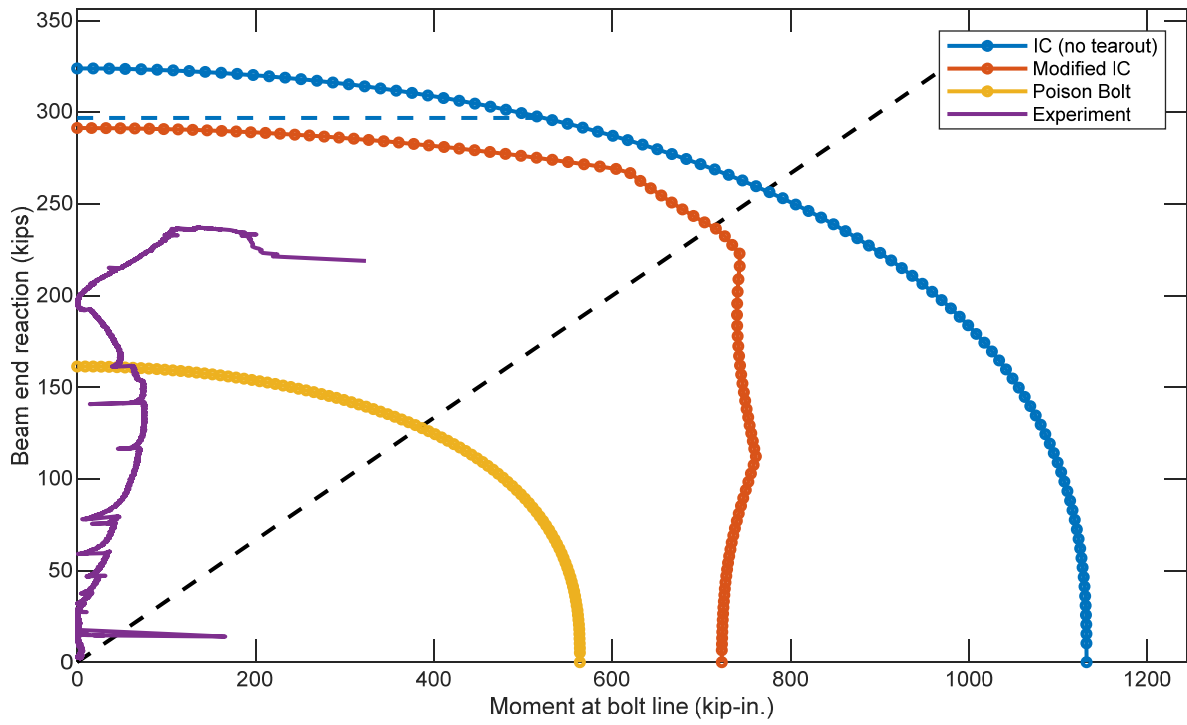
(g) Moment at bolt line vs. beam end reaction
Figure 35. Photographs and Results for Specimen 5C (continued)

(a) Connection before testing

(b) Connection after testing
Figure 36. Photographs and Results for Specimen 5D
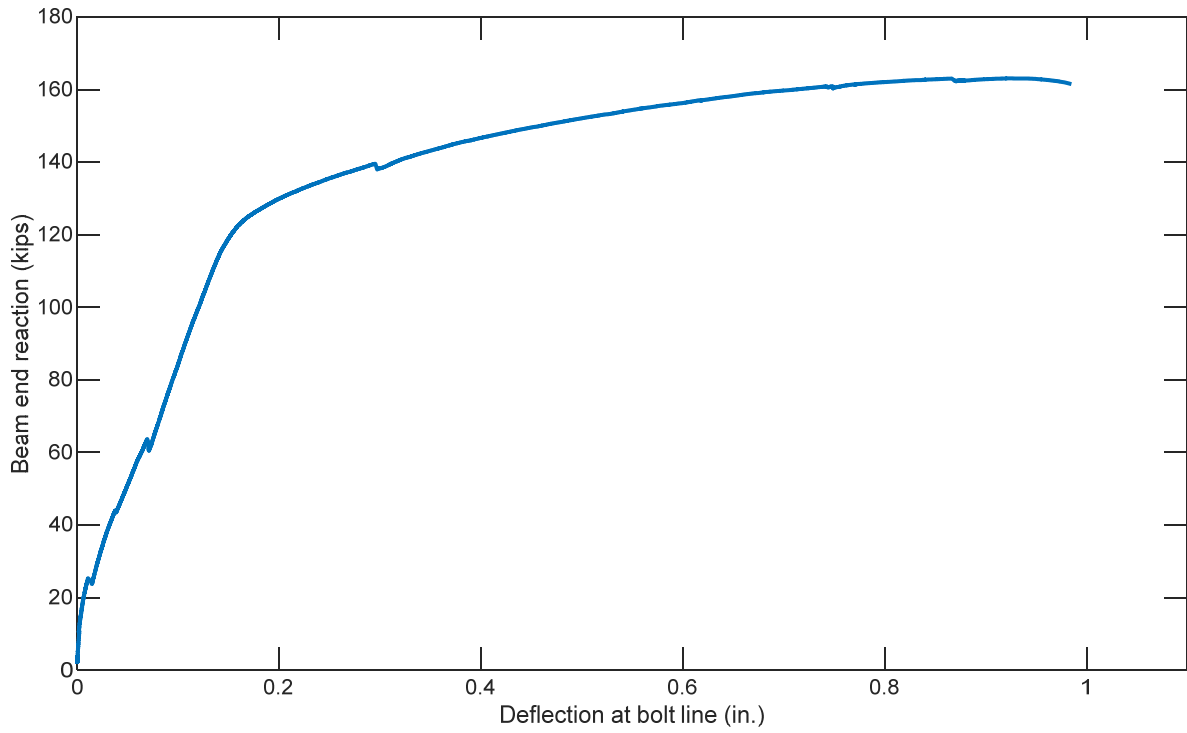
(c) Deflection at bolt line vs beam end reaction
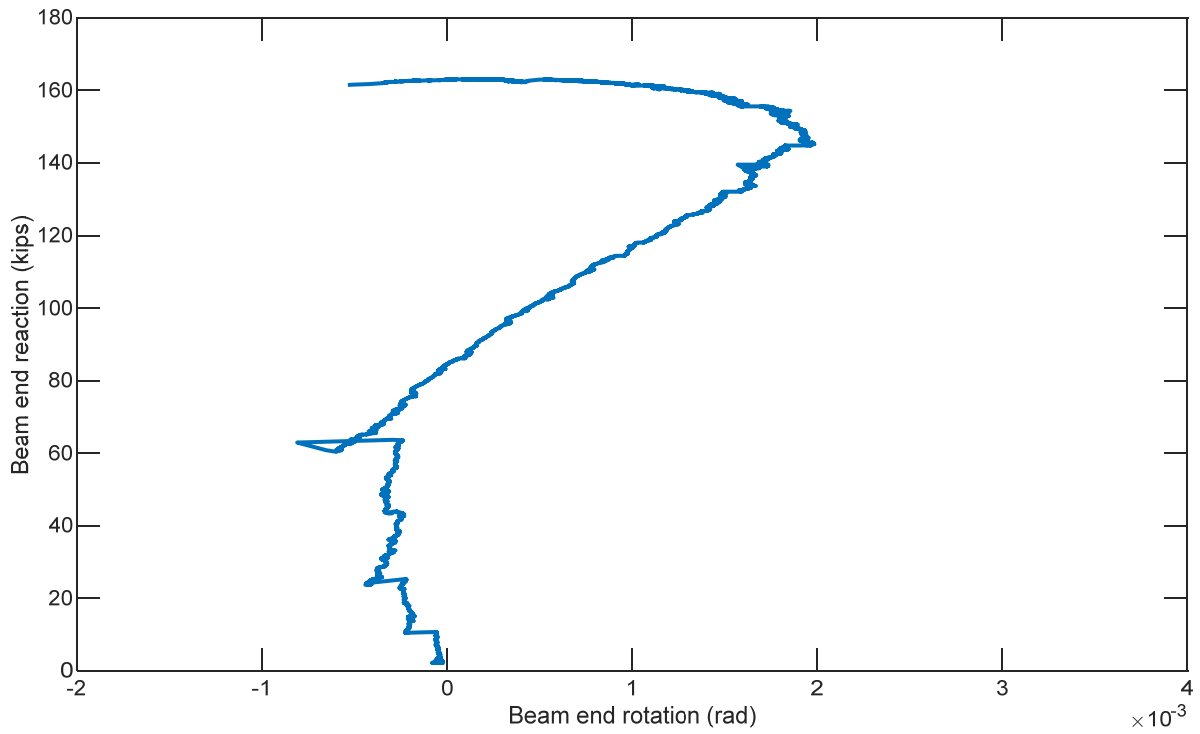
(d) Beam end rotation vs. beam end reaction
Figure 36. Photographs and Results for Specimen 5D (continued)
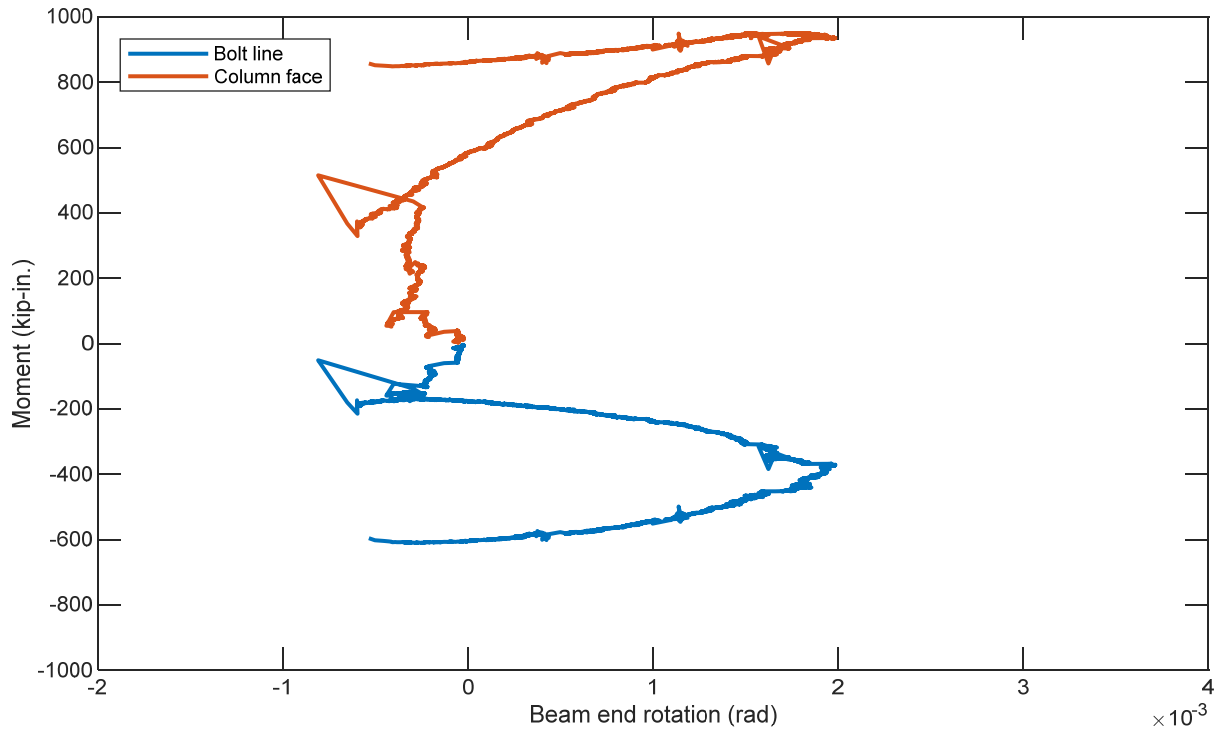
(e) Beam end rotation vs. moment at bolt line and column face
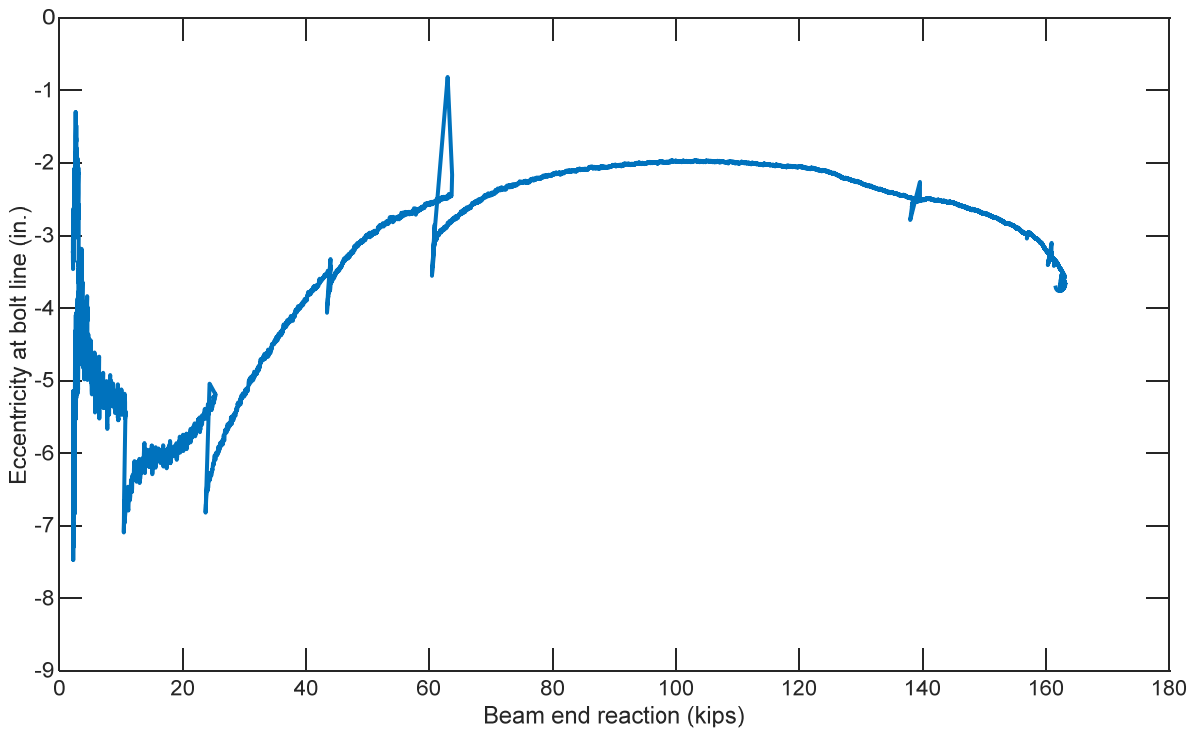
(f) Beam end reaction vs. eccentricity at bolt line
Figure 36. Photographs and Results for Specimen 5D (continued)
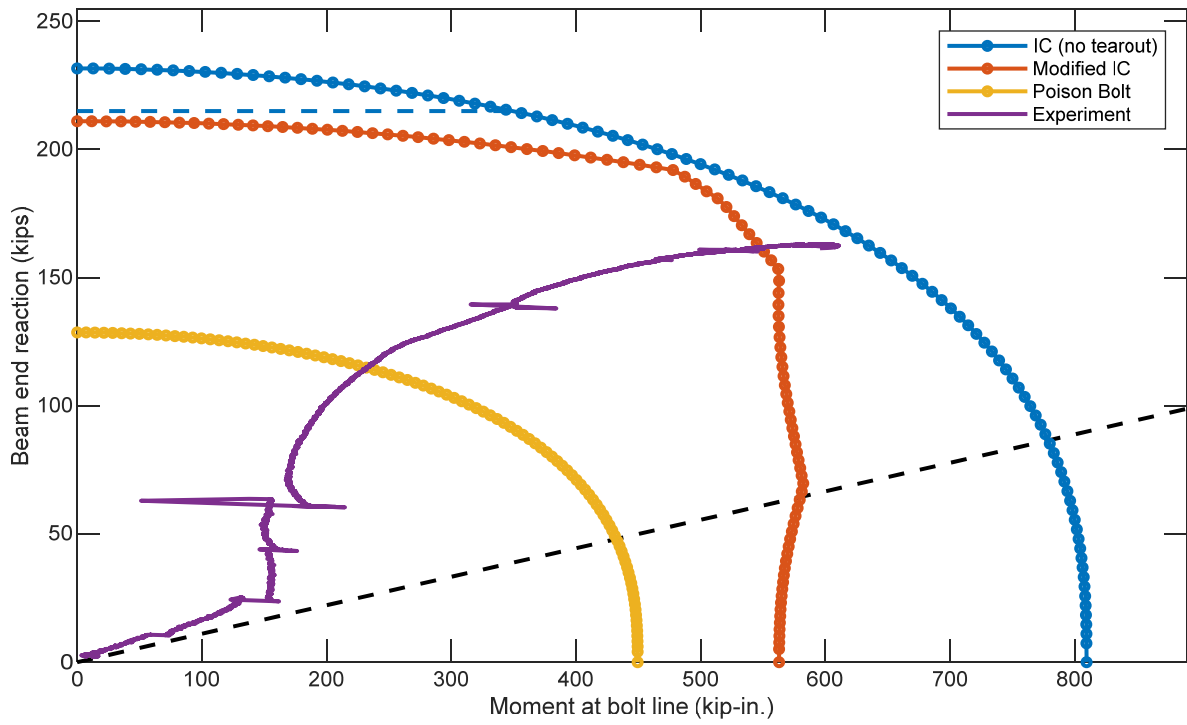
(g) Moment at bolt line vs. beam end reaction
Figure 36. Photographs and Results for Specimen 5D (continued)
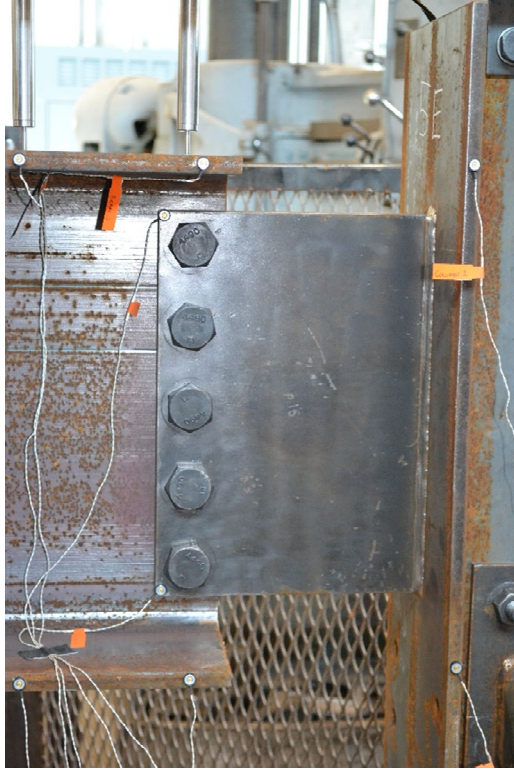
(a) Connection before testing
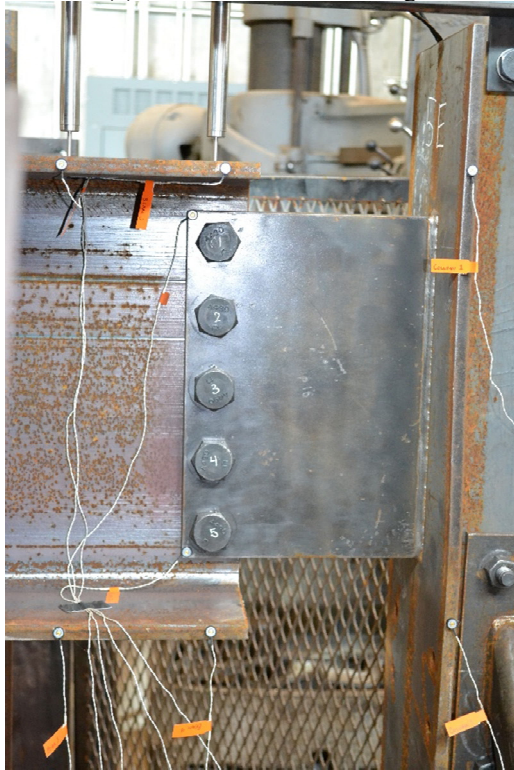
(b) Connection after testing
Figure 37. Photographs and Results for Specimen 5E
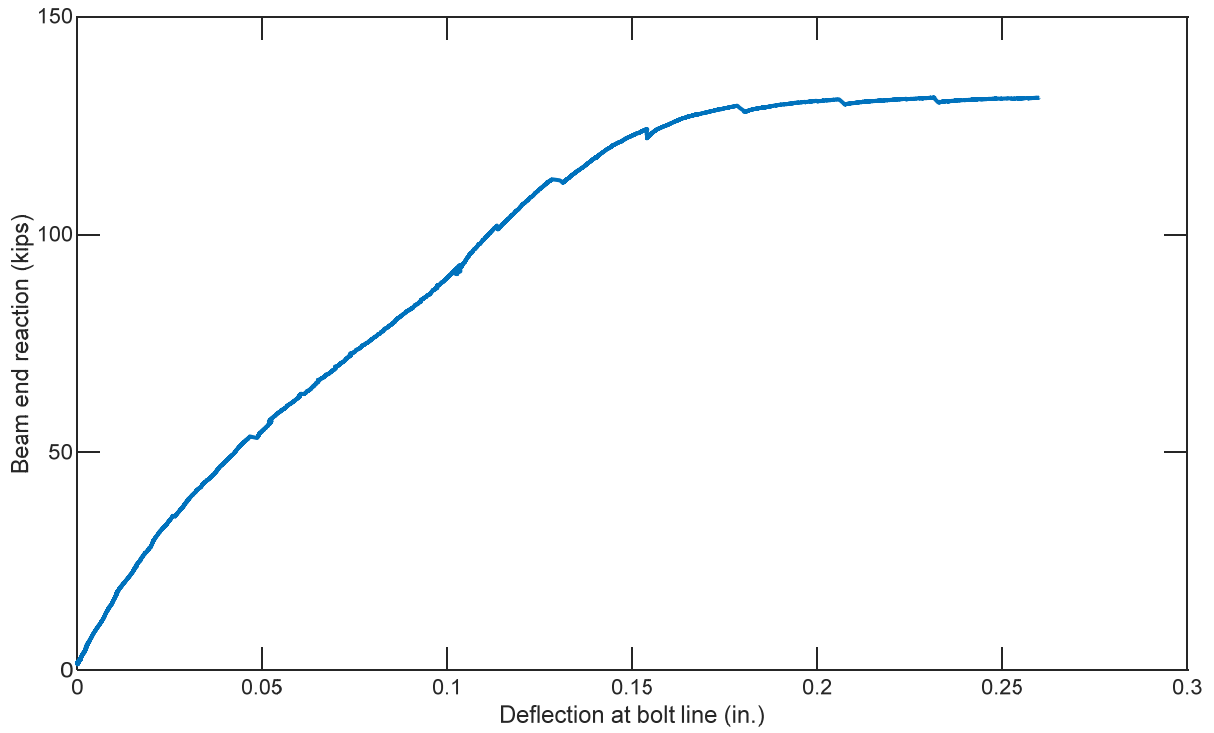
(c) Deflection at bolt line vs beam end reaction
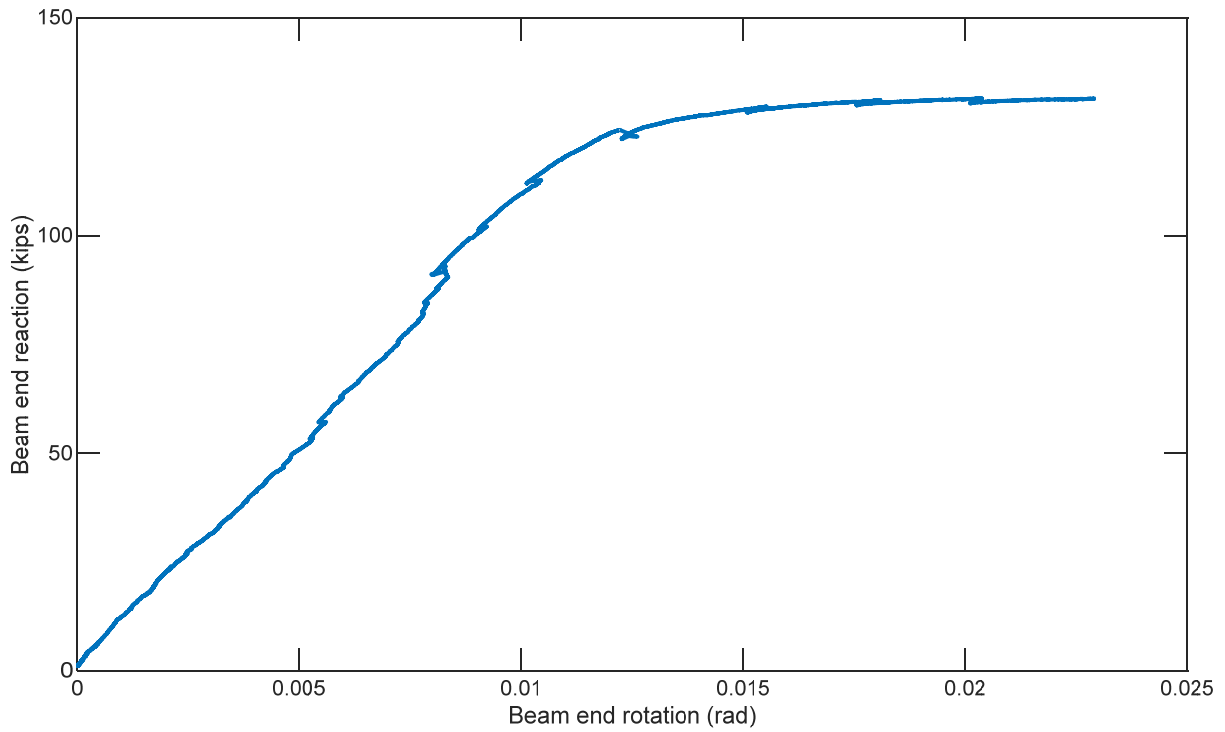
(d) Beam end rotation vs. beam end reaction

Figure 37. Photographs and Results for Specimen 5E (continued)
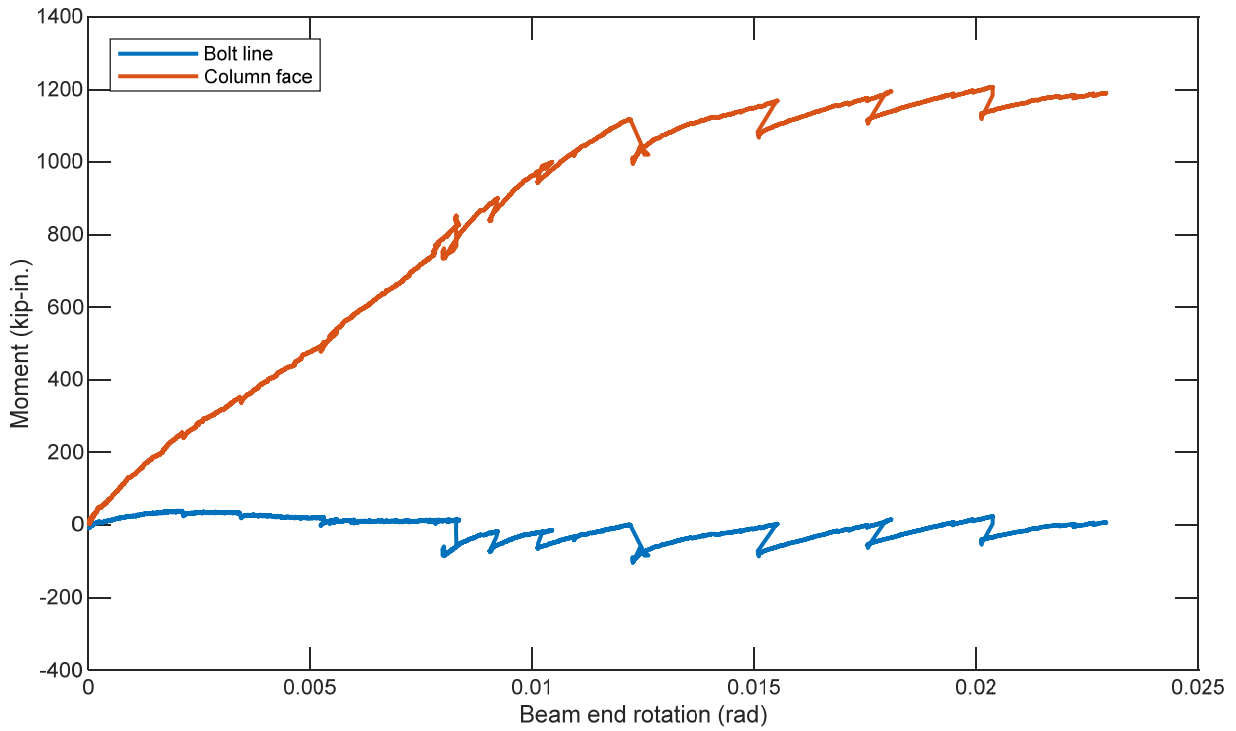
(e) Beam end rotation vs. moment at bolt line and column face
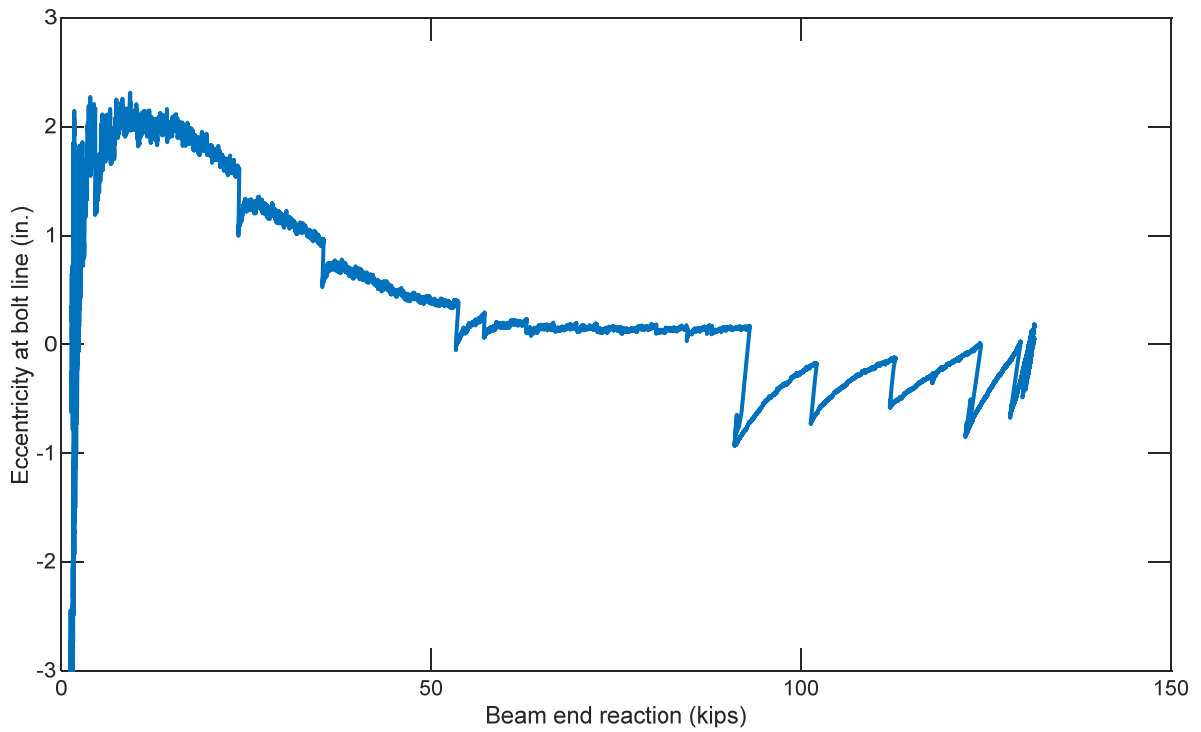
(f) Beam end reaction vs. eccentricity at bolt line
Figure 37. Photographs and Results for Specimen 5E (continued)

(g) Moment at bolt line vs. beam end reaction

Figure 37. Photographs and Results for Specimen 5E (continued)